SYNCHRONISATION ON NON-COMPACT MANIFOLDS

by

Louis Michel Ritchie

August 15, 2018

Thesis presented for the degree of Master of Philosophy in Physics
The University of Adelaide
Faculty of Sciences
School of Physical Sciences

Declaration

I certify that this work contains no material which has been accepted for the award of any other degree or diploma in my name, in any university or other tertiary institution and, to the best of my knowledge and belief, contains no material previously published or written by another person, except where due reference has been made in the text. In addition, I certify that no part of this work will, in the future, be used in a submission in my name, for any other degree or diploma in any university or other tertiary institution without the prior approval of the University of Adelaide and where applicable, any partner institution responsible for the joint-award of this degree. I acknowledge that copyright of published works contained within this thesis resides with the copyright holder(s) of those works. I also give permission for the digital version of my thesis to be made available on the web, via the University's digital research repository, the Library Search and also through web search engines, unless permission has been granted by the University to restrict access for a period of time. I acknowledge the support I have received for my research through the provision of an Australian Government Research Training Program Scholarship.

Signed by student:

Date: 15/08/2018

Signed by supervisor:

Date: 15/08/2018

Acknowledgements

Thank you to my supervisors, Max Lohe and Tony Williams, for their guidance, wisdom and senses of humour throughout the stages of my project and thank you to my friends and family for their love and support.

Abstract

The Kuramoto model is a widely studied model of phase synchronisation which continues to display novel and interesting emergent behaviours with its many extensions and generalisations. We formulate a non-compact version of the Kuramoto model by replacing the compact symmetry group $SO(2)$ with the non-compact group $SO(1,1)$. The N equations are similar to the Kuramoto equations, except that the trigonometric terms are replaced with hyperbolic functions. Solution trajectories are generally unbounded, lying on the unit hyperbola, but synchronisation occurs for any positive coupling constants and arbitrary driving parameters. We show solutions can develop singularities for negative coupling constants. We also develop a vector model of synchronisation on non-compact manifolds. By choosing the group $SO(1,2)$ trajectories are confined to a one-sheeted hyperboloid. This model also displays unbounded trajectories but can synchronise for negative couplings and restricted initial conditions. Singularities can occur for positive couplings or if the initial conditions are too widely distributed. We describe a physical interpretation of the $SO(1,1)$ model as a system of interacting relativistic particles in $1+1$ spacetime dimensions.

Contents

List of Figures

List of Publications

[1] L.M. Ritchie, M.A. Lohe, A.G. Williams, *Chaos* **28**, 053116 (2018).

Chapter 1

Introduction

1.1 Background

The emergent phenomenon of synchronisation in complex systems has been widely investigated, see the review articles [1–6], and is ubiquitous in physical and biological systems, for example the synchronous flashing of fireflies [7], neutrino oscillations [8], neuronal networks [9] and power grid networks [10]. Synchronisation (also called phase-locking) involves two or more interacting elements of a dynamical system whose properties become correlated in time, leading to the time evolution of the system as a collective entity. The most extensively-studied model of synchronisation is the Kuramoto model [11] along with its many extensions and generalizations (see [12–16] and [5] for examples). The popularity of the Kuramoto model (KM) arises from its mathematical simplicity while at the same time displaying a variety of synchronisation behaviours, as well as its many applications in realistic systems. The basic Kuramoto model consists of a population of N globally coupled i.e. all-to-all phase oscillators $\theta_i(t)$ with natural frequencies ω_i and coupling constant K. The governing equations for each of the oscillators are:

$$\dot{\theta}_i = \omega_i + \frac{K}{N}\sum_{j=1}^{N}\sin(\theta_j - \theta_i). \tag{1.1}$$

There are several models for the synchronisation of interacting nodes outside of the Kuramoto model. The "Tops" model, introduced in [17], is a model for the synchronisation of classical spins described by azimuthal and polar angles, rather than phase oscillators as in the KM. Another model which can show phase-locking is the statistical XY model, a lattice model describing the phases of plane-rotators at each lattice site [18, 19].

Apart from the globally coupled Kuramoto model, there are many other possible coupling configurations, such as scale-free networks, where the number of connections each node/oscillator has (the degree of a node) follows a power-law distribution [1,2]. To account for these complex network topologies the Kuramoto model must be modified by the inclusion of a coupling matrix:

$$\dot{\theta}_i = \omega_i + \frac{K}{N}\sum_{j=1}^{N} a_{ij}\sin(\theta_j - \theta_i). \tag{1.2}$$

where a_{ij} are the elements of the coupling matrix. For two nodes i and j that are coupled, for $i \neq j$, $a_{ij} = 1$ and is 0 otherwise. Other generalisations of the KM include stochastic models, which add white noise forcing terms $\xi_i(t)$ and tend to counteract synchronisation [4,5],

$$\dot{\theta}_i = \omega_i + \xi_i(t) + \frac{K}{N}\sum_{j=1}^{N} \sin(\theta_j - \theta_i), \tag{1.3}$$

and adaptive networks, where there is feedback between the dynamics of the nodes and the network topology, i.e. the dynamics of the nodes can alter the connectivity of the network [1,20]. It is well known [1,4] that for very weak coupling constants, the nodes oscillate independently at their natural frequencies, while for a larger coupling, the oscillators partially synchronise, and for sufficiently large coupling, the oscillators completely synchronise to a common mean frequency. Kuramoto's original analysis of the model was performed in the case of mean-field coupling i.e. by taking $N \to \infty$. Kuramoto showed that there is a critical value of the coupling constant K_C, below which the oscillators do not exhibit synchronous behaviour [11,21]. The collective behaviour, or order (the degree of synchronisation), of the system can be described by the (complex) order parameter,

$$e^{i\psi(t)}R(t) = \frac{1}{N}\sum_{j=1}^{N} e^{i\theta_j} \tag{1.4}$$

where the function $0 \leq R(t) \leq 1$ measures the phase coherence of the system and ψ is the average phase. A value of $R = 1$ corresponds to the fully synchronised state where all the phases are the same and $R = 0$ corresponds to the fully unsynchronised state where all the phases are uniformly distributed on the unit circle. In addition to synchronised and un-synchronised states, there are states called "chimera" states, named for the part-lion, part-serpent, part-goat creature of greek myth, in which a portion of the population is fully synchronised while another portion is desynchronised [5,22]. In [22], the authors studied a system of

two groups of oscillators in which each oscillator is coupled equally to all the others in its group, and less strongly to those in the other group; this is the simplest system which can show chimera states. They showed that chimera states emerge for certain initial conditions, and that chimera states can be stable, i.e. the order parameter of the desynchronised population is time independent, or they can "breathe", i.e. the order parameter oscillates with time.

The behaviour of the Kuramoto model is closely related to the properties of the rotation group $SO(2)$. For example, plane rotations $\theta_i(t) \to \theta_i(t) + \theta_0$ leave (1.1) invariant, for any constant θ_0, and are covariant under transformations $\theta_i \to \theta_i + \omega_0 t$, for constant frequency ω_0, shifting the natural frequencies ω_i to $\omega_i - \omega_0$. In fact, the Kuramoto equations (1.1) can be viewed as N dynamical equations for the 2×2 rotation matrices $R_i \in SO(2)$ parametrised by the angles θ_i. Matrix generalisations of the Kuramoto model exist wherein the rotation group of $SO(2)$ can be replaced by any compact, classical matrix Lie group [23, 24], and read as follows:

$$i\dot{U}_i U_j^\dagger = \Omega_i + \frac{iK}{2N} \sum_{j=1}^{N} \left(U_i U_j^\dagger - U_j U_i^\dagger \right) \tag{1.5}$$

where U_i is an $d \times d$ complex unitary matrix and $U_i^\dagger$ denotes its hermitian conjugate. Ω_i a $d \times d$ Hermitian matrix whose eigenvalues correspond to the natural frequencies of the i^{th} oscillator. The synchronisation properties of these matrix models are similar to those of the Kuramoto model. For example in [23], Lohe numerically investigated the $SU(2) \times SU(2)$ case and found that for sufficiently large K, the particles synchronise to a common frequency. In addition to the matrix models, there are n-vector models, whose trajectories are confined to the unit sphere S^{n-1}. For $n = 2$ the unit 2-vector is given by $\boldsymbol{x}_i = (\cos\theta_i, \sin\theta_i)$, and the vector equations reduce to the Kuramoto model. Vector models defined on the unit-sphere have similar properties to the Kuramoto model [23, 25]. A common feature of the Kuramoto model and its generalisations is that the trajectory at each node is restricted to a compact manifold, for example the unit circle in the case of the Kuramoto model but it is known that synchronisation can also occur in models that allow unbounded trajectories on non-compact manifolds [26]. Non-compact manifolds are important objects of study in physics and mathematics. For example the Lorentz group (which is also a manifold) is the group of all Lorentz transformations of Minkowski space, and is closely related to the special theory of relativity and the theory of electromagnetism. Another important non-compact manifold is de Sitter space, a vacuum solution to the Einstein field equations in general relativity.

In [26], the authors generalised the equations (1.5) to include non-compact matrix Lie groups, with trajectories on non-compact manifolds, and showed that the

emergent phenomenon of synchronisation can, for restricted initial values and sufficiently large coupling strength, be extended to matrix models with non-compact groups. The synchronisation behaviour between the group elements X_i, located at the i^{th} node/oscillator is described by the equations:

$$\dot{X}_i X_i^{-1} = \Omega_i + \frac{K}{2N} \sum_{j=1}^{N} \left[X_j X_i^{-1} - X_i X_j^{-1} \right]. \tag{1.6}$$

Ha et al. [26] also introduced a measure of synchronisation for general Lie groups, called the ensemble diameter, used to analyse the long-time behaviour, and proved global existence of solutions and emergence of phase-locked states i.e. synchronisation, for identical and nonidentical oscillators for some bounded set of initial conditions and sufficiently large coupling strength.

1.2 Aims and Methods

The general aim of this project is to investigate synchronisation properties of complex dynamical systems on certain non-compact manifolds. There have been intensive research efforts devoted to network systems defined on the unit circle, mainly the Kuramoto model and its many extensions, and necessary conditions which lead to synchronisation have been established and studied in depth. Comparatively little work has been carried out, however, for systems defined on non-compact manifolds, such as those which show relativistic symmetry, where the symmetry group could be the non-compact group $SO(1,1)$ or $SO(1,2)$. The specific aims of this thesis are:

- firstly, to study low-dimensional systems such as non-compact versions of the Kuramoto model defined on the non-compact groups $SO(1,1)$ and $SO(1,2)$ both analytically and numerically, and determine whether synchronisation occurs under special conditions, such as for restricted initial values and for different coupling constants, and how synchronisation can be measured for such examples. Both the vector and matrix models will be investigated for the $SO(1,1)$ system while the main focus for the $SO(1,2)$ system will be the vector model.

- The second aim is to investigate why some solutions to the non-compact Kuramoto models exist only locally, and how local existence can be extended to global existence.

- The third aim is to understand these systems physically, in terms of relativistic mechanics.

Some specific research questions that will be addressed include: How do we detect the onset of synchronisation for non-compact systems, and measure the degree of synchronisation when it occurs? Are there non-compact systems in which synchronisation occurs for all initial values? Do solutions exist globally for any given model, and if not, does this depend on the initial values? Why, in some cases, does local existence only hold, and can we then modify the model to avoid solution blow-ups? Does the synchronisation behaviour depend on the local dynamics at each node of the network, or is the asymptotic behaviour independent of the specific local dynamics?

To answer these questions, we apply Equations (1.6) to the non-compact group $SO(1,1)$, and study solutions and properties of the resulting equations of motion analytically where possible. We then confirm the analytic results numerically and perform numerical simulations to study the $SO(1,1)$ system in more depth, using a fourth-order Runge-Kutta algorithm with variable step-size via Matlab's inbuilt ode45 function. The vector model is then applied to 2-vectors constrained to motion on a hyperbola and is used to gain physical insight into the $SO(1,1)$ matrix model, as the vector model resulted in the same equations of motion. We then apply the vector model to 3-vectors constrained to a hyperboloid of one sheet, and study the resulting equations both analytically and numerically.

The rest of this thesis is organised as follows: In chapter 2 we formulate a hyperbolic form of the Kuramoto model by choosing the non-compact group $SO(1,1)$ as the symmetry group for equations (1.6). We then describe the emergent dynamical properties of the hyperbolic model, such as synchronisation and unbounded and singular trajectories using exact solutions for $N = 2$ particles. We also describe general transformation properties of $SO(1,n)$ models. Chapter 3 contains a numerical study of the $SO(1,1)$ model for $N > 2$, and compares the results to the ordinary Kuramoto system. Chapter 4 describes the hyperbolic vector model in $1+1$ dimensions and its physical interpretation in terms of relativistic particle dynamics. Chapter five extends the study of synchronisation on non-compact manifolds to higher dimensions with the vector hyperboloid model with $SO(1,2)$ symmetry. This chapter includes an analytical and numerical study of the resulting equations of motion. The final chapter summarises the work contained in this thesis and suggests possible future research directions.

Chapter 2

The Hyperbolic Kuramoto model

In this chapter we apply the equations (1.6) to the non-compact group $SO(1,1)$ to formulate a hyperbolic form of the Kuramoto model. We then define what is meant by synchronisation for this model and show analytically that for $N = 2$, the system synchronises for any positive coupling, while for negative coupling it blows apart very rapidly, resulting in trajectories which become singular at some finite time. We also describe some general transformation properties of models defined on the non-compact groups $SO(1,n)$ and introduce quantitative measures of synchronisation for the hyperbolic Kuramoto model.

2.1 Example on the Compact Group $SO(2)$

The elements of the Special Orthogonal Group $SO(n)$ are given by the $n \times n$ rotation matrices R_i with the properties $R_i^T R_i = R_i R_i^T = I_n$, $R_i^T = R_i^{-1}$, and $\det R_i = 1$. Let Ω_i be $n \times n$ antisymmetric matrices for $i = 1, \ldots, N$ and note the matrices Ω_i are proportional to the generators of $SO(n)$ (i.e. they span the Lie Algebra $\mathfrak{so}_n$) and their eigenvalues are the natural frequencies of the i^{th} oscillator. For general elements R_i of the group we have the following system of equations, similar to (1.5), for more details see [23]:

$$\dot{R}_i R_i^T = \Omega_i - \frac{K}{2N} \sum_{j=1}^{N} \left(R_i R_j^T - R_j R_i^T \right). \tag{2.1}$$

The ordinary Kuramoto Model (1.1) can be considered as a special case of (2.1), namely for the rotation group $SO(2)$ whose elements are given by:

$$R_i = \begin{pmatrix} \cos\theta_i & \sin\theta_i \\ -\sin\theta_i & \cos\theta_i \end{pmatrix}$$

for angles θ_i. By choosing $\Omega_i = \begin{pmatrix} 0 & \omega_i \\ -\omega_i & 0 \end{pmatrix} \in \mathfrak{so}_2$ we regain the Kuramoto Model.

2.2 The $SO(1,1)$ Hyperbolic Kuramoto model

In [26], Ha et al. proposed a generalisation of the Kuramoto model to general matrix Lie Groups $\mathbb{G}$, where the phase of each particle is considered to be an element X_i of the group $\mathbb{G}$ and the synchronous behaviour among the group elements is described by the equations:

$$\dot{X}_i X_i^{-1} = \Omega_i + \frac{K}{2N} \sum_{j=1}^{N} \left[X_j X_i^{-1} - X_i X_j^{-1} \right]. \tag{2.2}$$

To make sure the solutions $X_i(t)$ stay on the group $\mathbb{G}$, the RHS of the above equations must be in $\mathfrak{g}$, the Lie Algebra associated with $\mathbb{G}$. Note that for the compact group $SO(n)$, we have $X_i^{-1} = X_i^T$ and we recover (2.1). The equations of motion (1.6) apply for any Matrix Lie group $\mathbb{G}$. By choosing the non-compact group $SO(1,1)$, which can be interpreted as the hyperbolic rotations just as $SO(2)$ represents circular rotations, we have:

$$X_i = \begin{pmatrix} \cosh \alpha_i & \sinh \alpha_i \\ \sinh \alpha_i & \cosh \alpha_i \end{pmatrix}$$

for arbitrary parameter $\alpha_i(t)$ and we choose:

$$\Omega_i = \begin{pmatrix} 0 & \omega_i \\ \omega_i & 0 \end{pmatrix}$$

such that $\Omega_i \in \mathfrak{so}(1,1)$, i.e. Ω_i satisfies $\Omega_i^T G + G\Omega_i = 0$, where $G = \begin{pmatrix} 1 & 0 \\ 0 & -1 \end{pmatrix}$ is the metric, which is used to define the scalar product of two vectors in this hyperbolic space and hence defines the notion of a distance or interval, and also defines the matrix inverse X_i^{-1}. The inverse X_i^{-1} is given by $GX_i^T G$. Hence (1.6) becomes:

$$\dot{X}_i G X_i^T G = \Omega_i + \frac{K}{2N} \sum_{j=1}^{N} \left[X_j G X_i^T G - X_i G X_j^T G \right]. \tag{2.3}$$

The LHS of (2.3) is:

$$\begin{aligned}\dot{X}_i G X_i^T G &= \dot{\alpha}_i \begin{pmatrix} \sinh\alpha_i & \cosh\alpha_i \\ \cosh\alpha_i & \sinh\alpha_i \end{pmatrix} \begin{pmatrix} \cosh\alpha_i & -\sinh\alpha_i \\ -\sinh\alpha_i & \cosh\alpha_i \end{pmatrix} \\ &= \dot{\alpha}_i \begin{pmatrix} 0 & 1 \\ 1 & 0 \end{pmatrix}\end{aligned}$$

and the term in the sum is:

$$\begin{aligned}&X_j G X_i^T G - X_i G X_j^T G = \\ &\begin{pmatrix} \cosh\alpha_j & \sinh\alpha_j \\ \sinh\alpha_j & \cosh\alpha_j \end{pmatrix} \begin{pmatrix} \cosh\alpha_i & -\sinh\alpha_i \\ -\sinh\alpha_i & \cosh\alpha_i \end{pmatrix} \\ &\qquad - \begin{pmatrix} \cosh\alpha_i & \sinh\alpha_i \\ \sinh\alpha_i & \cosh\alpha_i \end{pmatrix} \begin{pmatrix} \cosh\alpha_j & -\sinh\alpha_j \\ -\sinh\alpha_j & \cosh\alpha_j \end{pmatrix} \\ &\qquad = 2 \begin{pmatrix} 0 & -\sinh(\alpha_i - \alpha_j) \\ -\sinh(\alpha_i - \alpha_j) & 0 \end{pmatrix}.\end{aligned}$$

Putting the LHS and RHS together gives us:

$$\dot{\alpha}_i \begin{pmatrix} 0 & 1 \\ 1 & 0 \end{pmatrix} = \begin{pmatrix} 0 & \omega_i \\ \omega_i & 0 \end{pmatrix} + \frac{K}{2N} \sum_{j=1}^{N} 2 \begin{pmatrix} 0 & -\sinh(\alpha_i - \alpha_j) \\ -\sinh(\alpha_i - \alpha_j) & 0 \end{pmatrix}.$$

Hence we arrive at the following result,

$$\dot{\alpha}_i = \omega_i + \frac{K}{N} \sum_{j=1}^{N} \sinh(\alpha_j - \alpha_i) \tag{2.4}$$

which is a hyperbolic form of the regular Kuramoto model (1.1). Note that this is very similar to the Kuramoto model, except that the trigonometric term has been replaced by a hyperbolic term.

2.3 Properties of the Hyperbolic model

2.3.1 Definition of Synchronisation

In the Kuramoto model, synchronised, or phase-locked states were travelling-wave solutions with constant frequency ω_{av} [26]:

$$\theta_i(t) = \theta_i^{\infty} + \omega_{av} t. \tag{2.5}$$

As in the Kuramoto model, synchronisation in the hyperbolic model means that solutions to (2.4) take the linear asymptotic form (this is explicitly shown for a 2 particle system in 2.3.2):

$$\alpha_i(t) = \alpha_i^\infty + \omega_{av} t \tag{2.6}$$

where α_i^∞ is a constant determined by the initial conditions and the parameters of the system and $\omega_{av} = \frac{1}{N}\sum_{i=1}^{N} \omega_i$. To show that ω_{av} is the mean of the driving terms ω_i, we substitute the asymptotic solutions (2.6) into the hyperbolic model (2.4) and sum over the indices i:

$$\omega_{av} = \omega_i + \frac{K}{N}\sum_{j=1}^{N} \sinh(\alpha_j^\infty - \alpha_i^\infty)$$

$$\sum_{i=1}^{N} \omega_{av} = \sum_{i=1}^{N} \omega_i + \frac{K}{N}\sum_{i,j=1}^{N} \sinh(\alpha_j^\infty - \alpha_i^\infty).$$

The sum over i and j vanishes by antisymmetry and we are left with:

$$\omega_{av} = \frac{1}{N}\sum_{i=1}^{N} \omega_i. \tag{2.7}$$

Hence the usual notion of synchronisation remains essentially the same when the KM is extended to the non-compact group $SO(1,1)$, with the caveat that the synchronised solutions cannot be described as travelling-wave solutions, since ω_{av} is no longer a rotational frequency. In terms of the matrices $X_i(t)$, which are solutions to (2.3) and are elements of the group $SO(1,1)$, the system is considered to be in a phase-locked (synchronised) state if the quantity $X_i(t)X_j^{-1}(t)$ approaches a constant value for all i, j [26] (Definition 2.3), which is equivalent to stating that the quantity $\alpha_i(t) - \alpha_j(t)$ approaches a constant in the limit $t \to \infty$ for all i, j. Hence provided that $\alpha_i(t) - \alpha_j(t)$ approaches a constant value for all pairs of i and j, which can be ensured by suitably restricting the initial conditions (as will be made evident from the form of the solutions in the following section), the sinh function will not diverge, and synchronisation will be possible.

2.3.2 Formation of synchronised states for N=2

To understand the formation of synchronised states, we can analytically solve (2.4) for the simple $N = 2$ case. For two nodes, with identical $\omega_i = \omega$ and positive

(attractive) interaction term, the equations (2.4) reduce to:

$$\dot{\alpha}_1 = \omega + \frac{K}{2}\sinh(\alpha_2 - \alpha_1)$$
$$\dot{\alpha}_2 = \omega - \frac{K}{2}\sinh(\alpha_2 - \alpha_1).$$

Subtracting $\dot{\alpha}_2$ from $\dot{\alpha}_1$ and defining a new variable α gives:

$$\begin{aligned}\Rightarrow \dot{\alpha} &\equiv \dot{\alpha}_1 - \dot{\alpha}_2 \\ &= K\sinh(\alpha_2 - \alpha_1) = -K\sinh(\alpha).\end{aligned}$$

The solution to this non-linear O.D.E is:

$$\alpha(t) = 2\tanh^{-1}(ce^{-Kt}) \tag{2.8}$$

where the constant c is determined by the initial condition $\alpha(0) = \alpha^0 = 2\tanh^{-1}(c)$ i.e. $c = \tanh\left(\frac{\alpha^0}{2}\right)$ where $\alpha^0 = \alpha_1(0) - \alpha_2(0)$. This solution only tracks the separation of the nodes over time, but if we define a new variable ρ such that $\dot{\rho} \equiv \dot{\alpha}_1 + \dot{\alpha}_2$, then our equation for $\dot{\rho}$ becomes:

$$\begin{aligned}\dot{\rho} &= \dot{\alpha}_1 + \dot{\alpha}_2 = 2\omega \\ \Rightarrow \rho(t) &= \rho^0 + 2\omega t\end{aligned} \tag{2.9}$$

where $\rho^0 = \alpha_1(0) + \alpha_2(0)$. Now we add (2.8) and (2.9) to get:

$$\begin{aligned}\alpha(t) + \rho(t) &= 2\tanh^{-1}\left(ce^{-Kt}\right) + \rho^0 + 2\omega t \\ &= (\alpha_1 - \alpha_2) + (\alpha_1 + \alpha_2) \\ &= 2\alpha_1(t).\end{aligned}$$

Hence the synchronisation solutions for α_1 and α_2 are:

$$\alpha_1(t) = \tanh^{-1}\left(ce^{-Kt}\right) + \frac{\rho^0}{2} + \omega t \tag{2.10}$$

$$\alpha_2(t) = -\tanh^{-1}\left(ce^{-Kt}\right) + \frac{\rho^0}{2} + \omega t \tag{2.11}$$

which are finite for all $t \geq 0$ and which, for $t \to \infty$, converge to the same straight line (See Figure 2.1a). This is also shown by the fact that the separation of the nodes $\alpha(t) \to 0$ as $t \to \infty$. More generally, we can consider the case when each node has a different ω_i, i.e. we have the two differential equations:

$$\dot{\alpha}_1 = \omega_1 - \frac{K}{2}\sinh(\alpha_1 - \alpha_2)$$
$$\dot{\alpha}_2 = \omega_2 + \frac{K}{2}\sinh(\alpha_1 - \alpha_2).$$

As before, we will define α as the difference between α_1 and α_2, and also define $\omega = |\omega_1 - \omega_2|$.

$$\begin{aligned} \Rightarrow \dot{\alpha} &\equiv \dot{\alpha}_1 - \dot{\alpha}_2 \\ &= \omega - K\sinh(\alpha). \end{aligned}$$

The solution to this non-linear O.D.E is obtained using [27]:

$$\alpha(t) = 2\tanh^{-1}\left(\frac{\mathcal{M}\tanh\left(\frac{\mathcal{M}}{2}(t-c)\right) - K}{\omega}\right) \tag{2.12}$$

where $\mathcal{M} = \sqrt{\omega^2 + K^2}$ and c is an integration constant given by the initial condition $\alpha(0)$. Note that this function is only real when the argument of the inverse hyperbolic tangent is between -1 and 1. This solution restricts the possible initial conditions $\alpha_0 = \alpha(t = 0)$. At $t = 0$ we have, using $\tanh(-\mathcal{M}c/2) < 1$

$$\begin{aligned} \omega\tanh\left(\frac{\alpha_0}{2}\right) &< \mathcal{M} - K \\ \omega\tanh\left(\frac{\alpha_0}{2}\right) &< \sqrt{\omega^2 + K^2} - K \end{aligned}$$

Hence

$$\frac{\omega}{|\omega|}\tanh\left(\frac{\alpha_0}{2}\right) < \sqrt{1 + \frac{K^2}{\omega^2}} - \frac{K}{|\omega|} \tag{2.13}$$

For positive K the RHS of (2.13) is less than one, hence the initial value α_0 cannot be arbitrarily large and positive. The above equation (2.12) for the difference between the two nodes has a similar form to the global phase difference between the centroids of two competing oscillator networks in a variation of the Kuramoto model [28] (Equation 21), the difference being that in (2.12) the separation is an inverse hyperbolic tangent function whereas in [28] the phase difference is an inverse tangent. As $t \to \infty$, the separation $\alpha(t)$ approaches a constant value (See Figure 2.1c), given by:

$$\lim_{t\to\infty}\alpha(t) = \alpha^{\infty} = 2\tanh^{-1}\left(\frac{\mathcal{M} - K}{\omega}\right).$$

Solving for α_1 and α_2 explicitly as above for identical nodes, we find:

$$\begin{aligned} \alpha_1(t) &= \frac{\alpha(t) + \rho(t)}{2} \\ \alpha_2(t) &= \frac{\rho(t) - \alpha(t)}{2} \end{aligned}$$

where $\rho(t) = (\omega_1 + \omega_2)t + \alpha_1(0) + \alpha_2(0)$. In the limit $t \to \infty$:

$$\alpha_1(t) = \frac{\alpha^\infty + \rho(t)}{2} \tag{2.14}$$

$$\alpha_2(t) = \frac{\rho(t) - \alpha^\infty}{2}. \tag{2.15}$$

This shows that α_1 and α_2 asymptotically trace out parallel straight lines separated by α^∞. To summarise, nodes with identical ω_i will converge to a single trajectory, while those with non-identical ω_i will follow parallel lines.

2.3.3 Unbounded trajectories and singularities

An interesting property of the hyperbolic equations, which is not present in the ordinary Kuramoto model, is that due to the hyperbolic nature of the interaction term, there is a possibility for unbounded trajectories, i.e. the particles will accelerate along their hyperbolic world-line towards infinity, as well as solutions which blow up/develop singularities in finite time. If $\alpha_j - \alpha_i$ becomes small as the system evolves (in the case of complete synchronisation $\alpha_j - \alpha_i \to 0 \quad \forall \quad i, j$), then the derivatives $\dot{\alpha}_i$ remain reasonably small, and the system is well behaved. If $\alpha_j - \alpha_i$ becomes large, then the derivatives become very large. This creates a positive feedback loop, which causes the system to explode apart very rapidly. This occurs whenever the interaction term is negative. Note that $N = 2$ is a special case where it is possible to have 1 negative coupling constant, and still have well-defined solutions for all time. These solutions neither blow up nor converge to the same line (i.e. perfect synchronisation), but are parallel for all time. this can be seen by reversing the sign of one of the interaction terms in the 2 equations of motion, resulting in $\dot{\alpha}_1 = \dot{\alpha}_2$. If we now reverse the sign of the interaction in (2.4), which is equivalent to introducing a repulsive interaction ($K < 0$), the equation for the separation of the two nodes becomes:

$$\begin{aligned} \Rightarrow \dot{\alpha} &\equiv \dot{\alpha}_1 - \dot{\alpha}_2 \\ &= -K \sinh(\alpha_2 - \alpha_1) = K \sinh(\alpha) \end{aligned}$$

whose solution is given by

$$\alpha(t) = 2 \tanh^{-1}(ce^{Kt}).$$

This solution $\alpha(t)$ is singular/undefined when the argument of the inverse hyperbolic tangent ce^{Kt} is equal to 1, where $c = \tanh\left(\frac{\alpha^0}{2}\right)$. By setting $ce^{Kt} = 1$ we can

calculate when the solution becomes singular:

$$\begin{aligned}\tanh\left(\frac{\alpha^0}{2}\right)e^{Kt} &= 1\\ \Rightarrow e^{Kt} &= \frac{1}{\tanh\left(\frac{\alpha^0}{2}\right)}\\ \Rightarrow Kt &= \log\left(\frac{1}{\tanh\left(\frac{\alpha^0}{2}\right)}\right).\end{aligned}$$

Hence in the case of $N = 2$ nodes, the separation of the nodes $\alpha(t)$ will blow up at time t given by:

$$t = \frac{1}{K}\log\left(\frac{1}{\tanh\left(\frac{\alpha^0}{2}\right)}\right).$$

By defining ρ as before, we can solve explicitly for $\alpha_1(t)$ and $\alpha_2(t)$:

$$\alpha_1(t) = \tanh^{-1}\left(ce^{Kt}\right) + \frac{\rho^0}{2} + \omega t \tag{2.16}$$

$$\alpha_2(t) = -\tanh^{-1}\left(ce^{Kt}\right) + \frac{\rho^0}{2} + \omega t \tag{2.17}$$

which diverge towards $+\infty$ and $-\infty$ for α_1 and α_2 respectively. These solutions are (unsurprisingly) the same as for the attractive coupling case, except the sign in the exponential has changed. This hyperbolic divergence/singularity is illustrated in Figure 2.1b.

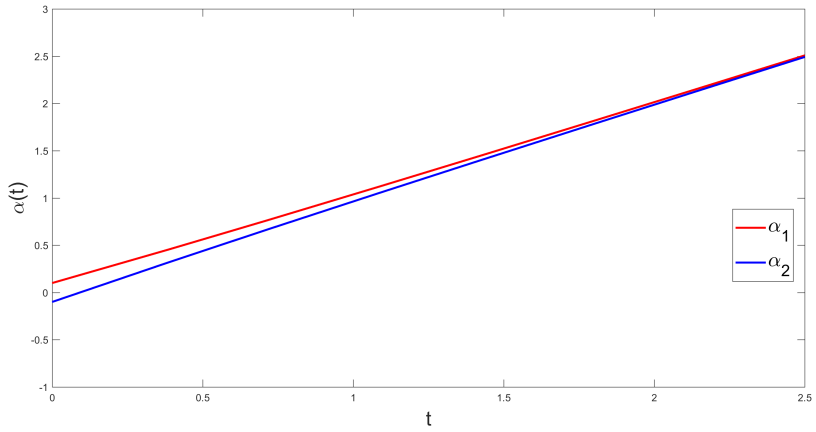

(a) Synchronisation of 2 nodes with identical $\omega_i = 1$ and initial conditions $\alpha_1(0) = 0.1 = -\alpha_2(0)$ and coupling $K = 1$

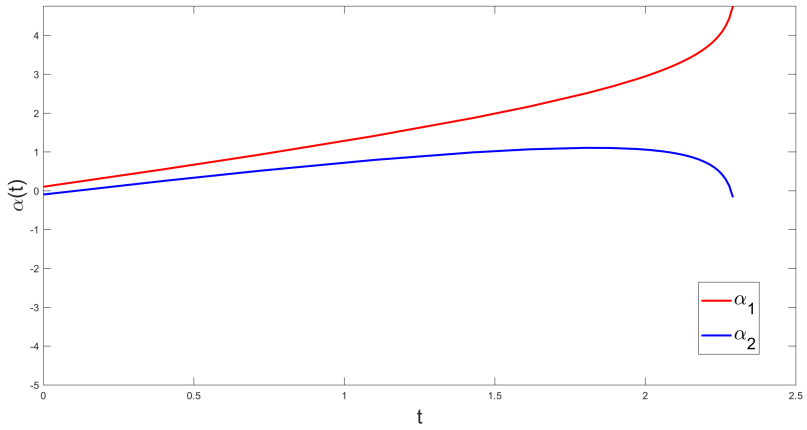

(b) Emergence of hyperbolic singularities for 2 nodes with identical $\omega_i = 1$, initial conditions $\alpha_1(0) = 0.1 = -\alpha_2(0)$ and $K = -1$. The Singularity occurs at $t \approx 2.3059$.

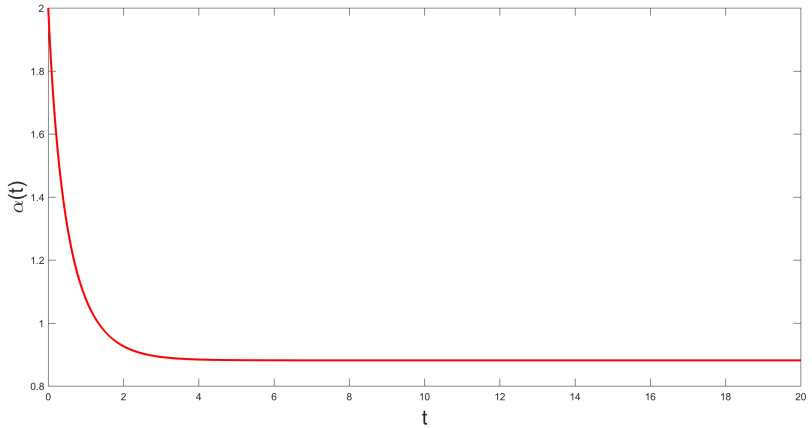

(c) The separation $\alpha(t)$ of 2 nodes with non-identical ω_i ($\omega_1 = 1$, $\omega_2 = 2$) and initial conditions $\alpha_1(0) = 1 = -\alpha_2(0)$. The separation reaches a constant value given of $\alpha_\infty \approx 0.88138$

Figure 2.1: Comparison of the synchronisation and blow-up of solutions for $N = 2$ nodes.

2.3.4 Lorentz Transformations

We can also consider the symmetries of Equations (2.3) and (2.4). Recall (2.3):

$$\dot{X}_i G X_i^T G = \Omega_i + \frac{K}{2N} \sum_{j=1}^{N} \left[X_j G X_i^T G - X_i G X_j^T G \right].$$

Now we transform $X_i \to \Lambda X_i$, where $\Lambda \in SO(n,1)$ is a matrix of constants satisfying $\Lambda^T G \Lambda = G$ and $G\Lambda G \Lambda^T = I$, where G is the metric $diag(1,-1)$ i.e. Λ is a Lorentz matrix. The L.H.S transforms as:

$$\begin{aligned} \dot{X}_i X_i^{-1} &= \dot{X}_i G X_i^T G \\ &\to (\Lambda \dot{X}_i) G (\Lambda X_i)^T G \\ &= \Lambda \dot{X}_i G X_i^T \Lambda^T G. \end{aligned}$$

Now insert the identity $G\Lambda G\Lambda^T = I$:

$$\begin{aligned} &= \Lambda \dot{X}_i G X_i^T G \Lambda G \Lambda^T \Lambda^T G \\ &= \Lambda \dot{X}_i (G X_i^T G)(\Lambda G \Lambda^T) \Lambda^T G \\ &= \Lambda \dot{X}_i (G X_i^T G)(G \Lambda^T G) \\ &= \Lambda \dot{X}_i X_i^{-1} \Lambda^{-1}. \end{aligned}$$

The summation clearly transforms in the same way. So we have the following:

$$\Lambda \dot{X}_i X_i^{-1} \Lambda^{-1} = \Omega_i + \frac{K}{2N} \sum_{j=1}^{N} \left[\Lambda X_j X_i^{-1} \Lambda^{-1} - \Lambda X_i X_j^{-1} \Lambda^{-1} \right].$$

We can rewrite this by left multiplying by Λ^{-1} and right multiplying by Λ:

$$\Rightarrow \dot{X}_i X_i^{-1} = \Lambda^{-1} \Omega_i \Lambda + \frac{K}{2N} \sum_{j=1}^{N} \left[X_j X_i^{-1} - \ X_i X_j^{-1} \right].$$

Since $\Omega_i \in \mathfrak{so}(1,\mathfrak{n})$ and by a property of Lie algebras, $\Lambda^{-1}\Omega_i\Lambda \in \mathfrak{so}(1,\mathfrak{n}) \quad \forall \quad \Lambda \in SO(1,n)$ [29]. So the equations transform covariantly under general $SO(1,n)$ transformations. In the case of the Lorentz group in one spatial dimension $SO(1,1)$, $\Lambda^{-1}\Omega_i\Lambda = \Omega_i$, since the group is abelian. Hence the equations (2.3) are invariant under $SO(1,1)$ Lorentz transformations i.e. they are unchanged under a change in inertial reference frame. Note we could have transformed $X \to \Lambda X \Lambda^{-1}$ (i.e. a

similarity transformation) and arrived at the same answer.
In terms of the α_i's, (2.4) transforms under a hyperbolic rotation of the form $\alpha_i \to \alpha_i + \alpha_0$ where α_0 is an arbitrary constant. Hence $\dot{\alpha_i}$ is unchanged. The term in the sum is also left unchanged. Hence (2.4) is invariant under hyperbolic rotations/Lorentz boosts.

2.4 Measures of Synchronisation

One of the most commonly used synchronisation measures for the Kuramoto model is the order parameter $R(t)$ given by (1.4). This is a very convenient measure for the Kuramoto model, taking values between zero and one. The main disadvantage of this parameter is that it is only suitable for systems defined on the unit circle i.e. the Kuramoto model, and is meaningless for systems defined on non-compact manifolds. As in the Kuramoto model, there are several order parameters one can employ to analyse the long-term behaviour and quantify the 'order' of the synchronised state. In this section we describe and compare a range of order parameters in order to quantify the long-term synchronisation behaviour of (2.4). One such measure is the 'Ensemble Diameter' $D(\mathcal{X}(t))$, defined in [26], which is a basic Lyapunov function for the stability of the phase locked state:

$$D(\mathcal{X}(t)) \coloneqq \max_{1\leq i,j\leq N} \|X_i(t)X_j^{-1}(t) - I_d\| \tag{2.18}$$

where $\mathcal{X}(t) := \{X_1(t), \ldots, X_N(t)\}$, $X_i(t) \in SO(1,1)$ are the matrices $\begin{pmatrix} \cosh\alpha_i & \sinh\alpha_i \\ \sinh\alpha_i & \cosh\alpha_i \end{pmatrix}$ with determinant 1, I_d is the $d \times d$ Identity matrix and the inverse $X_i^{-1}(t)$ is given by $GX_i^{\dagger}G$, where G is the metric $G = diag(1,-1)$. $\|A\|$ is the Frobenius norm for $d \times d$ complex matrices $A = (a_{ij})$:

$$\|A\| = \left[\sum_{i,j=1}^{d} |a_{ij}|^2\right]^2 = \left[tr(AA^{\dagger})\right]^{\frac{1}{2}}.$$

If $\omega_i = 0 \quad \forall \quad i$, then the diameter decreases exponentially to zero (See Figure 2.2), in agreement with [26] (section 4.2). If the parameters ω_i are distributed then the diameters often drop before increasing and finally settling to some value, rather than simply decreasing exponentially. This drop corresponds to the point where the nodes are closest together, i.e. when they cluster before crossing-over during the initial transient period. This is illustrated in Figure 2.3.

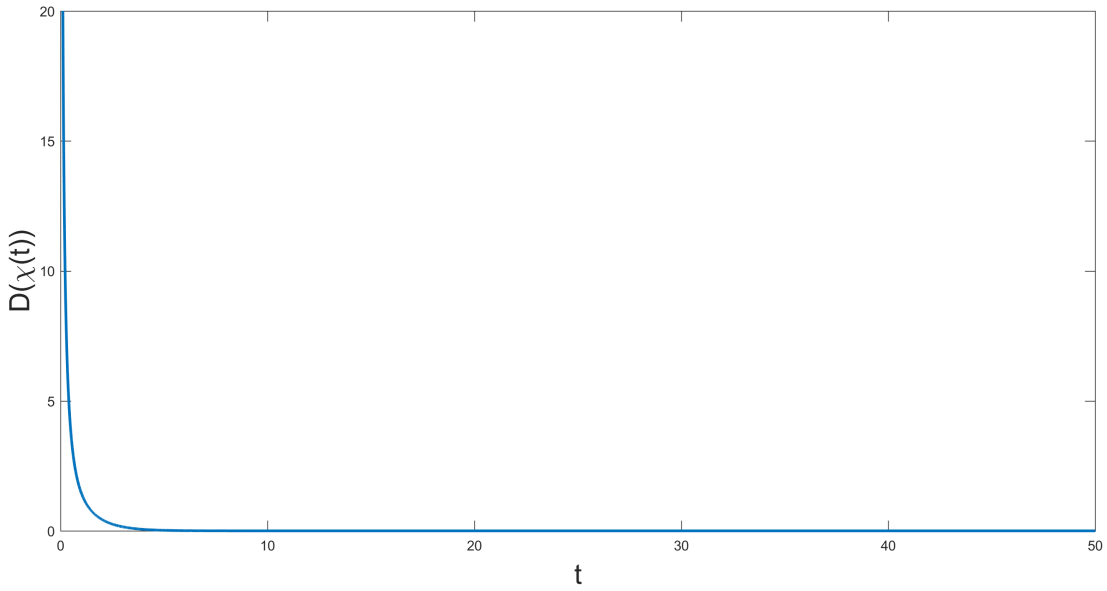

Figure 2.2: The Ensemble Diameter approaches 0 when $\omega_i = 0 \quad \forall \quad i$ with random initial conditions, in agreement with [26].

Another measure of synchronisation is the so-called disorder parameter $r(t)$ which measures the average deviation of the nodes from their mean trajectory:

$$r(t) \coloneqq \frac{1}{N} \sum_{i=1}^{N} \|\alpha_i(t) - \alpha_{cm}(t)\| \tag{2.19}$$

where $\alpha_{cm}(t) = \frac{1}{N} \sum_{i=1}^{N} \alpha_i(t)$ is the 'centre-of-mass' point of the nodes at time t. $r(t)$ is termed a 'disorder' parameter since it is small for trajectories which are closely correlated and large for widely separated trajectories. At synchronisation this parameter will reach a constant value. $r = 0$ means the system is completely synchronised.

The hyperbolic phase-difference $P(t)$ is a very simple measure of the separation between the hyperbolic angles α_i and is analogous to the phase-difference used in [30,31] for the ordinary Kuramoto model. Phase synchronisation occurs if $P(t)$ goes to a constant for large times. Complete synchronisation occurs if $P(t) \to 0$ for large times. $P(t)$ is given by:

$$P(t) \coloneqq \max_{1 \leq i,j \leq N} |\alpha_j - \alpha_i|. \tag{2.20}$$

Another way to quantify the synchronisation of the systems is the order parameter $\xi(t)$, given by:

$$\xi(t) = \frac{1}{N} e^{-\omega_{av} t} \sum_{i=1}^{N} e^{\alpha_i(t)} \tag{2.21}$$

where ω_{av} is the mean of the ω_i. If partial synchronisation occurs, then $\xi(t) \to \frac{1}{N}\sum_{i=1}^{N} e^{\alpha_i^0}$, i.e. ξ approaches a constant value which is greater than unity. A value of $\xi = 1$ represents complete synchronisation. This is because complete synchronisation implies that all the trajectories α_i are asymptotically the same i.e.

$$\begin{aligned} \sum_{i=1}^{N} e^{\alpha_i(t)} &= N e^{\alpha(t)} \\ \Rightarrow \xi(t) &= \frac{1}{N} e^{-\omega_{av} t} N e^{\alpha(t)} \\ &= 1 \end{aligned}$$

since synchronised solutions are given by (2.6) and for complete synchronisation the asymptotic separations α_i^{∞} vanish.

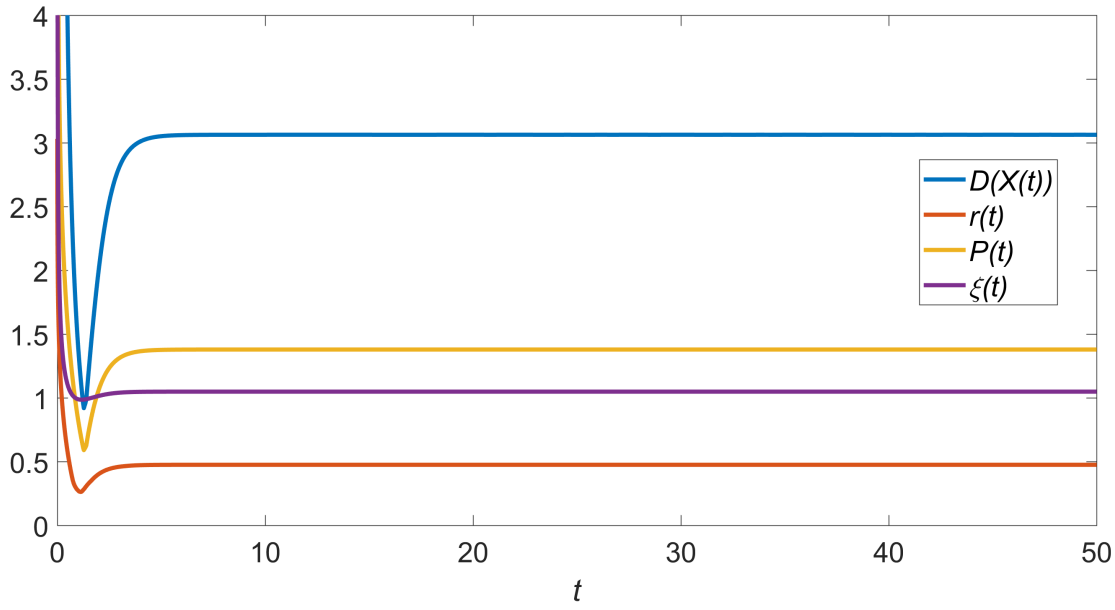

Figure 2.3: The Order parameters $D\left(X(t)\right)$, $r(t)$, $P(t)$ and $\xi(t)$ given random initial conditions and random ω_i. All of these synchronisation measures level out to a constant value at approximately the same time t. The transient behaviour at early times is also similar for each parameter.

Chapter 3

Numerical Results

In this section, we investigate properties of the hyperbolic Kuramoto model numerically and compare to those of the ordinary Kuramoto model. We also provide analytic explanations of the numerical results where possible. Numerical simulations were performed on a Dell XPS 13 laptop with an Intel i7-6500U processor. The equations (2.4) are solved for a system of $N = 20$ nodes with MATLAB's inbuilt ode45 function, which uses a 4^{th}-order Runge-Kutte algorithm with adaptive step-size. The initial conditions $\alpha_i(0)$ are randomly chosen from the uniform distribution on the interval [-3,3]. The ω_i's are similarly chosen at random from the interval [-1,1]. Unit coupling constant was used in §3.2 and §3.3. Solutions to the Kuramoto equations asymptotically tend towards:

$$\theta_i(t) = \theta_i^{\infty} + \Omega t$$

where Ω is the mean of the natural frequencies ω_i (this can be shown using the same method as in §2.3) and θ_i^{∞} is a constant. This asymptotic behaviour is also observed in the hyperbolic model (See Figure 3.1), with the caveat that the ω_i can no longer be interpreted as frequencies.

3.1 Coupling Constant

3.1.1 Critical Coupling

An important feature of the Kuramoto model is that there is a critical coupling constant, below which the oscillators do not synchronise [21]. By substituting the

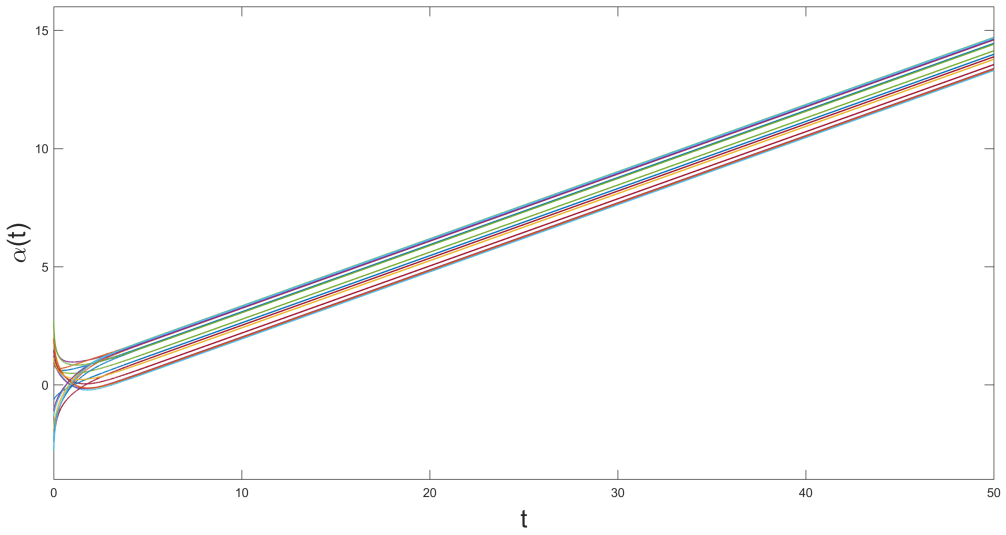

Figure 3.1: Synchronisation solutions $\alpha_i(t)$ given random initial conditions and random ω_i. At synchronisation, all the trajectories have the same slope given by the mean of the ω_i's.

synchronisation solutions into the Kuramoto equations we obtain the equations:

$$\Omega - \omega_i = \frac{K}{N} \sum_{j=1}^{N} \sin(\theta_j^\infty - \theta_i^\infty).$$

Now using the triangle inequality and the boundedness of $\sin(\theta_j^\infty - \theta_i^\infty)$, we can obtain an estimate on the critical coupling:

$$\begin{aligned} |\Omega - \omega_i| &\leq \frac{K}{N} \sum_{j=1}^{N} |\sin(\theta_j^\infty - \theta_i^\infty)| \\ &\leq \frac{K}{N} \sum_{j=1}^{N} 1 = K \end{aligned}$$

i.e. in order for synchronisation to occur, we require:

$$K \geq \max_{1 \leq i \leq N} |\Omega - \omega_i|.$$

In contrast to the regular Kuramoto model, there is no critical coupling K_C for the hyperbolic Kuramoto model i.e. there is no coupling constant K_C below which the system does not synchronise with each particle moving with its own ω. K just changes how tightly particles cluster and effectively acts to scale the interaction,

i.e. K changes the time scale over which the system synchronises. Increasing the initial spread of the α_i^0's increases the time it takes to cluster together. Even for very widely spread initial values, the nodes still eventually cluster. Having a different coupling K_i for each node i doesn't affect the dynamics, as long as all the K_i are positive.

3.1.2 Negative Coupling

Recall the hyperbolic Kuramoto model (2.4):

$$\dot{\alpha}_i = \omega_i + \frac{K}{N}\sum_{j=1}^{N}\sinh(\alpha_j - \alpha_i).$$

For $K > 0$, the interaction term acts as a restoring force, so as the system evolves, $\alpha_j - \alpha_i$ becomes small (in the case of complete synchronisation $\alpha_j - \alpha_i \to 0$), so that the rate of change of the α_i's become small so that the system is well behaved and the trajectories are asymptotically stable. If $K < 0$, then the interaction term acts as a repulsive force, so that as the system evolves, $\alpha_j - \alpha_i$ becomes large, hence the derivatives become large, effectively creating a feedback loop, which causes the trajectories to be unstable and the system to explode apart very rapidly, creating singularities at some finite time (See Figure 3.2). This phenomenon is called 'Lyapunov instability' [19, 32]. For a mathematical argument on the stability of solutions using Lyapunov functions see Appendix I, section IIIC.

It is worth noting that it is possible to have one (and only one) node with a negative coupling constant and have solutions which do not blow up, as long as said coupling constant is very small compared to the positive couplings. Any node with negative coupling constant will diverge from those with the positive coupling constants, as well as any others with a negative coupling constant. Those nodes with positive coupling constants will remain together.

This differs from the Kuramoto model, wherein there are three different types of long term behaviours. The first is the incoherent state, where the oscillators are completely desynchronised and scattered around the unit circle. The second is what is called a π-state, wherein the positively coupled oscillators (called conformists in the literature) converge to a partially synchronised state, as do the negatively coupled oscillators (called contrarians). The two clusters are stationary and are separated by π. The last is a more general form of the π-state where the conformists and contrarians again form two partially synchronised clusters, but which travel around the circle at constant speed, and are separated by some constant phase not equal to π. As the percentage of conformists increases, so does the level of synchronisation i.e. the order parameter approaches unity [33–35].

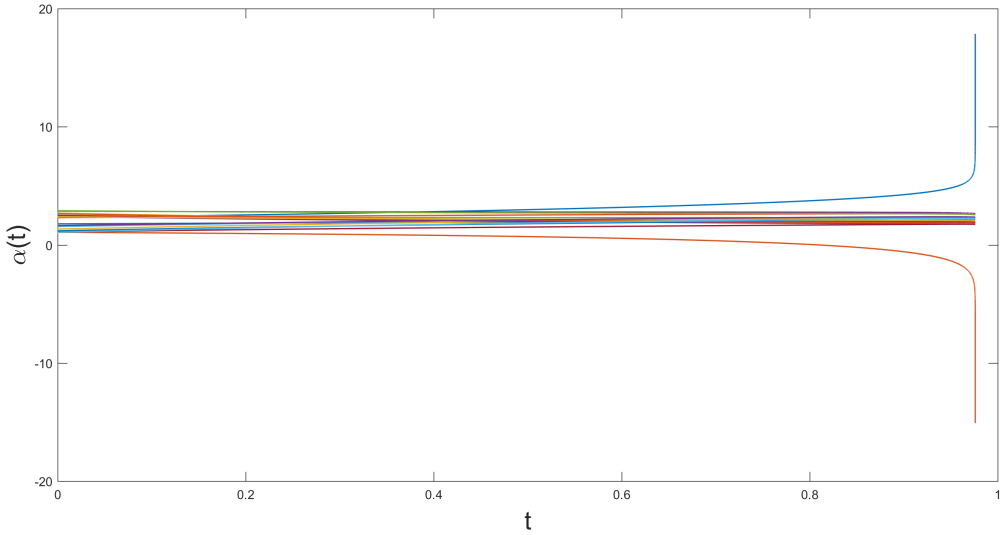

(a) Solution blow-up when 2 of the 20 nodes have negative coupling constants. The two nodes with negative coupling constant diverge from those with positive coupling constants, which cluster together. We have used initial conditions α_i^0 drawn randomly from the interval $[1, 3]$ and parameters ω_i drawn at random form the interval $[-1, 1]$.

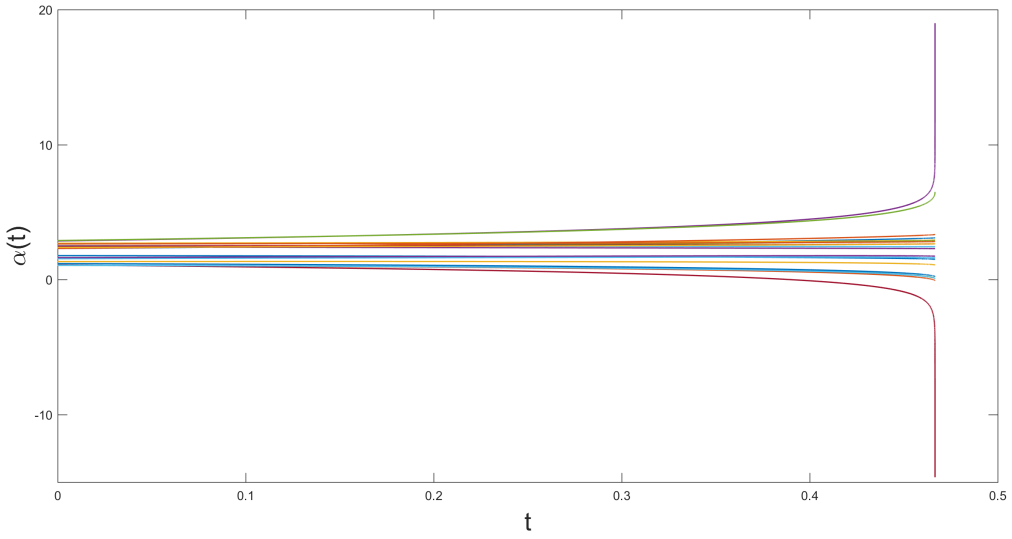

(b) Solution blow-up when all of the 20 nodes have negative coupling constants. We have used initial conditions α_i^0 drawn randomly from the interval $[1, 3]$ and parameters ω_i drawn at random form the interval $[-1, 1]$. Note how all the nodes are diverging from one another.

Figure 3.2: Solution blow-ups for 20 Nodes

3.2 Phase Lag

Phase lag parameters occur often in models of complex systems, for example in models of Josephson-junction arrays [36], and were first introduced in [37] as a way of modelling synchronised systems in which the synchronised frequency differed from the mean of the natural frequencies. Kuramoto models with phase lag take the form:

$$\dot{\theta}_i = \omega_i + \frac{K}{N}\sum_{j=1}^{N}\sin(\theta_j - \theta_i - \beta_i)$$

where β_i is the phase lag parameter. Phase lags (also called "frustrations") can be used to control the synchronised frequency of a system or to prevent synchronisation from occuring entirely [12, 15]. For example a phase lag of π is equivalent to have negative all-to-all coupling since $\sin(\theta - \pi) = -\sin\theta$, meaning synchronisation will not occur. For a synchronised system phase lag is equivalent to a time delayed coupling [12]. We will consider the following system of N equations,

$$\dot{\alpha}_i = \omega_i + \frac{K}{N}\sum_{j=1}^{N}\sinh(\alpha_j - \alpha_i - \beta_i) \tag{3.1}$$

where $\beta_i = \beta$ for each i is the (hyperbolic) phase lag angle. We find that the hyperbolic phase lag angle, as in the Kuramoto model, can be used to control the synchronisation frequency (which we call ω'_{av}) (Figure 3.3), but cannot prevent synchronisation from occurring entirely. This can be understood by looking at the interaction term of (3.1) in the synchronisation limit. As the system synchronises, $\alpha_j - \alpha_i \to 0 \quad \forall \quad i, j$ and $\omega_i \to \omega_{av} = \frac{1}{N}\sum_{i=1}^{N}\omega_i$:

$$\begin{aligned}
&\Rightarrow \frac{K}{N}\sum_{j=1}^{N}\sinh(\alpha_j - \alpha_i - \beta)\\
&\to \frac{K}{N}\sum_{j=1}^{N}\sinh(-\beta)\\
&= -\frac{K}{N}\sum_{j=1}^{N}\sinh(\beta).
\end{aligned}$$

Hence in the synchronisation limit,

$$\dot{\alpha}_i = \omega'_{av} = \omega_{av} - \frac{K}{N}\sum_{j=1}^{N}\sinh(\beta)$$

$$\Rightarrow \dot{\alpha}_i = \omega'_{av} = \omega_{av} - K\sinh(\beta). \tag{3.2}$$

So the synchronisation "frequency" ω'_{av} can be controlled by altering the lag parameter β, but since the hyperbolic sine function is unbounded, ω'_{av} can be decreased without limit, in contrast to the Kuramoto model.

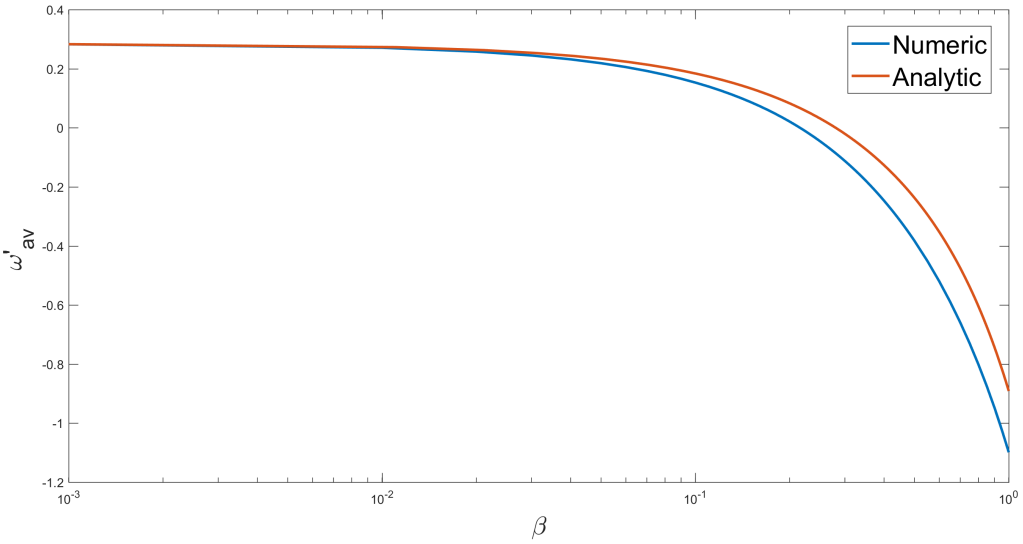

Figure 3.3: Effect of the Lag parameter β on the average slope ω'_{av} of the synchronised solutions. The analytic result (red) is that given by (3.2) which assumes perfect synchronisation. This is generally not the case, as shown by the blue curve.

3.3 External Fields

Another extension to the Kuramoto model is to add external fields, giving rise to richer dynamical behaviour. External fields (also known as "pinning") can model an external current applied to neurons or an oscillating current across Josephson junctions [4]. The equations describing the modified Kuramoto model then become:

$$\dot{\theta}_i = \omega_i + \frac{K}{N}\sum_{j=1}^{N}\sin(\theta_j - \theta_i) + A_i \sin\theta_i \tag{3.3}$$

where A_i is the amplitude of the external field/force. In [38], the authors considered the case $A_i = A$ and found two distinct regimes in the parameter space: states that were time-periodic and stable stationary synchronised states. For large A, the oscillators were entrained with the external field, while for small A, a portion of the oscillators were mutually synchronised in a periodic motion with frequency equal

to the mean of the natural frequencies. The phase transition from oscillatory to stationary occurred at $A = \omega$. We consider the effect of these sinusoidal external fields on the synchronisation properties of the hyperbolic Kuramoto model. The hyperbolic Kuramoto equations now read:

$$\dot{\alpha_i} = \omega_i + A\sin(\alpha_i) + \frac{K}{N}\sum_{j=1}^{N}\sinh(\alpha_j - \alpha_i).$$

For the uncoupled $K = 0$ case, the equations reduce to:

$$\dot{\alpha_i} = \omega_i + A\sin(\alpha_i).$$

For $\omega_i > A$ the solutions are periodic, with frequency $\sqrt{\omega_i^2 - A^2}/2\pi$:

$$\alpha_i(t) = 2\arctan\left(\frac{-A + \sqrt{-A^2+\omega_i^2}\tan\left(\frac{1}{2}\sqrt{-A^2+\omega_i^2}(t+c_i)\right)}{\omega_i}\right) \tag{3.4}$$

where c_i is determined by the initial conditions α^0:

$$c_i = \frac{2}{b_i}\arctan\left(\frac{A + \omega\tan(\frac{\alpha^0}{2})}{b_i}\right)$$

where $b_i = \sqrt{\omega_i^2 - A^2}$. For $A > \omega$ the solutions have the following form and are asymptotically stationary:

$$\alpha_i(t) = 2\arctan\left(\frac{-A + \sqrt{A^2-\omega_i^2}\tanh\left(\frac{1}{2}\sqrt{A^2-\omega_i^2}(c_i - t)\right)}{\omega_i}\right) \tag{3.5}$$

where the constant of integration c_i is:

$$c_i = \frac{2}{b_i}\tanh^{-1}\left(\frac{A + \omega\tan(\frac{\alpha^0}{2})}{b_i}\right)$$

where $b_i = \sqrt{A^2 - \omega_i^2}$. In the limit $A \to \infty$, the hyperbolic equations simplify to:

$$\dot{\alpha_i} = A\sin(\alpha_i)$$

with solutions:

$$\alpha_i(t) = 2\arctan\left(c_i e^{At}\right)$$

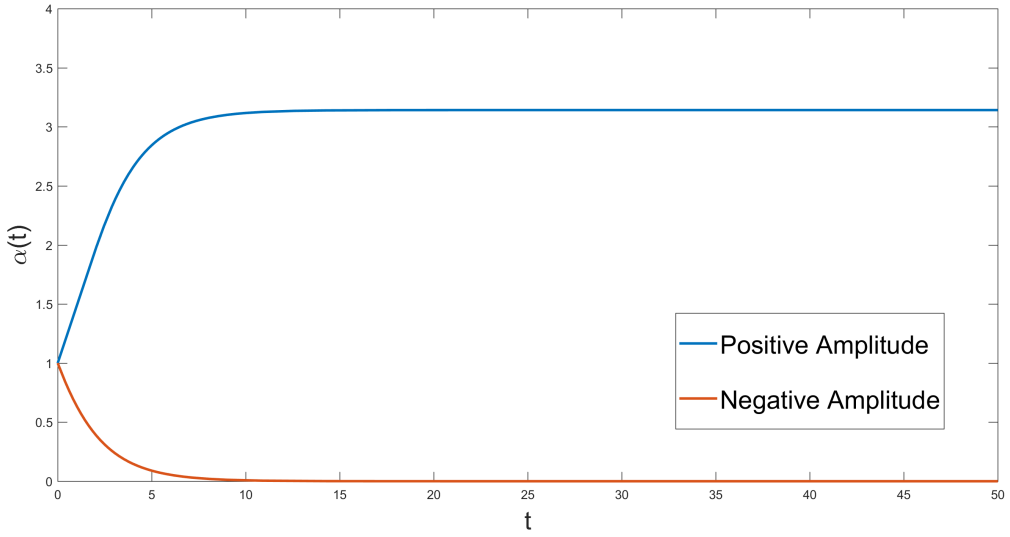

Figure 3.4: Solutions $\alpha(t)$ a single node in the limit $A \to \infty$ (or equivalently $\omega \to 0$, for positive and negative amplitude $A = \pm 0.5$ and initial condition $\alpha(0) = 1$. For positive A the solution tends towards π, while for negative amplitude $\alpha(t)$ goes to 0 for large times.

where $c_i = \tan(\frac{\alpha_i^0}{2})$. These solutions asymptote towards a constant value, namely π for $A > 0$ and 0 for $A < 0$ (See Figure 3.4). So $\dot{\alpha_i}(t) \to 0$ as $t \to \infty$ for each i, and therefore ω_{av}, the mean slope of the synchronised solutions goes to 0 for large A.

To study the interacting system with external fields, we performed numerical simulations for $N = 20$ nodes with random initial conditions and ω_i. For amplitudes A less than the mean of the parameters ω_i, the solutions were periodic, while for amplitudes large than the mean of the ω_i, the solutions became asymptotically stationary, as illustrated in Figure 3.5 and Figure 3.6. Hence there is a phase transition between the two regimes which occurs at $A = \omega_{AV}$, as observed for the ordinary Kuramoto model in [38]. In terms of the synchronisation properties, the order parameters do not settle to a final steady value when the amplitude is small, indicating that the system has not synchronised (or only very partially synchronised), while for large amplitudes the order parameters approach a constant value for large times (See Figure 3.7). Hence the effect of external fields is to force the nodes into a stationary synchronised state.

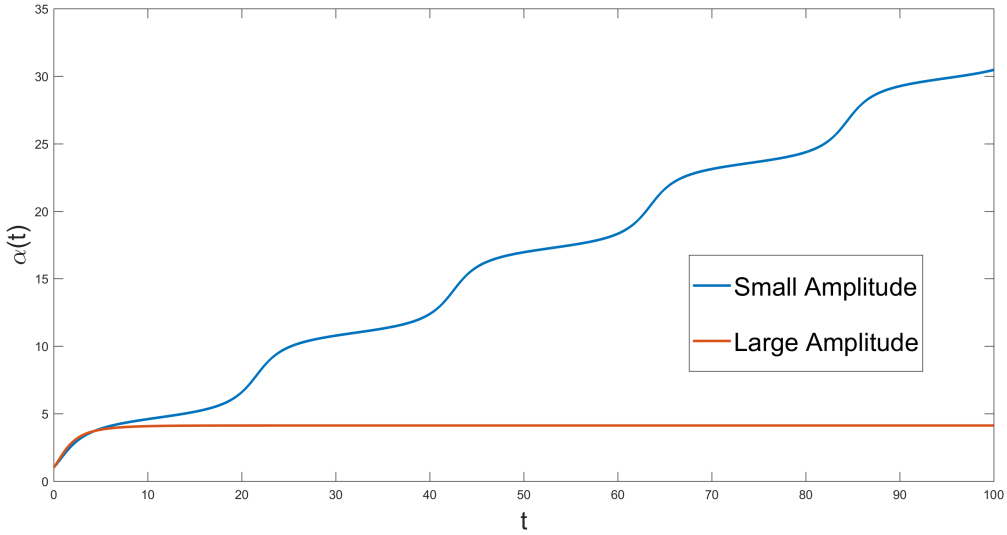

Figure 3.5: Solutions $\alpha(t)$ for a single node for $A < \omega$ (blue) and $A > \omega$ (red). The driving parameter ω was 0.5. The large amplitude solution has $A = 0.6$ and the small amplitude solution has $A = 0.4$. For amplitudes below ω the solutions are periodic, while for large amplitudes the solution become stationary.

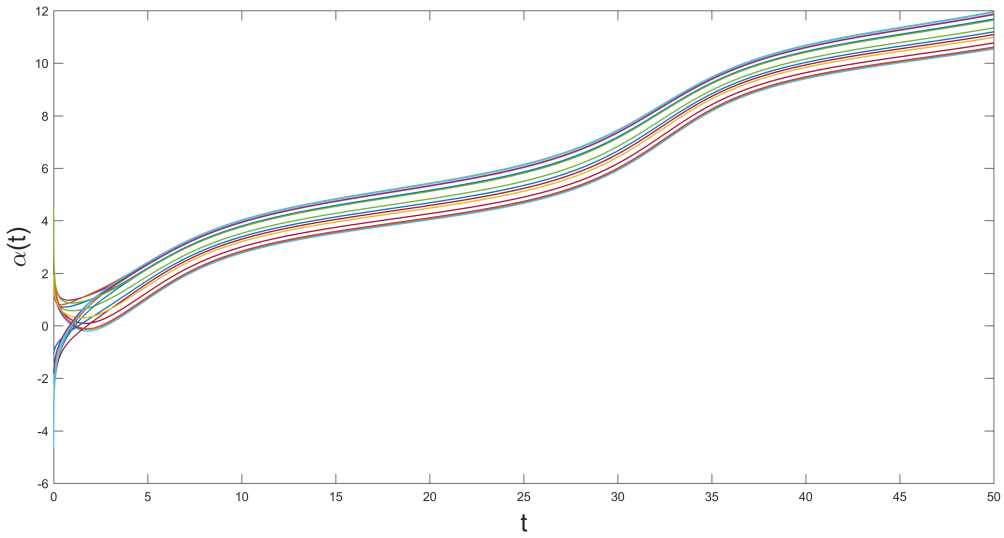

(a) Solutions $\alpha_i(t)$ with external field amplitude $A = 0.2$ for $N = 20$ nodes, with random initial conditions $-5 \leq \alpha_i^0 \leq 5$ and $-1 \leq \omega_i \leq 1$. The mean of the ω_i is 0.2841 (i.e. greater than the amplitude A.

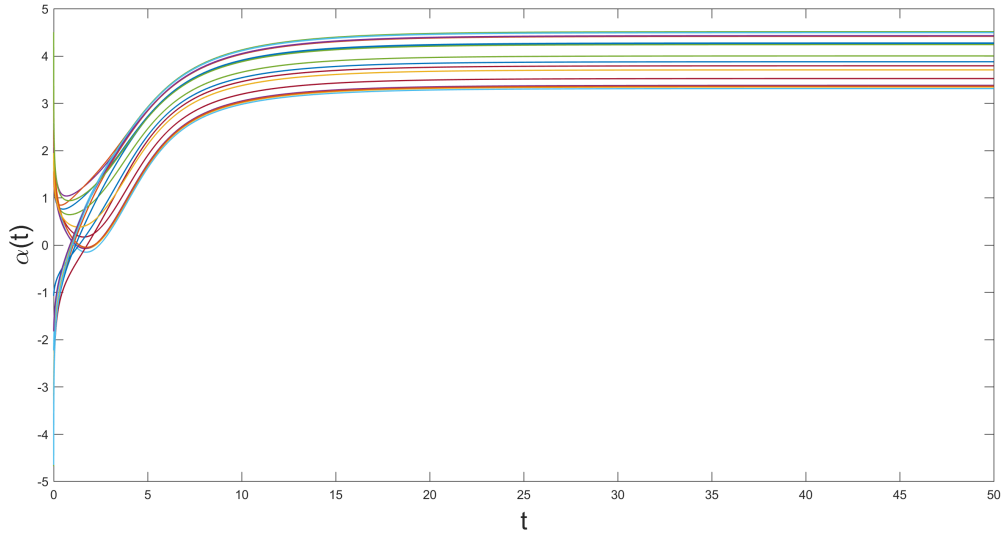

(b) Solutions $\alpha_i(t)$ with external field amplitude $A = 0.4$ for $N = 20$ nodes, with random initial conditions $-5 \leq \alpha_i^0 \leq 5$ and $-1 \leq \omega_i \leq 1$. The mean of the ω_i is 0.2841 (i.e. less than the amplitude A.

Figure 3.6: Solutions $\alpha_i(t)$ for 20 nodes with external fields highlighting the phase transition from partially synchronised periodic solutions to stationary synchronised solutions with increasing amplitudes.

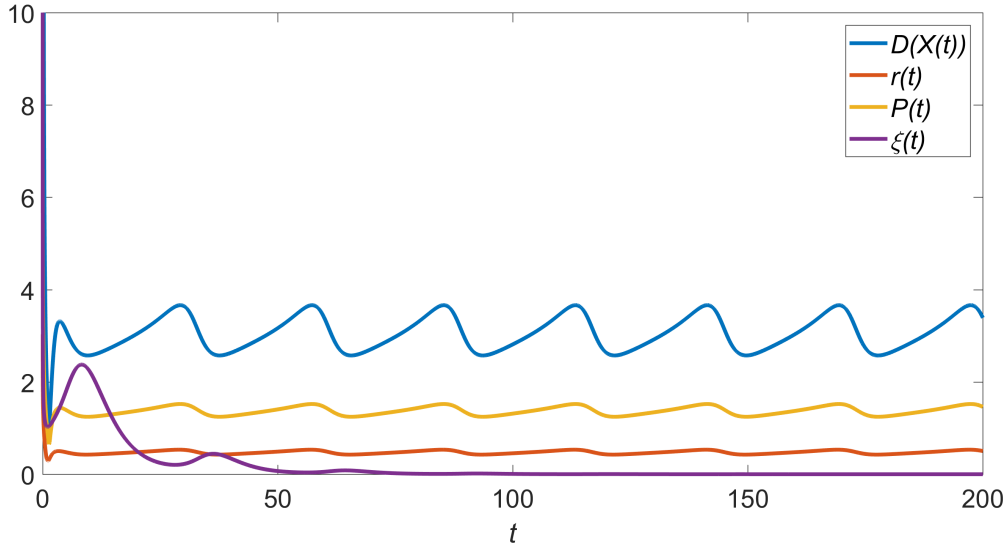

(a) Order parameters for a system with external fields with a small amplitude $A = 0.2$. The oscillatory behaviour of the parameters show that the system has not synchronised.

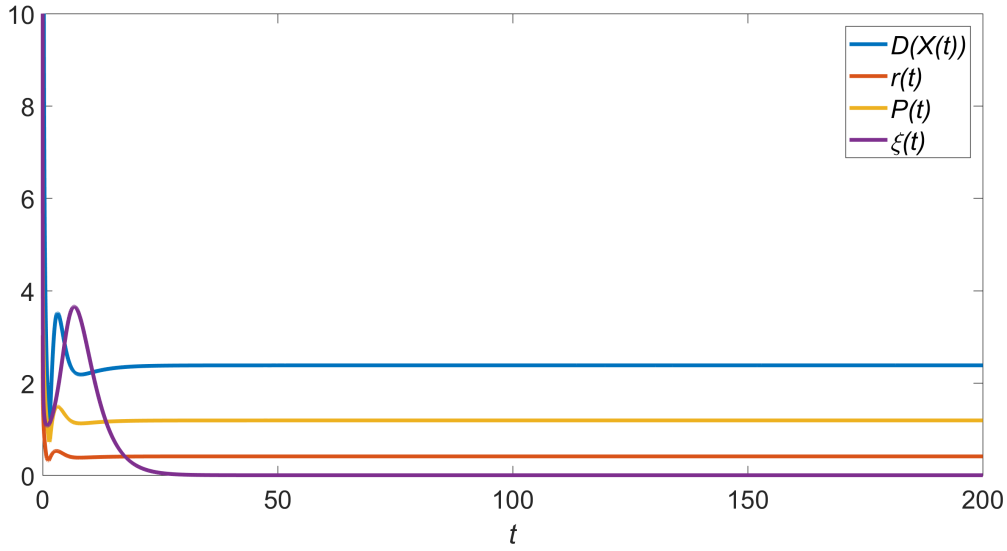

(b) Order parameters for a system with external fields with a large amplitude $A = 0.4$. The order parameters all reach a constant value, which shows that the system has synchronised.

Figure 3.7: Order parameters $D\left(X(t)\right), r(t), P(t), \xi(t)$ for 20 nodes with external fields showing the phase transition from partially synchronised to synchronised with increasing amplitudes. The initial conditions for the small and large amplitude cases are identical, as the ω_i, which have a mean of 0.2841.

Chapter 4

Vector generalisation of the hyperbolic Kuramoto model

In [23], Lohe provided a vector generalisation of the Kuramoto model where each node i is associated with an n-vector $\boldsymbol{x}_i$ in $\mathbb{R}^n$. By choosing $n = 2$, and parametrising the 2-vector as $\boldsymbol{x}_i = (\cos\theta_i, \sin\theta_i)$, which preserves (euclidean) distance, all trajectories are confined to the unit circle and the ordinary Kuramoto model is regained. The vector equations of motion are:

$$\dot{\boldsymbol{x}}_i = \Omega_i \boldsymbol{x}_i + \frac{K}{N} \sum_{j=1}^{N} [(\boldsymbol{x}_i \cdot \boldsymbol{x}_i)\boldsymbol{x}_j - (\boldsymbol{x}_j \cdot \boldsymbol{x}_i)\boldsymbol{x}_i] \tag{4.1}$$

where Ω_i is an antisymmetric $n \times n$ matrix in the Lie algebra of $SO(n)$. For $n = 2$ choose $\Omega_i = \begin{pmatrix} 0 & -\omega_i \\ \omega_i & 0 \end{pmatrix}$ and make the length preserving parametrisation $\boldsymbol{x}_i = (\cos\theta_i, \sin\theta_i)^T$ to constrain motion to the unit circle and hence regain the ordinary Kuramoto Model (1.1).

4.1 Non-compact manifolds: The Unit Hyperbola $SO(1,1)$

We can generalise (4.1) to non-compact groups by introduction of an indefinite metric $G = diag(1, \ldots, 1, -1 \ldots, -1)$ with p entries of $+1$ and q entries of -1, so the scalar dot product $\boldsymbol{x}_i \cdot \boldsymbol{x}_i$ is replaced by the Lorentz inner product $\langle \boldsymbol{x}_i, \boldsymbol{x}_i \rangle = \boldsymbol{x}_i^T G \boldsymbol{x}_i$. Hence $\boldsymbol{x}_i$ is a $(p+q)$-vector in Minkowski space and our equations of

motion read:

$$\dot{\boldsymbol{x}}_i = \Omega_i \boldsymbol{x}_i + \frac{K}{N} \sum_{j=1}^{N} \left[\langle \boldsymbol{x}_i, \boldsymbol{x}_i \rangle \boldsymbol{x}_j - \langle \boldsymbol{x}_i, \boldsymbol{x}_j \rangle \boldsymbol{x}_i \right] \tag{4.2}$$

where Ω_i is an $n \times n$ matrix in the Lie algebra $\mathfrak{so}(1,n)$ that satisfies $Tr(\Omega) = 0$ and $\Omega^T G + G\Omega = 0$. Note that $\dot{\boldsymbol{x}}_i = \frac{d}{ds}\boldsymbol{x}_i$, where s is a strictly increasing parameter of motion, rather than time. The reason for this will become clear in §4.2 when we come to a physical interpretation of the model. For $p = q = 1$, we have the metric $G = diag(1,-1)$ and we choose $\Omega_i = \begin{pmatrix} 0 & \omega_i \\ \omega_i & 0 \end{pmatrix}$.

If we now take the inner product of (4.2) with $\boldsymbol{x}_i$ (effectively left-multiplying the left and right hand sides by $\boldsymbol{x}_i^T G$, we get:

$$\langle \boldsymbol{x}_i, \dot{\boldsymbol{x}}_i \rangle = \langle \boldsymbol{x}_i, \Omega_i \boldsymbol{x}_i \rangle + \frac{K}{N} \sum_{j=1}^{N} \left[\langle \boldsymbol{x}_i, \boldsymbol{x}_i \rangle \langle \boldsymbol{x}_i, \boldsymbol{x}_j \rangle - \langle \boldsymbol{x}_i, \boldsymbol{x}_j \rangle \langle \boldsymbol{x}_i, \boldsymbol{x}_i \rangle \right].$$

Notice that the right hand side is zero by symmetry and hence $\langle \boldsymbol{x}_i, \dot{\boldsymbol{x}}_i \rangle = 0$ and therefore $\langle \boldsymbol{x}_i, \boldsymbol{x}_i \rangle$ is constant, and so by choosing $\langle \boldsymbol{x}_i, \boldsymbol{x}_i \rangle = -1$, all trajectories lie on an $(n-1)$-dimensional hyperboloid. Note that we could have chosen the value of the inner product to be any constant we like and which was different for each i i.e. $\langle \boldsymbol{x}_i, \boldsymbol{x}_i \rangle = -\lambda_i^2$. This would have the effect of constricting each particle to their own hyperbolae (See Appendix I for further details). After parametrizing the 2-vector as $\boldsymbol{x}_i = (\sinh \alpha_i, \cosh \alpha_i)^T$, where $\alpha_i(s) \in \mathbb{R}$, we recover the hyperbolic version of the Kuramoto model:

$$\dot{\alpha}_i = \omega_i - \frac{K}{N} \sum_{j=1}^{N} \sinh(\alpha_j - \alpha_i).$$

We can arbitrarily choose $K < 0$ so we have an attractive interaction term, thus avoiding singular solutions (see section 3.1).

4.2 Relativistic Interpretation

In this section, we describe a physical interpretation of the hyperbolic version of the Kuramoto model in terms of relativistic mechanics. In §4.1 we parametrised our two component Minkowski vector in terms of the hyperbolic functions $\cosh \alpha$ and $\sinh \alpha$ in order to derive a hyperbolic generalisation of the Kuramoto model. If we now define the components of said vector such that:

$$\sinh \alpha_i = x_i^0 = t_i \tag{4.3}$$

is the time component and

$$\cosh \alpha_i = x_i^1 = x_i \tag{4.4}$$

is the spatial component, i.e. $\boldsymbol{x}_i = (\sinh \alpha_i, \cosh \alpha_i)^T$, then we can interpret α_i physically as the rapidity of the i^{th} particle. Each of the particles then follows a hyperbolic path in spacetime with speed v_i given by the tangent to the curve at each point on the hyperbola (See Figure 4.1). As shown in §2.3, the hyperbolic Kuramoto model is also Lorentz invariant, i.e. it is invariant under transformations of the form $\alpha_i \to \alpha_i + \alpha_0$ for constant α_0.

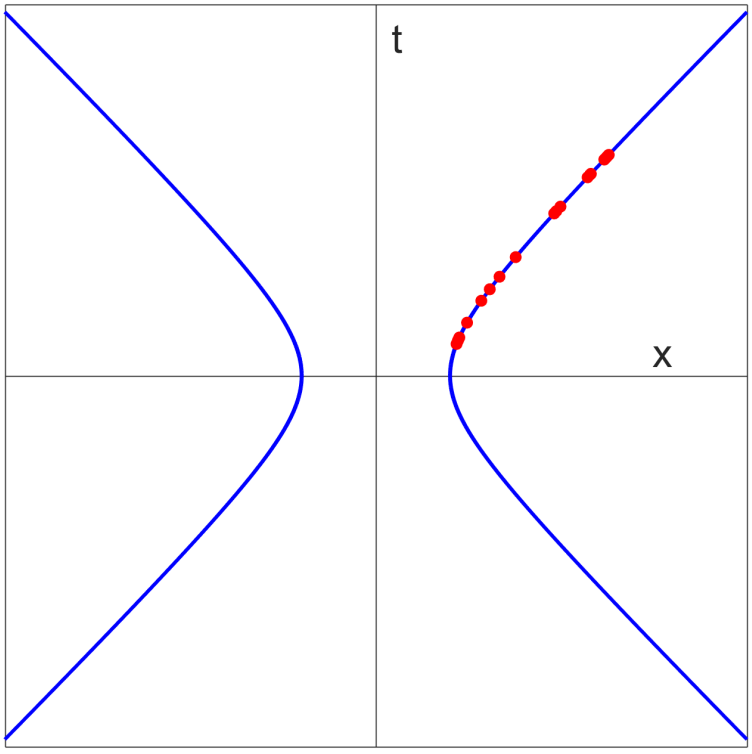

Figure 4.1: The hyperbola is the worldine of the particles, i.e. each of the particles follows a hyperbolic path in space-time. Geometrically, the rapidity α is the hyperbolic angle between the x-axis and a point on the hyperbola. The velocity of the particle (or speed in the case of one spatial dimension) is given by the hyperbolic tangent $v = \tanh \alpha$.

4.2.1 Lorentz factor and relativistic kinematics

The familiar Lorentz factor γ in special relativity for a particle with velocity $\vec{v}$ is given by:

$$\gamma = \frac{1}{\sqrt{1 - v^2}}$$

where we have set $c = 1$. If we choose $\boldsymbol{x}_i = (t_i, x_i) = (\sinh \alpha_i(s), \cosh \alpha_i(s))$ as above in (4.3) and (4.4), i.e. a space-like vector, then we can calculate the particles' velocity $v_i = \frac{dx_i}{dt_i}$ according to:

$$\begin{aligned} \vec{v_i} = \frac{d\vec{r_i}}{dt_i} = \frac{dx_i^1}{dx_i^0} = \frac{d\cosh\alpha_i}{d\sinh\alpha_i} &= \frac{d\cosh\alpha_i}{ds}\left(\frac{d\sinh\alpha_i}{ds}\right)^{-1} \\ &= \frac{\sinh\alpha_i}{\cosh\alpha_i} = \tanh\alpha_i. \end{aligned}$$

Hence the Lorentz factor γ_i is:

$$\gamma_i = \frac{1}{\sqrt{1 - \tanh^2\alpha_i}} = \cosh\alpha_i$$

which is greater than or equal to 1 (since $\tanh\alpha_i$ asymptotically approaches 1) and agrees with the definition of the relativistic Lorentz factor γ if we identify α_i as rapidity. Also $\vec{v_i} = \tanh\alpha_i$ then follows the definition of relativistic velocity and rapidity (See Figure 4.2).

Note that if we were to use the parametrisation $\boldsymbol{x}_i = (x_i^0, x_i^1) = (\cosh\alpha_i, \sinh\alpha_i)$, we would get:

$$\vec{v_i} = \frac{d\vec{r_i}}{dt_i} = \frac{dx_i^1}{dx_i^0} = \frac{d\sinh\alpha_i}{d\cosh\alpha_i}.$$

Then,

$$\begin{aligned} \vec{v_i} = \frac{d\sinh\alpha_i}{d\cosh\alpha_i} &= \frac{d\sinh\alpha_i}{d\alpha_i}\left(\frac{d\cosh\alpha_i}{d\alpha_i}\right)^{-1} \\ &= \frac{\cosh\alpha_i}{\sinh\alpha_i} = \coth\alpha_i \\ &\Rightarrow \gamma_i = \frac{1}{\sqrt{1 - \coth^2\alpha_i}} \end{aligned}$$

which can be complex, since the particle's speed given by $\coth\alpha_i$ is unbounded. This is clearly unphysical. The relativistic 2-momentum is given by $\boldsymbol{P}_i = (E_i/c, p_i) = (\gamma_i mc, \gamma_i m v_i)$, where $m = c = 1$. Hence the energy and momentum of each particle is $\cosh\alpha_i$ and $\sinh\alpha_i$. The Minkowski inner product of $\boldsymbol{P}_i$ with itself then gives

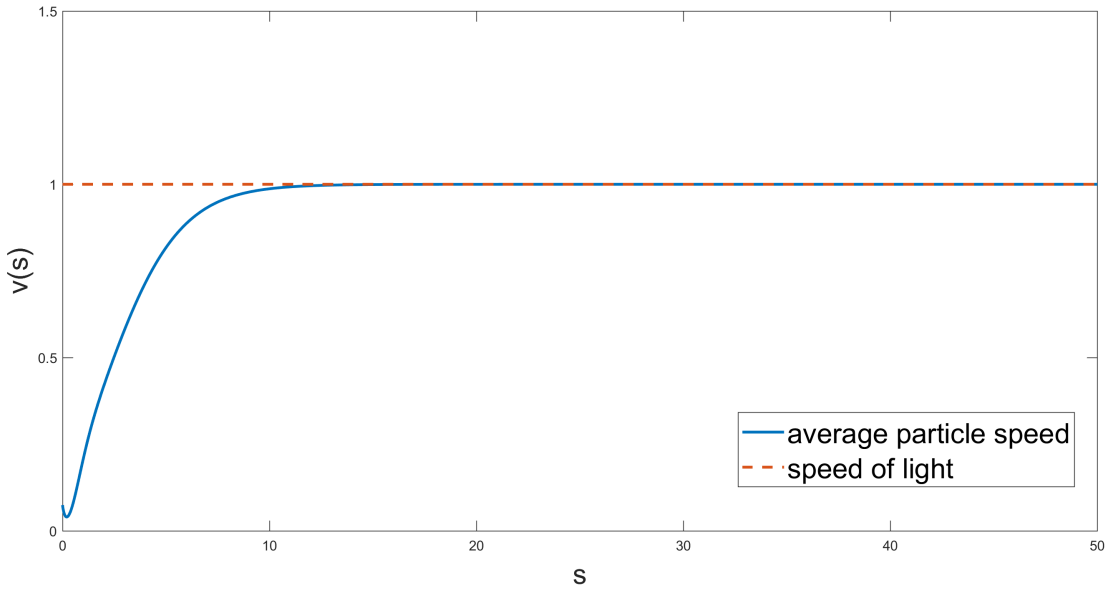

Figure 4.2: Average particle speed of 20 particles with random initial conditions and ω_i. The relativistic speed v is given by the hyperbolic tangent of the particles' rapidity α. The speed of the particles asymptotically approaches the speed of light $c = 1$.

the invariant energy-momentum relation $E_i^2 - p_i^2 = 1$. In a relativistic system interactions are not instantaneous, whereas the interactions between particles in (2.4) are assumed to be instantaneous, so in order for the relativistic interpretation to take effect, we must include a time delay σ_{ij} to account for the finite travel time for signals between particles i and j. Hence the equations now read:

$$\dot{\alpha}_i = \omega_i - \frac{K}{N} \sum_{j=1}^{N} \sinh\left(\alpha_j(s - \sigma_{ij}) - \alpha_i(s)\right).$$

Although we have not modelled the effect of a time-delay in the hyperbolic model, it has been previously noted that small uniform time delays have no qualitative effect on synchronisation in the Kuramoto model [39, 40].

4.2.2 Spacetime Interval

Let $\boldsymbol{x}_i = (x_i^0, x_i^1)$ and $\boldsymbol{x}_j = (x_j^0, x_j^1)$ be 2 space-like vectors in Minkowski space, with time and space components of $\boldsymbol{x}_i$ given by $\sinh \alpha_i$ and $\cosh \alpha_i$ respectively.

Then the spacetime interval I is given by:

$$\begin{aligned} I &= (\Delta x^0)^2 - (\Delta x^1)^2 \\ &= (x_i^0 - x_j^0)^2 - (x_i^1 - x_j^1)^2 \\ &= (x_i^0)^2 - 2x_i^0 x_j^0 + (x_j^0)^2 - (x_i^1)^2 + 2x_i^1 x_j^1 - (x_j^1)^2 \\ &= -1 + 2x_i^0 x_j^0 - 2x_i^1 x_j^1 - 1 \\ &= -2 + 2\cosh(\alpha_i - \alpha_j) \end{aligned}$$

which (since $\cosh\alpha > 1 \quad \forall \quad \alpha$) is always greater than or equal to zero. Hence for $\alpha_i \neq \alpha_j$ the space-time separation is strictly greater than zero. This corresponds to a time-like separation i.e. events can be causally related. If instead we choose the components as $(\cosh\alpha_i, \sinh\alpha_i)$, making the scalar product positive, then we would get $I = 2 - 2\cosh(\alpha_i - \alpha_j)$ which is less than zero (space-like separation), meaning no two events can be causally related, which is again unphysical.

4.2.3 Proper time

In special relativity, the lack of an absolute reference frame means that each particle/reference frame has its own "proper" time τ_i (i.e. the time measured by the moving particle) [41], given by $dt_i = \gamma_i(v_i)d\tau_i$, where t_i is the time measured by an observer (coordinate time) and $\gamma_i(v_i)$ is the Lorentz factor $\gamma_i(v_i) = \frac{1}{\sqrt{1-\beta_i^2}}$, with $\beta_i = \frac{v_i}{c}$. γ_i can also be expressed in terms of the particle's rapidity α_i such that:

$$\frac{dt_i}{d\tau_i} = \gamma_i(v_i) = \cosh\alpha_i. \tag{4.5}$$

In the $SO(1,1)$ model we have chosen the time-like direction to be parametrised as $t_i = \sinh\alpha_i$ for each i and our equations of motion are parametrised using an arbitrary parameter s. If we differentiate t with respect to this parameter s we find:

$$\frac{dt_i}{ds} = \frac{d\sinh\alpha_i(s)}{ds} = \frac{d\alpha_i}{ds}\cosh\alpha_i(s). \tag{4.6}$$

For a single particle system $\frac{d\alpha}{ds}$ is simply the parameter ω and $\cosh\alpha$ we showed above to be the Lorentz factor γ. Hence

$$\frac{dt}{ds} = \omega\cosh\alpha = \omega\gamma(v). \tag{4.7}$$

We now compare this result to the relativistic definition of proper time (4.5) to show that

$$ds = \omega d\tau. \tag{4.8}$$

Hence for a one-particle system, the evolution parameter s is proportional to the particle's proper time and since s is an arbitrary parameter we can easily rescale s by a factor ω such that $\frac{dt}{ds} = \frac{dt}{d\tau}$. For an N particle system, there is no common proper time unless all the particles have the same speed, i.e. they are synchronised, at which point we simply replace ω with $\omega_{av} = \frac{1}{N}\sum_{i=1}^{N} \omega_i$.

The proper time for each particle must also be an increasing function of s. For random initial conditions α_i^0 and random parameters ω_i, the particles can, for small s, travel backwards with respect to time. This can be avoided by choosing the parameters ω_i sufficiently large so that the RHS of (2.4) is always positive. This parameter shift $\omega_i \to \omega_i + \omega_0$, for some ω_0 is equivalent to shifting the rapidities α_i to $\alpha_i - \omega_0 s$.

Chapter 5

The $SO(1,2)$ Vector Hyperboloid Model

In this chapter we formulate and study a vector model of synchronisation on the non-compact manifold $SO(1,2)$. Recall the vector generalisation of the Kuramoto model to the non-compact Minkowski space:

$$\dot{\boldsymbol{x}}_i = \Omega_i \boldsymbol{x}_i + \frac{K}{N} \sum_{j=1}^{N} \left[\langle \boldsymbol{x}_i, \boldsymbol{x}_i \rangle \boldsymbol{x}_j - \langle \boldsymbol{x}_i, \boldsymbol{x}_j \rangle \boldsymbol{x}_i \right]. \tag{5.1}$$

If we now make $\boldsymbol{x}_i$ a 3-vector (which satisfies the requirement $\langle \boldsymbol{x}_i, \boldsymbol{x}_i \rangle = -1$, we can choose the parametrisation $\boldsymbol{x}_i = (\sinh \alpha_i, \cosh \alpha_i \cos \theta_i, \cosh \alpha_i \sin \theta_i)^T$ which constrains the particles to motion on a one-sheeted hyperboloid, whose symmetry group is $SO(1,2)$. The hyperboloid of one sheet is an important object in differential geometry and general relativity where it is a model of 2-dimensional spacetime (de Sitter space). We choose the 3×3 driving matrix Ω_i to be a general element of the Lie algebra of $SO(1,2)$ which satisfies $\Omega_i^T G + G\Omega_i = 0$ for each i, for the metric $G = \mathrm{diag}(1,-1,-1)$, i.e. we select:

$$\Omega_i = \begin{pmatrix} 0 & \eta_i & \beta_i \\ \eta_i & 0 & -\omega_i \\ \beta_i & \omega_i & 0 \end{pmatrix}. \tag{5.2}$$

Substituting our parametrisation for $\boldsymbol{x}_i$ and Ω_i into (5.1), we arrive at the $3N$ equations of motion:

$$\dot{\alpha}_i = \eta_i \cos\theta_i + \beta_i \sin\theta_i + \frac{K}{N}\sum_{j=1}^{N}[\cos(\theta_i-\theta_j)\cosh\alpha_j \sinh\alpha_i - \cosh\alpha_i \sinh\alpha_j] \tag{5.3}$$

$$\dot{\alpha}_i \sinh\alpha_i \cos\theta_i - \dot{\theta}_i \sin\theta_i \cosh\alpha_i = \eta_i \sinh\alpha_i - \omega_i \cosh\alpha_i \sin\theta_i \tag{5.4}$$

$$+\frac{K}{N}\sum_{j=1}^{N}[-\cosh\alpha_j\cos\theta_j - \cosh\alpha_i\cos\theta_i(\sinh\alpha_i\sinh\alpha_j - \cos(\theta_i-\theta_j)\cosh\alpha_i\cosh\alpha_j]$$

$$\dot{\alpha}_i \sinh\alpha_i \sin\theta_i + \dot{\theta}_i \cos\theta_i \cosh\alpha_i = \beta_i \sinh\alpha_i + \omega_i \cosh\alpha_i \cos\theta_i \tag{5.5}$$

$$+\frac{K}{N}\sum_{j=1}^{N}[-\cosh\alpha_j\sin\theta_j - \cosh\alpha_i\sin\theta_i(\sinh\alpha_i\sinh\alpha_j - \cos(\theta_i-\theta_j)\cosh\alpha_i\cosh\alpha_j]\,.$$

We can reduce these $3N$ equations to $2N$ equations by multiplying (5.4) by $\sin\theta_i$ and subtracting (5.5) multiplied by $\cos\theta_i$ to yield:

$$\dot{\alpha}_i = \eta_i\cos\theta_i + \beta_i\sin\theta_i + \frac{K}{N}\sum_{j=1}^{N}[\cos(\theta_i-\theta_j)\cosh\alpha_j\sinh\alpha_i - \cosh\alpha_i\sinh\alpha_j] \tag{5.6}$$

$$\dot{\theta}_i = \tanh\alpha_i(\beta_i\cos\theta_i - \eta_i\sin\theta_i) + \omega_i - \frac{K}{N\cosh\alpha_i}\sum_{j=1}^{N}[\cosh\alpha_j\sin(\theta_j-\theta_i)]\,. \tag{5.7}$$

These are our defining equations for the hyperbolic Kuramoto model in $1+2$ dimensions. Note that if we were to set $\theta = 0$ in (5.6), then we arrive back at the hyperbolic model (2.4), and if we set $\alpha = 0$ in (5.7) we regain the ordinary Kuramoto model (1.1). Also, by setting $\alpha = 0$ and $\eta = \beta = 0$ in (5.6), the equation reduces to $\dot{\alpha}_i = 0$, which makes sense as we are effectively choosing the $SO(2)$ subgroup of $SO(1,2)$. Similarly, setting $\theta = 0$ and $\omega = \beta = 0$ in (5.7) means we are choosing the $SO(1,1)$ subgroup, leaving us with $\dot{\theta}_i = 0$.

5.1 Exact Solutions for One Particle

In this section we solve for the motion of a single particle moving on the hyperboloid surface with parameters ω, β, η, and show how the equations can be reduced to the Kuramoto model and the hyperbolic model by considering the subgroups of $SO(1,2)$. We will use the vector equation (4.2) rather than the equations of motion (5.6) and (5.7). For $N = 1$, the equations (4.2) reduce to the simple matrix ordinary differential equation:

$$\dot{\boldsymbol{x}} = \Omega\boldsymbol{x} \tag{5.8}$$

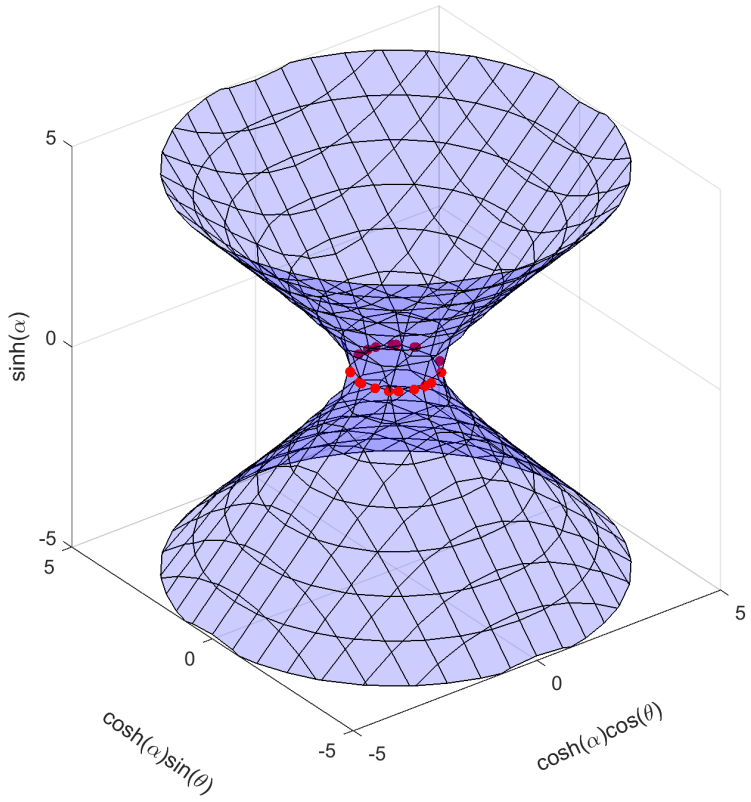

Figure 5.1: In the hyperboloid vector model, the particles (red) are constrained to motion on a 2-dimensional hyperboloid of one sheet. Each particle i has driving parameters $\omega_i, \eta_i, \beta_i$.

where Ω is as before:

$$\Omega = \begin{pmatrix} 0 & \eta & \beta \\ \eta & 0 & -\omega \\ \beta & \omega & 0 \end{pmatrix}.$$

We can write these equations component-wise:

$$\begin{pmatrix} \dot{x}_1 \\ \dot{x}_2 \\ \dot{x}_2 \end{pmatrix} = \begin{pmatrix} 0 & \eta & \beta \\ \eta & 0 & -\omega \\ \beta & \omega & 0 \end{pmatrix} \begin{pmatrix} x_1 \\ x_2 \\ x_3 \end{pmatrix}.$$

We can solve this single particle system for $x_1(s), x_2(s), x_3(s)$ using an eigenvalue approach. The characteristic polynomial obtained using the characteristic equation $\det(\Omega - \lambda I_3) = 0$ is:

$$(\beta^2 + \eta^2 - \omega^2)\lambda - \lambda^3 = 0 \tag{5.9}$$

where I_3 is the 3×3 identity matrix. Solving for λ gives the eigenvalues:

$$\lambda_1 = 0, \quad \lambda_2 = \Delta, \quad \lambda_3 = -\Delta \tag{5.10}$$

where the quantity Δ is given by:

$$\Delta = \sqrt{\beta^2 + \eta^2 - \omega^2}. \tag{5.11}$$

The corresponding eigenvectors $\boldsymbol{v}_i$ are determined by solving the equation $(\Omega - \lambda_i I_3)\boldsymbol{v}_i = 0$ using Gaussian elimination:

$$V = \begin{pmatrix} \frac{\omega}{\eta} & \frac{-\omega\eta+\beta\Delta}{\beta^2-\omega^2} & \frac{-\omega\eta-\beta\Delta}{\beta^2-\omega^2} \\ -\frac{\beta}{\eta} & \frac{\beta\eta-\omega\Delta}{\beta^2-\omega^2} & \frac{\beta\eta+\omega\Delta}{\beta^2-\omega^2} \\ 1 & 1 & 1 \end{pmatrix} \tag{5.12}$$

where the columns of V give the eigenvectors i.e. $V = (\boldsymbol{v}_1|\boldsymbol{v}_2|\boldsymbol{v}_3)$. We now look for general solutions of the form:

$$\boldsymbol{x}(s) = ae^{\lambda_1 s}\boldsymbol{v}_1 + be^{\lambda_2 s}\boldsymbol{v}_2 + ce^{\lambda_3 s}\boldsymbol{v}_3 \tag{5.13}$$

where a, b, c are constants given by the initial conditions α_0 and θ_0. For $s = 0$, (5.13) reduces to:

$$\boldsymbol{x}(0) = a\boldsymbol{v}_1 + b\boldsymbol{v}_2 + c\boldsymbol{v}_3 \tag{5.14}$$

or in matrix form:

$$\boldsymbol{x}(0) = V \begin{pmatrix} a \\ b \\ c \end{pmatrix}.$$

Hence the coefficients a,b and c (the explicit form of the constants are presented in Appendix II) are given by:

$$\begin{pmatrix} a \\ b \\ c \end{pmatrix} = V^{-1}\boldsymbol{x}(0)$$

where $\boldsymbol{x}(0) = \boldsymbol{x}_0$ is given by the initial conditions:

$$\boldsymbol{x}_0 = \begin{pmatrix} \sinh\alpha_0 \\ \cosh\alpha_0\cos\theta_0 \\ \cosh\alpha_0\sin\theta_0 \end{pmatrix}$$

From the general solution (5.13) we see that depending on whether the eigenvalues are real or imaginary, different dynamics emerge. If $\Delta^2 = \beta^2 + \eta^2 - \omega^2$ is less

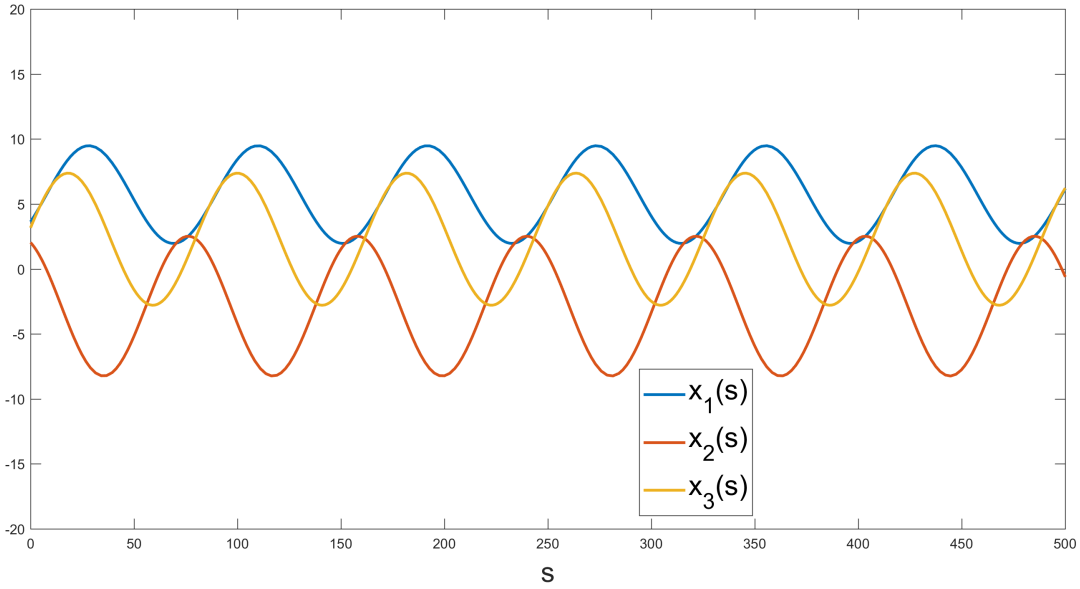

Figure 5.2: Components $x_1(s), x_2(s), x_3(s)$ of the exact solutions for a single particle. Each component corresponds to one of the vector components. The parameters used were $\omega = 0.1, \beta = 0.05, \eta = 0.04$ giving a Δ^2 value of -0.0059. The initial conditions were $\alpha_0 = 2, \theta_0 = 1$.

than zero, then the eigenvalues are imaginary (with the exception of the zero mode $\lambda_1 = 0$) and the solutions α_i and θ_i are periodic with an angular frequency given by the absolute value of the eigenvalue (See Figure 5.3). In terms of the particles' trajectory on the hyperboloid surface, this corresponds to the particle oscillating up and down in the α-direction while rotating around the hyperboloid with an undulating velocity. The amplitudes are governed by the constants a, b, c and the eigenvectors $\boldsymbol{v}_1, \boldsymbol{v}_2, \boldsymbol{v}_3$. If $\Delta^2 > 0$ then the eigenvalues are real, yielding a linear asymptotic solution $\alpha(s)$ with slope $\sqrt{\beta^2 + \eta^2 - \omega^2}$ and a stationary asymptotic solution $\theta(s)$ shown in Figure 5.4. This means the particle simply shoots outs to infinity at a constant velocity while remaining at a fixed angle i.e. on a hyperbola.

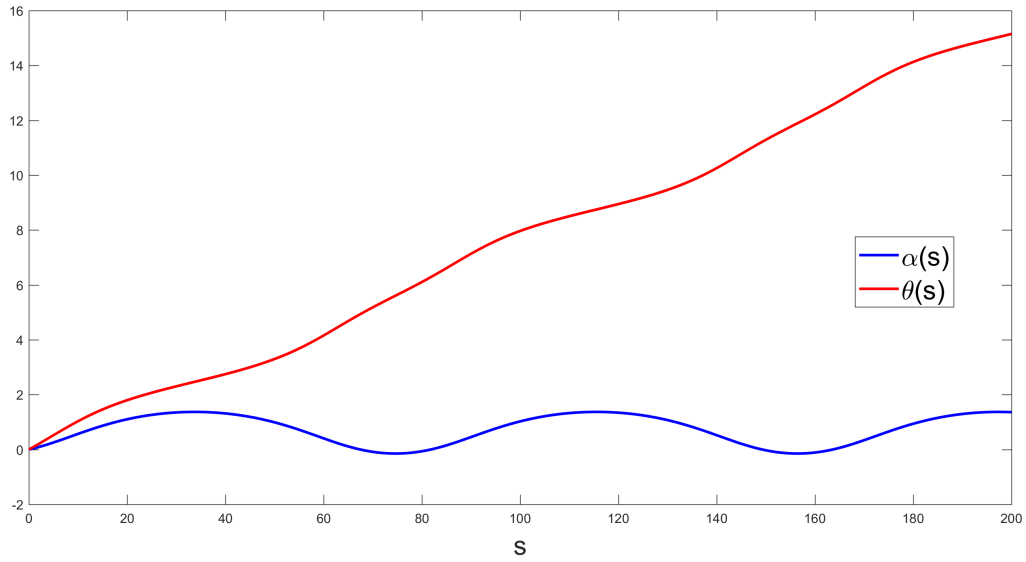

Figure 5.3: Exact solutions for $N = 1$ with parameters $\omega = 0.1, \beta = 0.05, \eta = 0.04$ ($\Delta^2 = -0.0059$) and random initial conditions α_0, θ_0. A value of $\Delta^2 < 0$ means the solutions $\alpha(s)$ and $\theta(s)$ are periodic.

A special case occurs if $\Delta^2 = 0$ where all three eigenvalues are zero, in which case we must look for new solutions of the form:

$$\boldsymbol{x}(s) = \frac{1}{2}s^2 e^{\lambda_1 s}\boldsymbol{u}_1 + s e^{\lambda_2 s}\boldsymbol{u}_2 + e^{\lambda_3 s}\boldsymbol{u}_3 \tag{5.15}$$

where the eigenvectors $\boldsymbol{u}_i$ satisfy $(\Omega - \lambda I_3)\boldsymbol{u}_2 = \boldsymbol{u}_1$ and $(\Omega - \lambda I_3)\boldsymbol{u}_3 = \boldsymbol{u}_2$. In this case the solution $\alpha(s)$ will be inverse hyperbolic functions, as shown in Figure 5.5, and the angular component $\theta(s)$ tends towards a constant, meaning the particle moves up along a hyperbola with a decreasing velocity. Note that for all three types of motion described, the single particle state is equivalent to the fully synchronised N particle state, since at synchronisation $\alpha_j - \alpha_i \to 0$ and $\theta_j - \theta_i \to 0$, hence the 1 particle solutions can be applied to the N particle system at synchronisation.

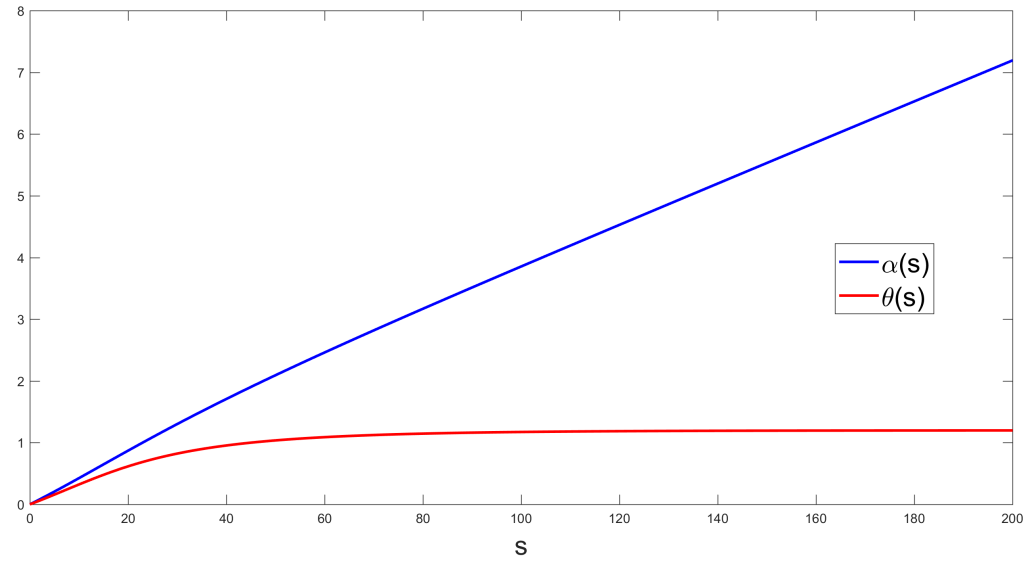

Figure 5.4: Exact solutions $\alpha(s)$ and $\theta(s)$ for a single particle. The parameters used were $\omega = 0.03, \beta = 0.02, \eta = 0.04$ giving a Δ^2 value of 0.0011, yielding a linear asymptotic solution $\alpha(s)$ and a stationary angular solution $\theta(s)$. The initial conditions were generated randomly.

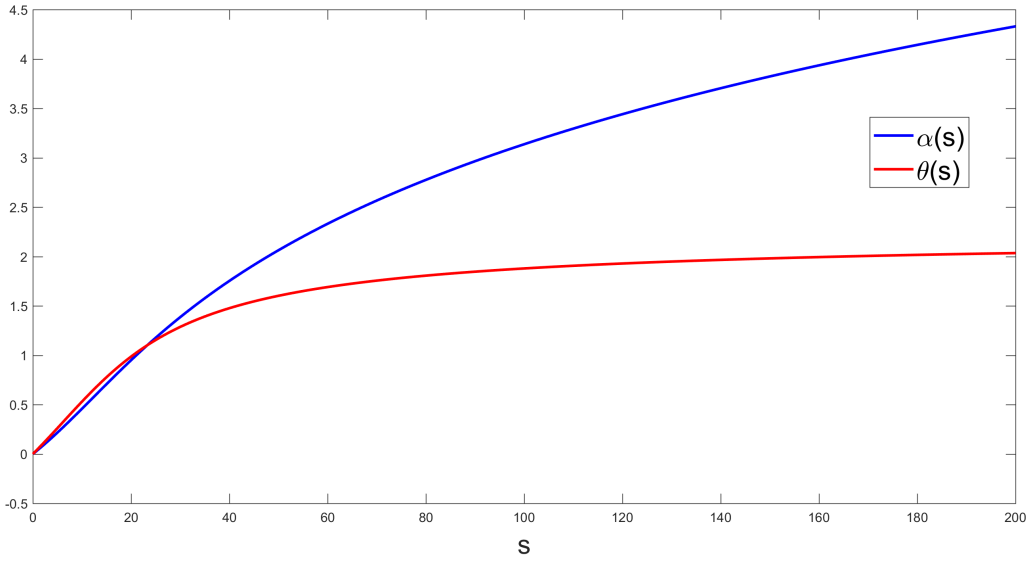

Figure 5.5: Exact solutions $\alpha(s)$ and $\theta(s)$ for a single particle. The parameters used were $\omega = 0.05, \beta = 0.04, \eta = 0.03$ giving a Δ^2 value of 0, yielding an inverse hyperbolic asymptotic solution $\alpha(s)$ and a stationary angular solution $\theta(s)$. The initial conditions were generated randomly.

5.1.1 1 particle solutions for the SO(2) subgroup

We now show how the vector hyperboloid model can be reduced to the ordinary Kuramoto model and the 1-dimensional hyperbolic model by considering the subgroups of the system's symmetry group $SO(1,2)$, namely $SO(2)$ and $SO(1,1)$. For the $SO(2)$ subgroup ($\eta = \beta = 0$), i.e. the Kuramoto model, we parametrised the 2-vector as $(x_1, x_2) = (\cos\theta, \sin\theta)$ and we have the antisymmetric matrix

$$\Omega = \begin{pmatrix} 0 & -\omega \\ \omega & 0 \end{pmatrix}$$

with eigenvalues $\lambda_1 = -i\omega$ and $\lambda_2 = i\omega$. The columns of V give the corresponding eigenvectors $\boldsymbol{v}_1$ and $\boldsymbol{v}_2$:

$$V = \begin{pmatrix} -i & i \\ 1 & 1 \end{pmatrix}.$$

Again we look for solutions of exponential form:

$$\boldsymbol{x}(s) = ae^{\lambda_1 s}\boldsymbol{v}_1 + be^{\lambda_2 s}\boldsymbol{v}_2 \tag{5.16}$$

where a and b are given by $\begin{pmatrix} a \\ b \end{pmatrix} = V^{-1}\boldsymbol{x}(0)$. Hence the solutions $x_1(s)$ and $x_2(s)$ are:

$$\begin{aligned} x_1(s) &= \frac{-i}{2}(i\cos\theta_0 + \sin\theta_0)e^{-i\omega s} + \frac{i}{2}(-i\cos\theta_0 + \sin\theta_0)e^{i\omega s} \\ &= \frac{1}{2}(e^{-i\theta_0}e^{-i\omega s} + e^{i\theta_0}e^{i\omega s}) \\ &= \cos(\theta_0 + \omega s). \end{aligned}$$

Hence $\cos\theta(s) = \cos(\theta_0 + \omega s)$ i.e. $\theta(s) = \theta_0 + \omega s$. Likewise for $x_2(s)$ we get $\sin\theta(s) = \sin(\theta_0 + \omega s)$ i.e. $\theta(s) = \theta_0 + \omega s$. This is consistent with the ordinary Kuramoto model, where a one-particle system has the simple differential equation $\dot{\theta} = \omega$. This can also be seen by setting $\eta = \beta = 0$ in (5.7).

5.1.2 1 particle solutions for the SO(1,1) subgroup

For the $SO(1,1)$ subgroup ($\omega = \beta = 0$) we parametrised the 2-vector as $(x_0, x_1) = (\sinh\alpha, \cosh\alpha)$ and we have the matrix

$$\Omega = \begin{pmatrix} 0 & \eta \\ \eta & 0 \end{pmatrix}$$

with eigenvalues $\lambda_1 = \eta$ and $\lambda_2 = -\eta$. The columns of V give the corresponding eigenvectors $\boldsymbol{v}_1$ and $\boldsymbol{v}_2$):

$$V = \begin{pmatrix} 1 & -1 \\ 1 & 1 \end{pmatrix}.$$

Again we look for solutions of exponential form:

$$\boldsymbol{x}(s) = ae^{\lambda_1 s}\boldsymbol{v}_1 + be^{\lambda_2 s}\boldsymbol{v}_2 \tag{5.17}$$

where a and b are given by $\begin{pmatrix} a \\ b \end{pmatrix} = V^{-1}\boldsymbol{x}(0)$. Hence the solutions $x_1(s)$ and $x_2(s)$ are:

$$\begin{aligned} x_1(s) &= \frac{1}{2}(\cosh\alpha_0 + \sinh\alpha_0)e^{\eta s} - \frac{1}{2}(\cosh\alpha_0 - \sinh\alpha_0)e^{-\eta s} \\ &= \frac{1}{2}(e^{-\alpha_0}e^{-\eta s} + e^{\alpha_0}e^{\eta s}) \\ &= \sinh(\alpha_0 + \eta s). \end{aligned}$$

Hence $\sinh\alpha(s) = \sinh(\alpha_0 + \eta s)$ i.e. $\alpha(s) = \alpha_0 + \eta s$. Likewise for $x_2(s)$ we get $\cosh\alpha(s) = \cosh(\alpha_0 + \eta s)$ i.e. $\alpha(s) = \alpha_0 + \eta s$, in agreement with the 1-dimensional hyperbolic model, which, for a single particle has equation $\dot{\alpha} = \eta$. Setting $\omega = \beta = 0$ in (5.6) gives the same result.

5.2 Definition and Measures of Synchronisation

In the 1-dimensional hyperbolic model and the Kuramoto model, particles/oscillators were considered synchronised, or phase locked if their trajectories approached parallel lines or if they completely coincided, in the case of complete synchronised. This definition can be used in the hyperboloid model, with the caveat that synchronised trajectories need not only be linear functions, but can also have periodic or hyperbolic s dependence. To measure the onset of synchronisation we will use the Kuramoto order parameter $R(s)$ (1.4) to measure synchronisation in the θ-direction and the disorder parameter $r(s)$ (2.19) to measure synchronisation in the α-direction. In addition to these 1-dimensional measures, we introduce a 2-dimensional measure of synchronisation based on the Minkowski inner-product between any two particles on the hyperboloid surface. For any two particles i and

j with coordinates $\boldsymbol{x}_i$ and $\boldsymbol{x}_j$, the separation, or interval $\mathcal{I}_{ij}(s)$ between them is:

$$\begin{aligned}\mathcal{I}_{ij}(s) &= \langle \boldsymbol{x}_i - \boldsymbol{x}_j, \boldsymbol{x}_i - \boldsymbol{x}_j \rangle \\ &= (x_i^0 - x_j^0)^2 - (x_i^1 - x_j^1)^2 - (x_i^2 - x_j^2)^2 \\ &= \sinh^2\alpha_i + \sinh^2\alpha_j - 2\sinh\alpha_i \sinh\alpha_j - \cosh^2\alpha_i(\cos^2\theta_i + \sin^2\theta_i) \\ &- \cosh^2\alpha_j(\cos^2\theta_j + \sin^2\theta_j) + 2\cosh\alpha_i\cosh\alpha_j(\cos\theta_i\cos\theta_j + \sin\theta_i\sin\theta_j) \\ &= -2 - 2\left(\sinh\alpha_i\sinh\alpha_j - \cosh\alpha_i\cosh\alpha_j\cos(\theta_i - \theta_j)\right)\end{aligned}$$

This interval can therefore be either positive or negative, because we are in a non-euclidean, hyperbolic space. Using the above interval $\mathcal{I}$, we define the (dis)order parameter $I(s)$, which is zero for synchronised systems:

$$I(s) = \frac{1}{N^2}\sum_{i,j=1}^{N} |-1 - \sinh\alpha_j\alpha_i + \cosh\alpha_j\cosh\alpha_i\cos(\theta_j - \theta_i)|. \tag{5.18}$$

5.3 Exact Solutions for two particles

In order to gain some basic understanding of the properties of this complicated hyperboloid system, such as synchronisation and the possibility of the solutions developing hyperbolic singularities, as observed in 2.3, we will take the simplest interacting system and consider what happens when we have only 2 particles. For 2 particles with identical parameters η, β, ω we have the four equations of motion:

$$\dot{\alpha_1} = \eta\cos\theta_1 + \beta\sin\theta_1 + \frac{K}{N}\left[\cos(\theta_1 - \theta_2)\cosh\alpha_2\sinh\alpha_1 - \cosh\alpha_1\sinh\alpha_2\right] \tag{5.19}$$

$$\dot{\alpha_2} = \eta\cos\theta_2 + \beta\sin\theta_2 + \frac{K}{N}\left[\cos(\theta_2 - \theta_1)\cosh\alpha_1\sinh\alpha_2 - \cosh\alpha_2\sinh\alpha_1\right] \tag{5.20}$$

$$\dot{\theta_1} = \tanh\alpha_1(\beta\cos\theta_1 - \eta\sin\theta_1) + \omega - \frac{K}{N\cosh\alpha_1}\cosh\alpha_2\sin(\theta_2 - \theta_1) \tag{5.21}$$

$$\dot{\theta_2} = \tanh\alpha_2(\beta\cos\theta_2 - \eta\sin\theta_2) + \omega - \frac{K}{N\cosh\alpha_2}\cosh\alpha_1\sin(\theta_1 - \theta_2). \tag{5.22}$$

We will simplify the equations further by setting $\eta = \beta = 0$. We could also have set $\omega = 0$, effectively making the matrix $\Omega = 0$, but the effect of ω is simply to introduce a linear (slope ω) time dependence into the angular solutions θ_i, hence keeping $\omega \neq 0$ is just as simple as removing it. In essence we are ignoring the particles' individual behaviours and considering only the effect of the interaction terms. Taking the difference of the equations for $\dot{\alpha_i}$ and for $\dot{\theta_i}$ leaves us with the equations:

$$\dot{\alpha} = \frac{K}{N} \sinh \alpha \, (\cos \theta + 1) \tag{5.23}$$

$$\dot{\theta} = \frac{K}{N} \sin \theta \left(\frac{\cosh^2 \alpha_2 + \cosh^2 \alpha_1}{\cosh \alpha_1 \cosh \alpha_2} \right) \tag{5.24}$$

where $\alpha \equiv \alpha_1 - \alpha_2$ and $\theta \equiv \theta_1 - \theta_2$. We will also define $\rho \equiv \alpha_1 + \alpha_2$ and $\phi \equiv \theta_1 - \theta_2$ such that:

$$\dot{\rho} = \frac{K}{N} \sinh \rho \, (\cos \theta - 1) \tag{5.25}$$

$$\dot{\phi} = 2\omega + \frac{K}{N} \sin \theta \left(\frac{\cosh^2 \alpha_2 - \cosh^2 \alpha_1}{\cosh \alpha_1 \cosh \alpha_2} \right). \tag{5.26}$$

We can find exact solutions for $\theta_i(s)$ and $\alpha_i(s)$ using the above sum and difference equations for certain cases with restricted initial conditions.

5.3.1 Case 1

The simplest two-particle system is when both particles start at the same point i.e. $\theta_1^0 = \theta_2^0, \alpha_1^0 = \alpha_2^0$, in which case the sum and difference equations of motion simplify greatly:

$$\dot{\alpha} = 0$$

$$\dot{\theta} = 0.$$

Hence the separation in both the θ- and α-directions is constant, i.e. $\theta(s) = \theta_1^0 - \theta_2^0$ and $\alpha(s) = \alpha_1^0 - \alpha_2^0$. We now use (5.26) to get $\dot{\phi} = 2\omega$. By integrating we obtain:

$$\phi(s) = 2\omega s + \phi^0$$

. Adding the equations for $\theta(s)$ and $\phi(s)$ gives us the solutions for θ_1 and θ_2:

$$\theta_1(s) = 2\omega s + \theta_1^0 \tag{5.27}$$

$$\theta_2(s) = 2\omega s + \theta_2^0. \tag{5.28}$$

Now we use (5.25) to observe that $\dot{\rho} = 0$ and hence that $\rho(s) = \alpha_1^0 + \alpha_2^0$. Finally we add $\rho(s)$ and $\alpha(s)$ to yield:

$$\alpha_1(s) = \alpha_1^0 \tag{5.29}$$

$$\alpha_2(s) = \alpha_2^0. \tag{5.30}$$

Hence if the particles start together, they will stay together. In this somewhat trivial case, the coupling constant can be either positive or negative without changing the solutions.

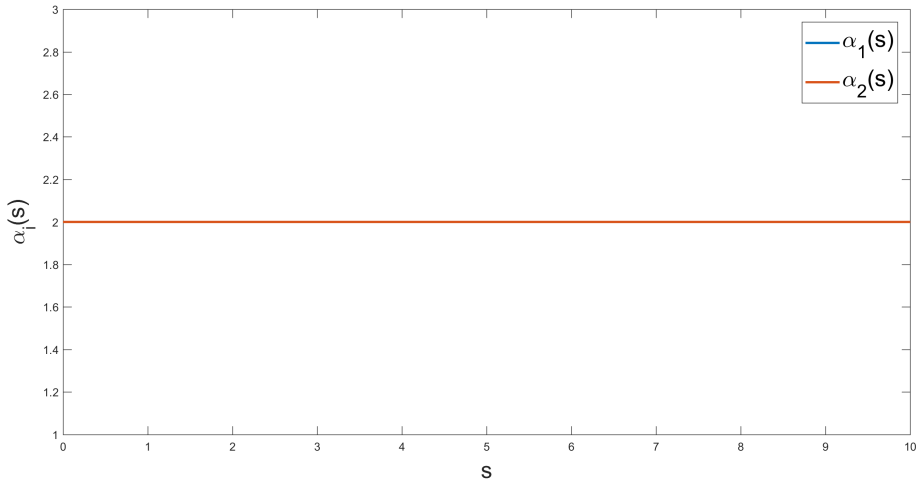

(a) Solutions $\alpha_i(s)$ for Case 1

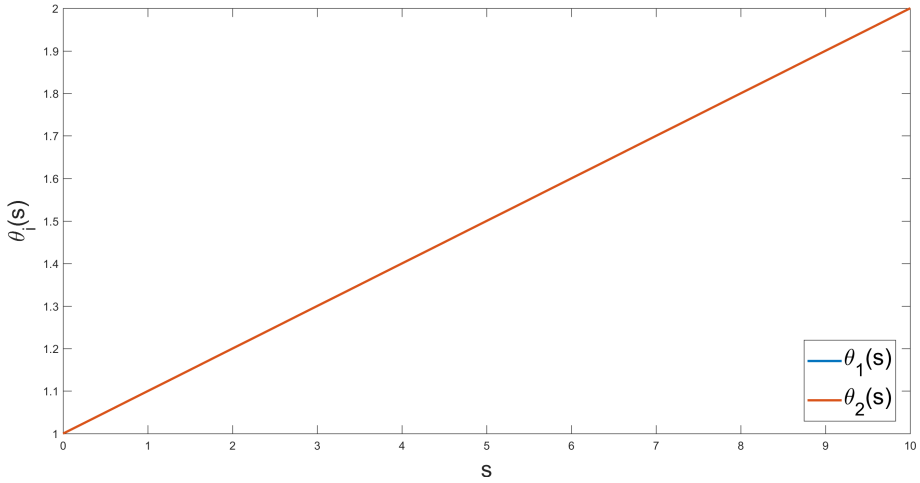

(b) Solutions $\theta_i(s)$ for Case 1

Figure 5.6: Solutions for $N = 2$ where the initial conditions are identical for each particle i.e. $\theta_1^0 = \theta_2^0 = 1, \alpha_1^0 = \alpha_2^0 = 2$. In this case, the particles remain together always for positive or negative coupling constant K. The slope of the angular solutions θ_i is $\omega = 0.1$. A coupling constant of $K = -0.1$ was used.

5.3.2 Case 2

The next case is to consider what happens when $\theta_1^0 = \theta_2^0, \alpha_1^0 = -\alpha_2^0$. The equations of motion (for the differences α and θ reduce to:

$$\dot{\theta} = 0$$

$$\dot{\alpha} = K \sinh \alpha$$

with solutions:

$$\theta(s) = \theta^0 = \theta_1^0 - \theta_2^0 \tag{5.31}$$

$$\alpha(s) = 2\tanh^{-1}\left(ce^{Ks}\right) \tag{5.32}$$

where $c = \tanh\left(\frac{\alpha_1^0 - \alpha_2^0}{2}\right)$. The equations for $\dot{\rho}$ and $\dot{\phi}$ reduce to

$$\dot{\rho} = 0 \tag{5.33}$$

$$\dot{\phi} = 2\omega \tag{5.34}$$

with solutions

$$\phi(s) = 2\omega s + \theta_1^0 + \theta_2^0 \tag{5.35}$$

and

$$\rho(s) = \alpha_1^0 + \alpha_2^0. \tag{5.36}$$

Combining θ with ϕ and α with ρ as before, the solutions for α_i for each particle are:

$$\alpha_1(s) = -\tanh^{-1}(ce^{Ks}) + \frac{\alpha_1^0 + \alpha_2^0}{2} \tag{5.37}$$

$$\alpha_2(s) = \tanh^{-1}(ce^{Ks}) + \frac{\alpha_1^0 + \alpha_2^0}{2} \tag{5.38}$$

while for θ_i we have as before:

$$\theta_1(s) = 2\omega s + \theta_1^0 \tag{5.39}$$

$$\theta_2(s) = 2\omega s + \theta_2^0. \tag{5.40}$$

The solutions α_i develop the same hyperbolic singularities observed in 2.3 if the coupling K is positive, while for $K < 0$, the solutions converge to a single trajectory at $\alpha = 0$ (i.e. at the waist of the hyperboloid). The angular solution θ_i are linear in s i.e. the particles move around the hyperboloid at a constant speed $\frac{d\theta_i}{ds}$.

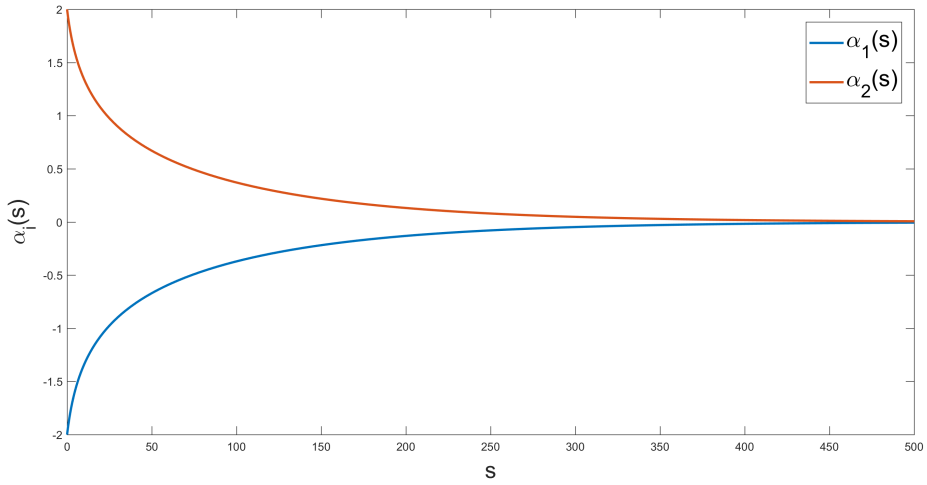

(a) Solutions $\alpha_i(s)$ for Case 2

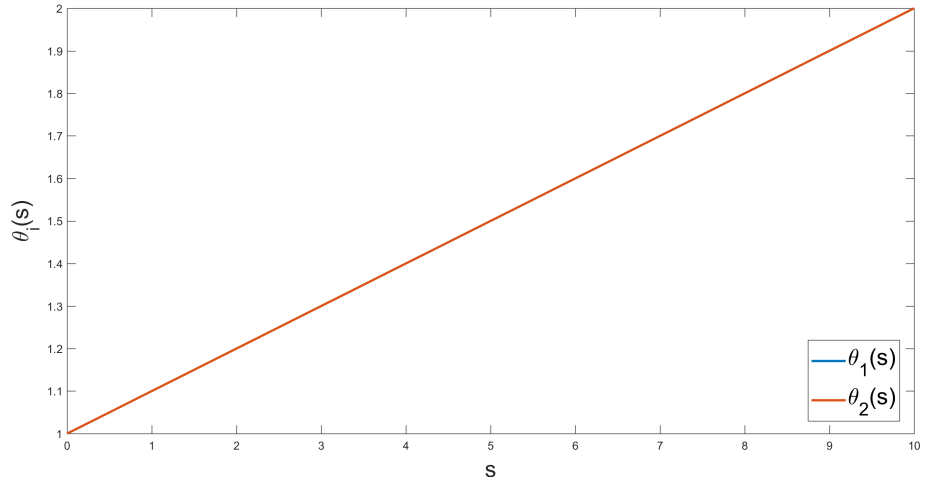

(b) Solutions $\theta_i(s)$ for Case 2

Figure 5.7: Solutions for $N = 2$ with the initial conditions $\theta_1^0 = \theta_2^0 = 1, \alpha_1^0 = -\alpha_2^0 = -2$. α_1 and α_2 converge to the same asymptotic value at the waist of the hyperboloid $\alpha = 0$, while the angular components remain together always, with slope ω (chosen to be 0.1). A coupling constant of $K = -0.1$ was used.

5.3.3 Case 3

We now consider what happens when $\theta_1^0 = -\theta_2^0, \alpha_1^0 = -\alpha_2^0$. Following the same analysis as before we get the following solutions $\alpha_i(s)$:

$$\alpha_1(s) = -\tanh^{-1}\left(\frac{c_2 e^{Ks}}{\sqrt{2c_1 e^{2Ks}+1}}\right) + \frac{\alpha_1^0 + \alpha_2^0}{2} \tag{5.41}$$

$$\alpha_2(s) = \tanh^{-1}\left(\frac{c_2 e^{Ks}}{\sqrt{2c_1 e^{2Ks}+1}}\right) + \frac{\alpha_1^0+\alpha_2^0}{2} \tag{5.42}$$

where the integration constants $c_1 = \tan\left(\frac{\theta_1^0-\theta_2^0}{2}\right)$ and $c_2 = \tanh\left(\frac{\alpha_1^0-\alpha_2^0}{2}\right)\sqrt{2c_1+1}$. The angular solutions $\theta_i(s)$ are:

$$\theta_1(s) = -\tan^{-1}(c_1 e^{Ks}) + \frac{\theta_1^0+\theta_2^0}{2} + \omega s \tag{5.43}$$

$$\theta_2(s) = \tan^{-1}(c_1 e^{Ks}) + \frac{\theta_1^0+\theta_2^0}{2} + \omega s. \tag{5.44}$$

As in case 2, the solutions for α_i will develop hyperbolic singularities when $K > 0$, and will converge to a single solution for $K < 0$. Singularities and convergence (synchronisation) of solutions will develop slower than in case 2, due to the argument of the inverse hyperbolic tangent function being suppressed by a square root of an exponential time dependence. The angular solutions will asymptotically converge to the same straight line with slope ω when $K < 0$, while for $K > 0$ they diverge from each other, asymptotically approaching two straight lines with slope ω separated by a constant value of π.

5.3.4 Case 4

We now consider what happens when $\theta_1^0 = -\theta_2^0, \alpha_1^0 = \alpha_2^0$. Following the same analysis as before we get the following solutions $\alpha_i(s)$:

$$\alpha_1(s) = \alpha_2(s) = \tanh^{-1}\left(\frac{c_2 e^{-Ks}}{\sqrt{2c_1 e^{-2Ks}+1}}\right) + \frac{\alpha_1^0-\alpha_2^0}{2} \tag{5.45}$$

where the integration constants $c_1 = \tan\left(\frac{\theta_1^0-\theta_2^0}{2}\right)$ and $c_2 = \tanh\left(\frac{\alpha_1^0+\alpha_2^0}{2}\right)\sqrt{2c_1+1}$. The angular solutions $\theta_i(s)$ are:

$$\theta_1(s) = -\tan^{-1}(c_1 e^{Ks}) + \frac{\alpha_1^0+\alpha_2^0}{2} + \omega s \tag{5.46}$$

$$\theta_2(s) = \tan^{-1}(c_1 e^{Ks}) + \frac{\alpha_1^0+\alpha_2^0}{2} + \omega s. \tag{5.47}$$

For positive K the solutions α_i decay to zero together, and will develop hyperbolic singularities when the coupling constant is negative (the reverse of case 3). Likewise, the angular solutions are essentially the reverse of those in case 3, becoming

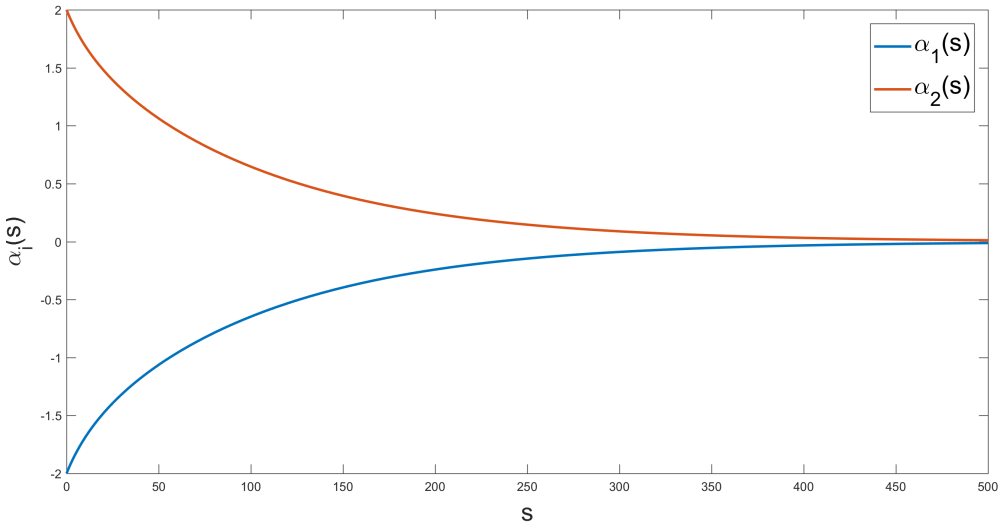

(a) Solutions $\alpha_i(s)$ for Case 3

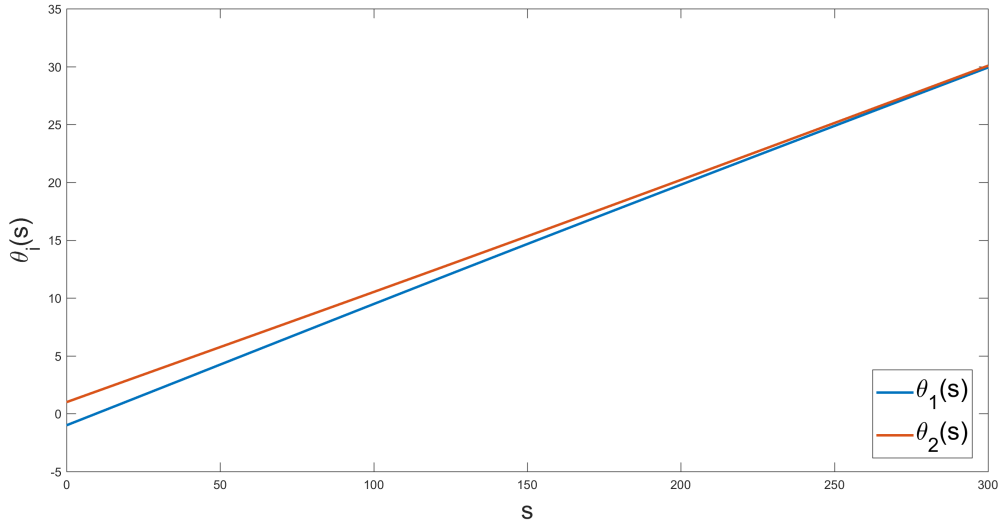

(b) Solutions $\theta_i(s)$ for Case 3

Figure 5.8: Solutions for $N = 2$ with the initial conditions $\theta_1^0 = -\theta_2^0, \alpha_1^0 = -\alpha_2^0$. The solutions for α converge to the same trajectory, as in case 2, but slower. The angular solutions also converge, to a single line with constant slope $\omega = 0.1$. $K = -0.1$

separated for positive K (asymptotically approaching straight lines split apart by π, and converging for negative K.

The different synchronisation behaviours of the two-particle systems considered are reflected by the Kuramoto order parameter (1.4) and the disorder parameter

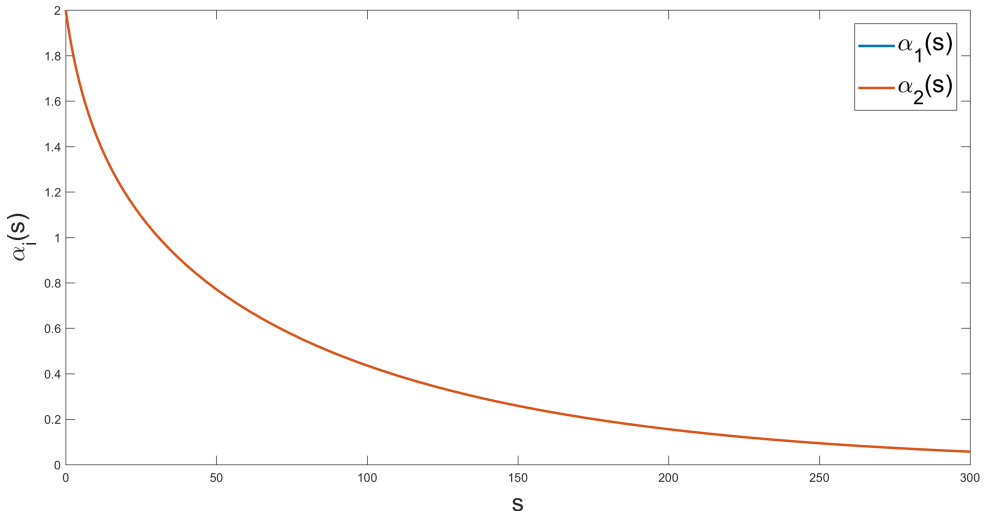

(a) Solutions $\alpha_i(s)$ for Case 4

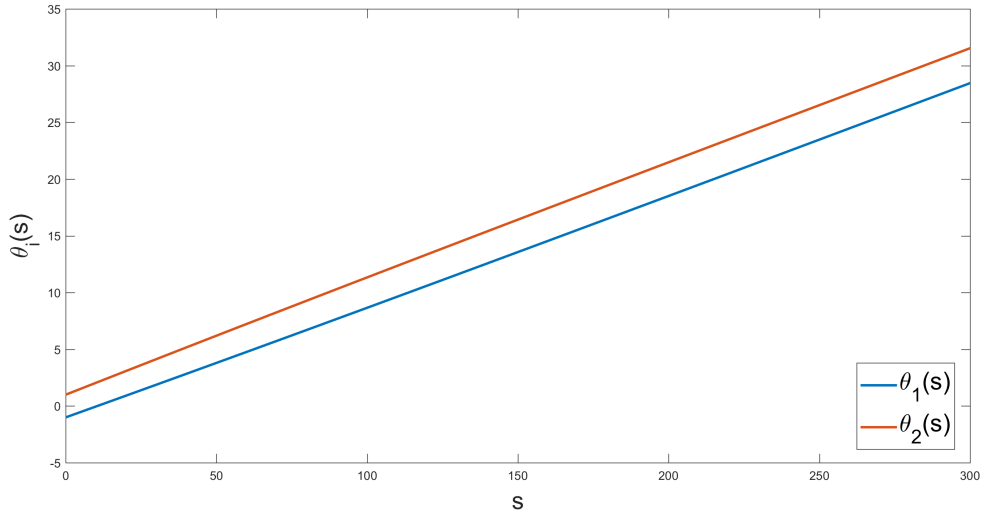

(b) Solutions $\theta_i(s)$ for Case 4

Figure 5.9: Solutions for $N = 2$ with the initial conditions $\theta_1^0 = -\theta_2^0 = -1, \alpha_1^0 = \alpha_2^0 = 2$. α_1 and α_2 both decay towards $\alpha = 0$ for positive K. θ_1 and θ_2 diverge slowly and approach parallel lines of slope $\omega = 0.1$ separated by π i.e. the particle are phase-locked on opposite sides of the circle. $K = 0.1$.

(2.19) in Figure 5.10. Recall that an order parameter with unit value corresponds to complete synchronisation, as does a disorder parameter of zero. Also note that each parameter measures synchronisation in a different direction/dimension. In Case 1, all initial conditions were identical, hence the particles always remained together, and so $R(s) = 1$ and $r(s) = 0$ for all values of s, while in Case 4

the equilibrium state was that the angular components $\theta_{1,2}(s)$ adopted an anti-synchronised configuration, with each particle locked on opposite sides of the circle, resulting in an order parameter of $R = 0$. The hyperbolic components always remained together, hence the disorder parameter was always zero. The long-term mean spacetime separations $I(s)$ for cases 1-3 was zero, showing synchronisation, while for case 4, $I(s)$ approached a value of 1.

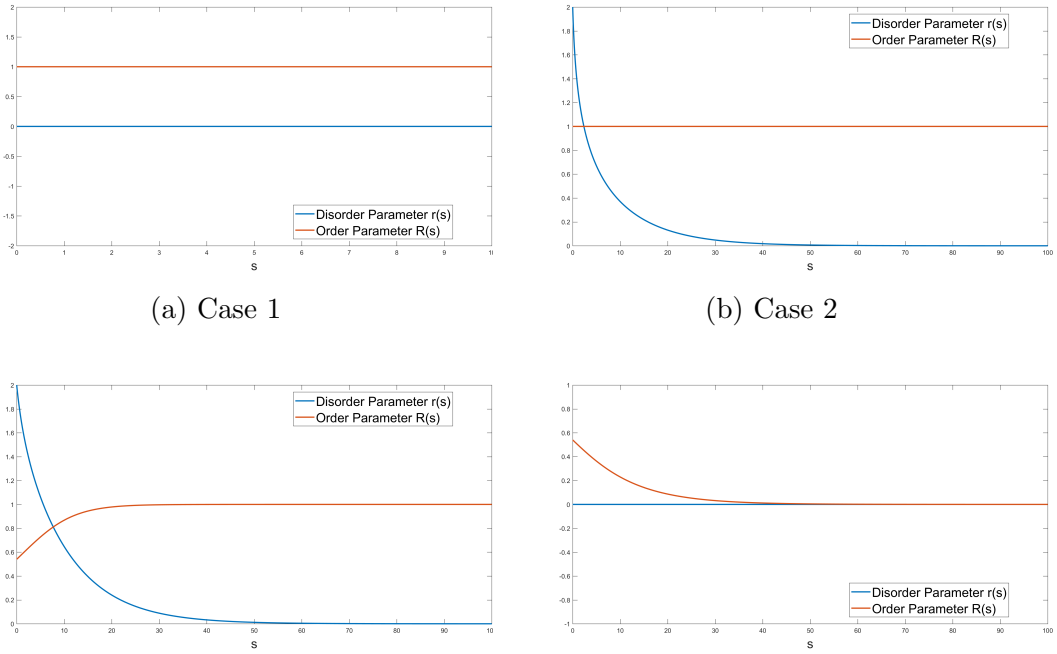

(a) Case 1

(b) Case 2

(c) Case 3

(d) Case 4

Figure 5.10: The disorder parameters and Kuramoto order parameters for the $N = 2$ solutions for the 2-dimensional hyperboloid model. Asymptotic values for the order and disorder parameters of 1 and 0 respectively, show that complete synchronisation occurs for cases 1-3. For case 4, the disorder parameter goes to 0, but the order parameter is 0, hence this system only partially synchronises i.e. it only synchronises in the α-direction.

By studying the hyperboloid model for a system of two particles with certain initial conditions, we have shown analytically that, as in the one dimensional hyperbolic model, solutions can converge, becoming completely synchronised, or only partially synchronise, with particle trajectories only converging to parallel lines. Solutions can also become singular at some finite time, depending on the sign of the coupling constant, as in the one dimensional model.

5.4 Numerical Results

In this section we investigate numerical properties of the vector hyperboloid model ((5.6) and (5.7)) for a system of $N = 20$ particles with either positive or negative coupling constant $K_i = K = \pm 1$ parameters $\beta_i, \eta_i, \omega_i$ and initial conditions α_i^0, θ_i^0. We describe the different types of solutions which emerge from the vector hyperboloid model such as bounded and unbounded trajectories, as well as the collective (synchronous or otherwise) behaviour of the system, and how this depends on the chosen initial conditions. Firstly we summarise numerical properties specific to $N = 2$.

5.4.1 Numerical Observations for N=2

To understand the two particle system for general initial conditions and parameters, we must rely on numerical results rather than exact results due to the complexity of the equations of motion. Synchronisation was best achieved when the initial hyperbolic angles α_i^0 were very close to the waist of the hyperboloid $\alpha = 0$. If either of the particles started too far from the waist (with both particles on the same side of the waist), then we encounter singularities consistent with those predicted in the exact results above. It is possible for the system to attain some level of synchronisation even when the particles start far away from the waist if, and only if, they start on opposite sides of the waist, e.g. if particle 1 starts at $\alpha_1^0 = 40$ and particle 2 starts at $\alpha_2^0 = -40$. This system will of course take much longer to reach synchronisation than if the particles had started much closer together. We also find that the system is insensitive to the choice of the initial angles θ_i^0.

5.4.2 Negative coupling

Setting the matrix $\Omega_i = 0$ for all i (i.e. setting the parameters $(\omega_i = \beta_i = \eta_i = 0)$ removes the "natural" behaviour of the particles, so the only dynamical behaviour arises from the coupling between particles. For negative (attractive) coupling $(K = -1)$, and initial conditions θ_i^0 distributed randomly around the hyperboloid i.e. between 0 and 2π, and initial α_i^0 spread randomly over a small region near the waist of the hyperboloid $(-1/1000 < \alpha_i^0 < 1/1000)$, then the system synchronises completely, with particles converging to the same *stationary* point. The initial conditions α_i^0 must be restricted to a small region around the waist for solutions to exist for all s; if they are too far from the waist (even if they are all close to each other), then we encounter singularities of the kind we observed in §5.3. If the initial conditions are spread *evenly* i.e. *symmetrically* above and below the

waist $\alpha = 0$, then the interval over which the particles are spread can be increased somewhat ($-1/100 < \alpha_i^0 < 1/100$) before developing hyperbolic singularities, in contrast to the $N = 2$ system, where the particles can start arbitrarily far away. The parameters η and β boost the stationary synchronised solutions $\alpha_i(s)$ up or down the hyperboloid linearly towards plus or minus infinity, respectively, i.e. they add a linear s-dependence with slope η or $-\beta$ to the stationary solutions. The angular solutions $\theta_i(s)$ remain stationary i.e. the solutions stay in the same vertical plane of the hyperboloid and do not rotate. If both boost parameters η and β are non zero, then the synchronised motion along the hyperboloid $\alpha_i(s)$ is linear with slope $\sqrt{\eta^2 + \beta^2}$. The parameter ω causes the stationary solutions to rotate around the hyperboloid at a constant frequency ω with constant α_i.

For general driving matrix $\Omega = \begin{pmatrix} 0 & \eta & \beta \\ \eta & 0 & -\omega \\ \beta & \omega & 0 \end{pmatrix}$, there are three different types of solutions (See Figure 5.11) for $\alpha_i(s)$ and $\theta_i(s)$, depending on the relative magnitudes of the driving parameters and hence the sign of Δ^2.

1. if $\Delta^2 = \beta^2 + \eta^2 - \omega^2 < 0$, then the eigenvalues of the matrix Ω (5.10) are imaginary, and so the solutions $\alpha_i(s)$ and $\theta_i(s)$ are periodic, with angular frequency given by the absolute value of the non-zero eigenvalue $\frac{|\sqrt{\beta^2+\eta^2-\omega^2}|}{2\pi}$ (See Figure 5.12). The angular solutions $\theta_i(s)$ also have a linear s-dependence with slope $\frac{|\sqrt{\beta^2+\eta^2-\omega^2}|}{2\pi}$.

2. if $\Delta^2 > 0$ then the eigenvalues are real and the synchronised solutions $\alpha_i(s)$ are linear in with slope $\sqrt{\beta^2 + \eta^2 - \omega^2}$ while the long term angular solutions θ_i are stationary.

3. The third (and special) case $\Delta^2 = 0$ gives solutions α_i which look like inverse hyperbolic functions, while the angular solutions are asymptotically stationary.

Note that the insets in Figure 5.11 all show convergence[1] of the particles' trajectories, demonstrating that synchronisation occurs for $K < 0$ and any value of Δ^2.

It is possible to have small random perturbations in the driving parameters so that the driving matrix Ω_i depends on i and still achieve synchronisation, and without singularities occurring, but only if ω_i is relatively large compared to the other

[1]The angular solutions seem to split into "clusters"; in fact these two clusters are separated by 2π in the angular direction (around the hyperboloid) i.e. they are all together.

two parameters, i.e. the motion in the α direction must be bounded (e.g. periodic). Even with this bounded periodic motion, large perturbations will cause hyperbolic singularities. If the α-motion is naturally unbounded, then any randomness (i dependence) in any of the parameters causes singularities. As we observed in the $1+1$ dimensional hyperbolic Kuramoto model §3, there is no critical coupling. The coupling constant K affects the time scale over which the system evolves e.g. a large coupling will cause the system to synchronise faster.

We can gain some numerical understanding of the N particles system and confirm the analytical results above using Fourier transforms to analyse the periodicity of the solutions. The mean Fourier spectrum is shown in Figure 5.12. This figure uses driving parameters $\omega = 0.3, \beta = 0.2, \eta = 0.1$, giving a Δ^2 value of -0.04 and a fundamental frequency (given by $\frac{1}{2\pi}|\sqrt{\eta^2 + \beta^2 - \omega^2}|$) of 0.0318. The large peak at zero in Figure 5.12 is due to a constant in the solutions $\alpha_i(s)$. From general solution (5.13) we see that the solution component corresponding to $\lambda_1 = 0$ has no time dependence (i.e. it is a zero mode). This peak also indicates the mean value of the the solutions $\alpha_i(s)$. The presence of harmonics, the progressively smaller peaks at integer multiples of the fundamental (linear) frequency means the periodic solutions are not pure sinusoids. Note that the Fourier spectrum only tells us that the particles oscillate at the same frequency; it does not give any information about whether the particle trajectories are synchronised in terms of their relative positions i.e. phase locked. The order and disorder parameters shown in Figure 5.13 show that this system fully synchronises, with an order parameter of unity and a disorder parameter of zero, at roughly $s = 10$.

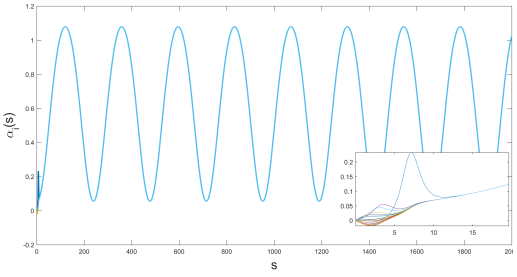

(a) Numerical Solutions $\alpha_i(s)$ with $K = -1$ and parameters $\omega = 0.03, \eta = \beta = 0.01$. $\Delta^2 < 0$.

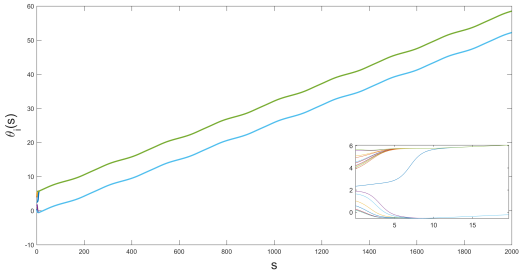

(b) Numerical Solutions $\theta_i(s)$ with $K = -1$ and parameters $\omega = 0.03, \eta = \beta = 0.01$. $\Delta^2 < 0$.

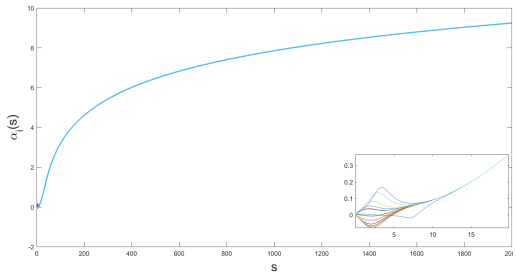

(c) Numerical Solutions $\alpha_i(s)$ with $K = -1$ and parameters $\omega = 0.05, \beta = 0.04, \eta = 0.03$. $\Delta^2 = 0$.

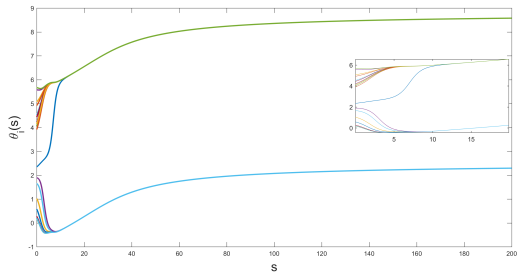

(d) Numerical Solutions $\theta_i(s)$ with $K = -1$ and parameters $\omega = 0.05, \beta = 0.04, \eta = 0.03$. $\Delta^2 = 0$.

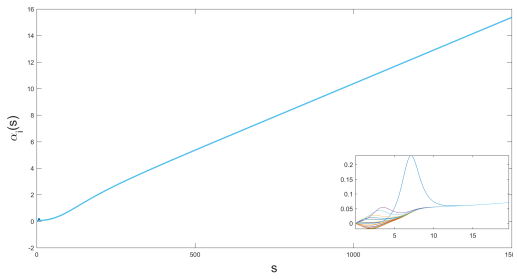

(e) Numerical Solutions $\alpha_i(s)$ with $K = -1$ and parameters $\omega = \beta = \eta = 0.01$. $\Delta^2 > 0$.

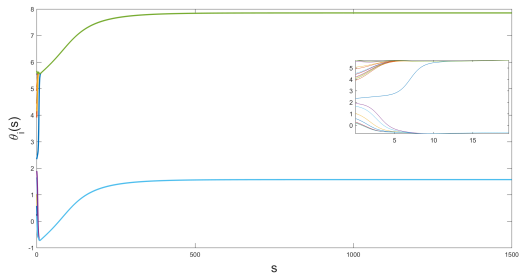

(f) Numerical Solutions $\theta_i(s)$ with $K = -1$ and parameters $\omega = \beta = \eta = 0.01$. $\Delta^2 > 0$.

Figure 5.11: N particle solutions for the Hyperboloid model with negative coupling. There are three different types of solutions, depending on the relative magnitude of the driving parameters and the sign of Δ^2 in (5.11): 5.11a and 5.11b show oscillatory behaviour, 5.11c and 5.11d show an inverse hyperbolic trajectory and 5.11e and 5.11f are linear. The inserts show the initial transient behaviour. Note that the angular solutions seem to split into "clusters"; in fact these two clusters are separated by 2π i.e. they are part of the same cluster.

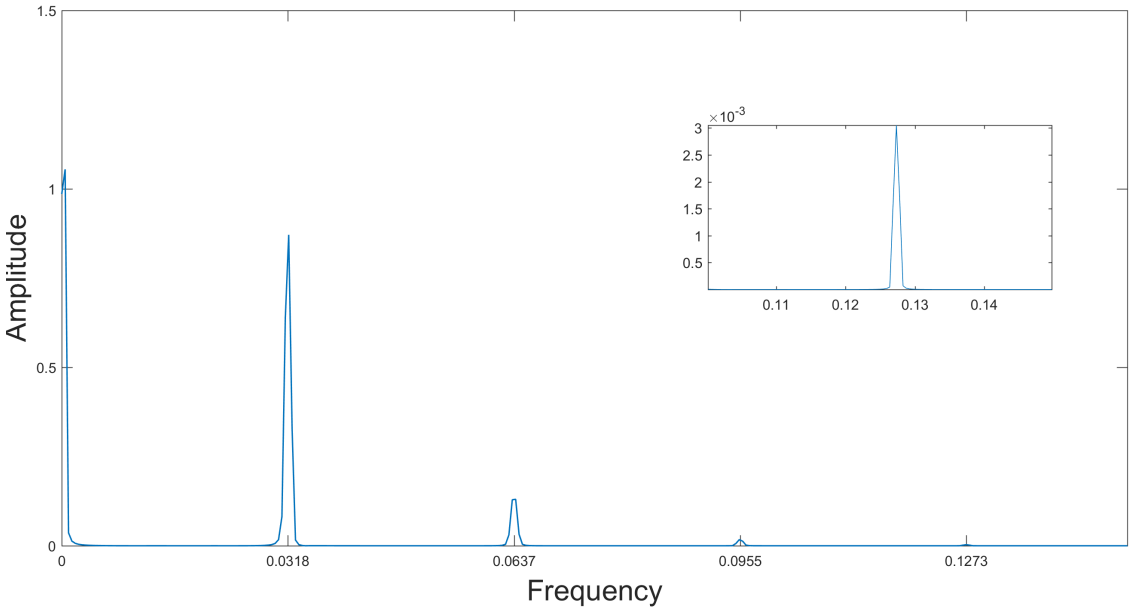

Figure 5.12: Mean Fourier Transform of $\alpha_i(s)$ of a 20 particle system with $K = -1$. The (fundamental) frequency is given by the absolute value of the eigenvalue $\sqrt{\beta^2 + \eta^2 - \omega^2}$ divided by 2π. The parameters used are $\omega = 0.3, \beta = 0.2, \eta = 0.1$, giving a Δ^2 value of -0.04, giving a fundamental frequency of 0.0318. The peak at 0 frequency is due to a constant in the s-domain. The inset shows the fourth harmonic at 4 times the fundamental frequnency. A Hanning window was applied to the numerical results to reduce spectral leakage [42], which arises from sampling a periodic signal over a finite time interval.

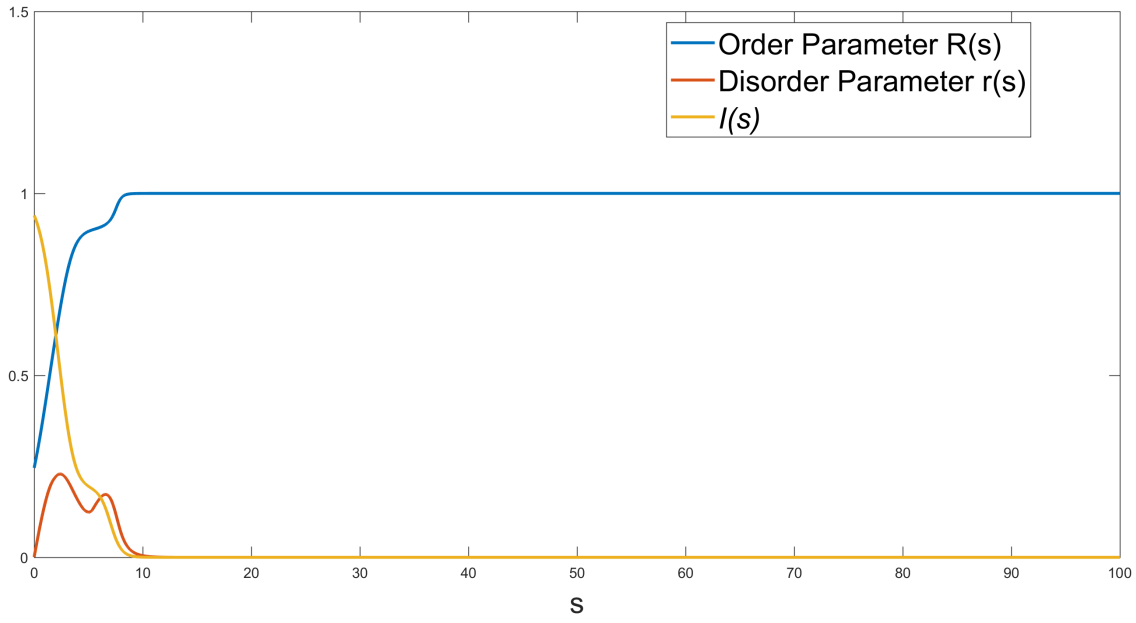

Figure 5.13: Kuramoto order parameter $R(s)$ and disorder parameter $r(s)$ for a system of $N = 20$ particles with negative coupling constant $K = -1$ and parameters $\omega = 0.3, \beta = 0.2, \eta = 0.1$ ($\Delta^2 = -0.04$). The asymptotic values of $R = 1$ and $r = 0$ indicate that the system has fully synchronised. Also shown is the mean separation $I(s)$, which goes to zero for synchronised systems.

5.4.3 Positive coupling

Reversing the sign of K makes the interactions between particles repulsive rather than attractive, hence the behaviour is quite different. When the coupling between particles was negative (attractive), we saw that the particles generally synchronised, unless the initial conditions were not tight enough. As we saw in the negative coupling case, there are three types of solutions depending on the relative sizes of the driving parameters: periodic, hyperbolic and linear. These are shown in Figure 5.15. However, if the coupling is positive, then the particles will often split into two very loose clusters which move apart in the α-direction, and which are anti-synchronised in the θ-direction, i.e. they are completely out-of-phase and synchronisation does not occur (see Figure 5.14). The initial conditions α_i^0, which can be chosen at random or evenly spaced, do not need to be as tightly restricted (they can be distributed over the interval $-1/10 < \alpha_i^0 < 1/10$) as the negatively coupled system to avoid singularities. If ω is small compared to η and β, meaning that the solutions are unbounded, then hyperbolic singularities can occur as the two clusters move apart, as illustrated in Figure 5.15e at $s = 1800$. We can avoid these singularities by choosing ω large enough to make the eigenvalues imaginary (i.e. $\Delta^2 > 0$), resulting in bounded periodic solutions, such as in Figure 5.15a.

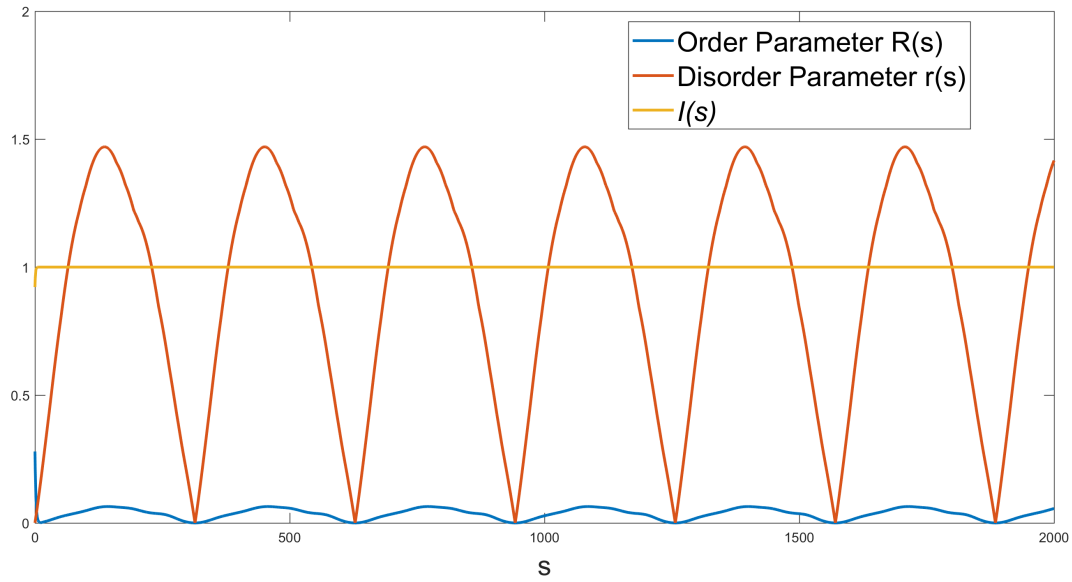

Figure 5.14: Order and Disorder parameters $R(s)$,$r(s)$ and $I(s)$ for the same system as in Figure 5.13, except with positive coupling $K = +1$. Neither of the synchronisation measures R or r approach a constant asymptotic value, hence the system does not synchronise. Also a value of $I \neq 0$ means the system is not synchronised

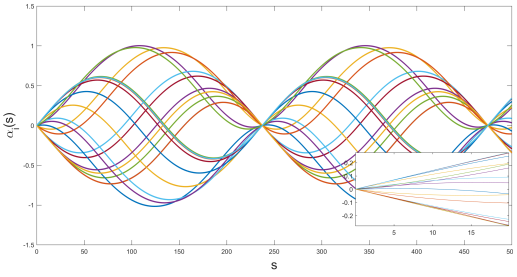

(a) Numerical Solutions $\alpha_i(s)$ with $K = 1$ and parameters $\omega = 0.03, \eta = \beta = 0.01$. $\Delta^2 < 0$.

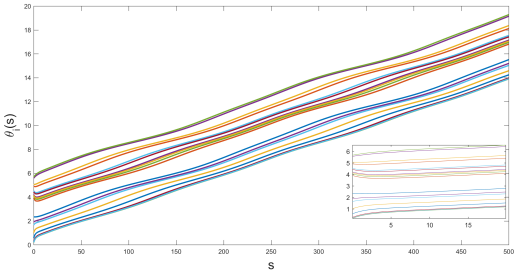

(b) Numerical Solutions $\theta_i(s)$ with $K = 1$ and parameters $\omega = 0.03, \eta = \beta = 0.01$. $\Delta^2 < 0$.

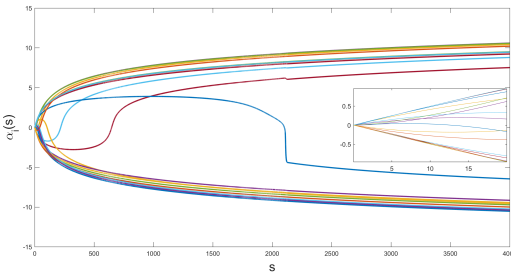

(c) Numerical Solutions $\alpha_i(s)$ with $K = 1$ and parameters $\omega = 0.05, \beta = 0.04, \eta = 0.03$. $\Delta^2 = 0$.

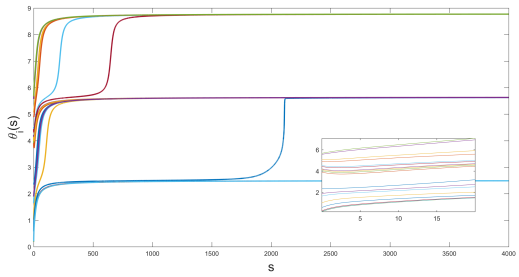

(d) Numerical Solutions $\theta_i(s)$ with $K = 1$ and parameters $\omega = 0.05, \beta = 0.04, \eta = 0.03$. $\Delta^2 = 0$.

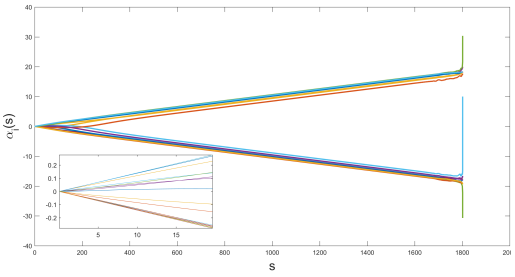

(e) Numerical Solutions $\alpha_i(s)$ with $K = 1$ and parameters $\omega = \beta = \eta = 0.01$. $\Delta^2 > 0$.

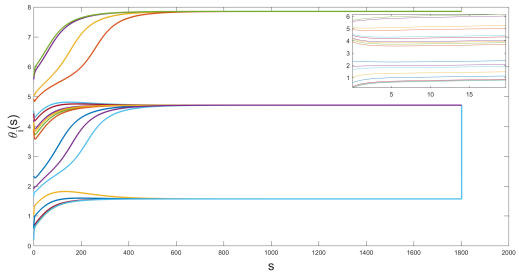

(f) Numerical Solutions $\theta_i(s)$ with $K = 1$ and parameters $\omega = \beta = \eta = 0.01$. $\Delta^2 > 0$.

Figure 5.15: N particle solutions for the Hyperboloid model with positive coupling. There are three different types of solutions, depending on the relative magnitude of the driving parameters and the sign of Δ^2 in (5.11): 5.15a and 5.15b show oscillatory behaviour, 5.15c and 5.15d show an inverse hyperbolic trajectory and 5.15e and 5.15f are linear. The inserts show the initial transient behaviour. Note, in 5.15d and Figure 5.15f, the solutions seem to separate into three clusters, however the top and bottom clusters are separated by 2π and are therefore part of the same cluster.

Chapter 6

Conclusion and Future Directions

The Kuramoto model is the most widely used model for the synchronisation of coupled phase oscillators. It can be expressed in matrix form where the matrices are elements of the rotation group $SO(2)$, which can be generalised to matrix models with elements belonging to any Lie group, compact or non-compact. In this thesis we have studied a hyperbolic form of the Kuramoto model by replacing the compact rotation group $SO(2)$ with the non-compact group $SO(1,1)$. The equations of motion are invariant under $SO(1,1)$ transformations, just as the Kuramoto model is invariant under $SO(2)$ transformations i.e. rotations. We solved the model exactly for a system of $N = 2$ nodes and studied its dynamics. This model varies from the Kuramoto model in that it allows unbounded trajectories, where the particles propagate out to infinity, and trajectories which may become singular in a finite time i.e. solutions may exist only locally rather than globally. However, provided solutions exist globally, which may be ensured by sufficiently restricting the initial conditions, the emergent phenomenon of synchronisation remains well-defined in this non-compact model and can be detected and quantified by synchronisation measures such as D, r, P, ξ. If the driving parameters ω_i are identical, then their trajectories coincide, leading to complete synchronisation; if the parameters ω_i are non-identical, then the trajectories trace out parallel paths and we have incomplete/partial synchronisation.

There is also no critical coupling constant for this hyperbolic Kuramoto model, unlike the ordinary KM [21]; synchronisation occurs whenever $K > 0$ and can still partially occur if there is negative coupling, as long as there is only one node with negative coupling, and as long as this negative coupling is much smaller than the positive couplings. The inclusion of more than one negatively coupled node caused the system to develop singularities. This is very different to the Kuramoto system, wherein the inclusion of repulsive interactions can cause desynchronised

states or π-states, where the conformists (attractive) and contrarians (repulsive) cluster separately from each other. Other modifications of the model, such as the inclusion of a (hyperbolic) phase lag or external fields were studied numerically and showed similar behaviours as in the ordinary Kuramoto system [15, 38]; the inclusion of a phase-lag can be used to control the synchronisation frequency, but cannot prevent synchronisation entirely, unlike in the KM. External fields, as in the KM, tend to counteract synchronisation for small field amplitudes and force the system into a stationary synchronised state for large amplitudes.

We have also developed a vector model of synchronisation for non-compact symmetry groups, in which particles are no longer constrained to motion on the unit circle as in the Kuramoto model. In choosing the one-dimensional Lorentz group $SO(1,1)$ we regain the hyperbolic Kuramoto model, in which particles move on the unit hyperbola. As the equations are invariant under Lorentz transformations, the vector model leads to a physical interpretation of the model as a system of N relativistic particles interacting in $1+1$ dimensional spacetime, where $\boldsymbol{x}_i = (x_i^0, x_i^1)$ are spacetime coordinates of a particle i. For a valid relativistic interpretation, the hyperbolic Kuramoto model requires choosing sufficiently large driving parameters ω_i such that the proper time is a strictly increasing function of s, and requires a modification which takes into account the finite time delay of particle interactions, which has not been numerically modelled in this thesis, but which is expected to have little effect on synchronisation [39, 40].

Another non-compact manifold on which synchronisation occurs is the $1+2$ dimensional Lorentz group $SO(1,2)$. We formulated a vector model of synchronisation for the non-compact symmetry group $SO(1,2)$, where particles interact on a one-sheeted hyperboloid. By fixing an angle, or a hyperbolic angle, the resulting equations of motion reduce to the hyperbolic, or the ordinary Kuramoto models respectively. Exact solutions for a single particle on the hyperboloid surface showed that there are three distinct trajectory types: oscillatory, linear and inverse hyperbolic trajectories. The equations were also solved exactly for a restricted subset of initial conditions for a system of two particles, and it was shown that, as in the one-dimensional model, synchronised states and singularities can both form depending on the coupling constant. The degree of synchronisation was measured in a number of ways; the Kuramoto order $R(s)$ parameter was used to quantify synchronisation in angular (θ) direction while the disorder parameter $r(s)$, used in the 1-dimensional model, was used to quantify synchronisation in the (α) direction. A 2-dimensional measure of synchronisation $I(s)$ was introduced, based on the Minkowski scalar product, to measure the overall synchronisation on the hyperboloid surface. The general 2-dimensional hyperboloid model displays a wide range of dynamic behaviour, such as unbounded and singular solutions as in the 1-dimensional hyperbolic Kuramoto model, and also exhibits three distinct types

of dynamics, depending on the relative magnitudes of the driving parameters. For $\Delta^2 = \beta^2 + \eta^2 - \omega^2 < 0$ the solutions are periodic, for $\Delta^2 > 0$ solutions are asymptotically linear and for $\Delta^2 = 0$ solutions are inverse hyperbolic functions. Each of these can exhibit synchronous, asynchronous or divergent/singular behaviour depending on the parameters of the system and the sign of the coupling constant. Trajectories generally synchronise for negative coupling and desynchronise for positive coupling. For both positive and negative coupling, solutions may exist only locally, i.e. they may develop singularities at some time if the initial conditions are not restricted to a small region near the waist of the hyperboloid.

As in the 1 dimensional hyperbolic model there is no critical coupling; synchronisation can occur for any $K < 0$. The vector model for $SO(1,2)$ has not yet led to a satisfactory relativistic interpretation, which may not be at all possible. It is well known that there is no satisfactory formulation for an interacting multi-particle system in classical relativistic mechanics except for some few special cases [41]. Indeed it seems that the $SO(1,1)$ model is one of those few special cases. Whether or not the $SO(1,2)$ vector model is another is unclear and is a possible topic for future study. Another possibility for future exploration is the generalisation of the *matrix* model to higher dimensional non-compact groups, in particular the group $SO(1,2)$. Whereas the one-dimensional vector and matrix models resulted in the same N equations of motion (for N particles), the matrix model for $SO(1,2)$ will not be the same as the vector model since the Lie group $SO(1,2)$ is a 3-parameter group, and will therefore lead to $3N$ coupled equations of motion rather than $2N$ for the vector model.

The results presented in this thesis are significant for several reasons. The first is that we have extended the Kuramoto model to non-compact manifolds and have shown that synchronisation is possible even when solution trajectories are unbounded, opening the door to the study of synchronisation in other models with unbounded trajectories. Secondly, the hyperbolic model can be interpreted as a relativistic interacting multi-particle dynamical system, something which is quite rare and therefore deserves further examination. The hyperbolic Kuramoto model has endless room for future investigation. Many of the generalisations and variations of the ordinary Kuramoto model could be applied to the non-compact version. Examples include time delayed couplings, which have been considered in this thesis but not explicitly modelled, the possibility of chimera states, and the effect of complex network topologies, such as small world networks or scale-free networks [1,2,6,18,43]. as well as networks in which there are multiple competing populations of oscillators [28]. In this thesis we have only considered the basic all-to-all network, where each particle/node is connected to every other. More complex network topologies and coupling configurations may lead to interesting dynamical behaviours.

Appendix I

This appendix contains a paper entitled "*Synchronization of relativistic particles in the hyperbolic Kuramoto model*" which has been published in the journal *Chaos* and which is based on the original research contained in this thesis.

CHAOS **28**, 053116 (2018)

Synchronization of relativistic particles in the hyperbolic Kuramoto model

Louis M. Ritchie,[a] M. A. Lohe,[b] and Anthony G. Williams[c]
Centre for Complex Systems and Structure of Matter, Department of Physics, University of Adelaide, Adelaide 5005, Australia

(Received 7 January 2018; accepted 7 May 2018; published online 23 May 2018)

We formulate a noncompact version of the Kuramoto model by replacing the invariance group $SO(2)$ of the plane rotations by the noncompact group $SO(1, 1)$. The N equations of the system are expressed in terms of hyperbolic angles α_i and are similar to those of the Kuramoto model, except that the trigonometric functions are replaced by hyperbolic functions. Trajectories are generally unbounded, nevertheless synchronization occurs for any positive couplings κ_i, arbitrary positive multiplicative parameters λ_i and arbitrary exponents ω_i. There are no critical values for the coupling constants. We measure the onset of synchronization by means of several order and disorder parameters. We show numerically and by means of exact solutions for $N = 2$ that solutions can develop singularities if the coupling constants are negative, or if the initial values are not suitably restricted. We describe a physical interpretation of the system as a cluster of interacting relativistic particles in $1 + 1$ dimensions, subject to linear repulsive forces with space-time trajectories parametrized by the rapidity α_i. The trajectories synchronize provided that the particle separations remain predominantly time-like, and the synchronized cluster can be viewed as a bound state of N relativistic particle constituents. We extend the defining equations of the system to higher dimensions by means of vector equations which are covariant with respect to $SO(p, q)$. *Published by AIP Publishing*. https://doi.org/10.1063/1.5021701

The Kuramoto model and its many extensions continue to provide new and interesting examples of the behavioural characteristics of complex dynamical systems, such as the properties of synchronized states, the role of critical couplings, the effects of nontrivial network topologies, and of distributed amplitudes of oscillation and link-dependent time delays. We formulate the Kuramoto model as the evolution equations of a system of $SO(2)$ rotation matrices, with nonlinear cubic interactions between connected nodes. We investigate a noncompact version of the Kuramoto model by replacing $SO(2)$ by the Lorentz group $SO(1, 1)$, leading to equations for the hyperbolic angles in which the trigonometric interactions are replaced by hyperbolic functions. This hyperbolic model has properties similar to those of the standard Kuramoto model in that the system synchronizes for positive coupling constants and positive amplitudes but differs in that there is no critical value for the coupling constants; instead, synchronization occurs for all positive couplings. Other differences are the appearance of unbounded trajectories and, in some cases, singularities in which solutions exist only locally for certain initial values. We present a physical interpretation of the model as a system of relativistic particles of unit mass in which the coordinate at each node is the rapidity of the corresponding particle. Trajectories are restricted to a space-time hyperbola and particles are propelled out to infinity with increasing speed as a synchronized cluster. Particles on different hyperbolas can also synchronize provided that the time-dependent network topology is not too sparse. This system represents a consistent relativistic multiparticle model with an arbitrary number of nodes.

I. INTRODUCTION

Synchronization is a ubiquitous phenomenon in physical, biological and other complex systems which has been widely investigated.[1–5] Synchronization involves two or more interacting elements of a dynamical system whose properties become correlated in time, leading to the evolution of the system as a collective entity. A widely studied model of synchronization is the Kuramoto model[6] along with its many extensions and generalizations.[5,7] The usefulness of this model arises from its amenability to both numerical and analytical investigations, while at the same time displaying a wide variety of synchronization behaviours. The Kuramoto model consists of a population of N harmonic oscillator variables $\theta_i(t)$ with natural frequencies ω_i and coupling constants κ_i, with the governing equations

$$\dot{\theta}_i = \omega_i + \frac{\kappa_i}{N}\sum_{j=1}^{N}\lambda_i\lambda_j \sin(\theta_j - \theta_i), \tag{1}$$

where we have included multiplicative parameters λ_i which denote the amplitudes of oscillation.[8] Such parameters were first introduced by Daido[9] in 1987 but have also been used in more recent applications.[10,11] One could also include nontrivial network couplings, distributed phase lag, time delay, etc.; see Ref. 5 for various generalizations. It is well known[1,4] that for weak couplings, the nodes oscillate almost independently, while for stronger couplings, the oscillators

[a]louis.ritchie@adelaide.edu.au
[b]Max.Lohe@adelaide.edu.au
[c]anthony.williams@adelaide.edu.au

partially synchronize, and for sufficiently large couplings, the oscillators phase lock with a common frequency.

The properties of the Kuramoto model are closely linked to those of the 2-dimensional rotation group, for example, (1) is invariant under plane rotations in which $\theta_i \to \theta_i + \theta_0$, for any constant angle θ_0. Equation (1) is also covariant with respect to rotating frames of reference, in which $\theta_i \to \theta_i + \omega_0 t$ for any constant frequency ω_0, leading to $\omega_i \to \omega_i - \omega_0$. The model (1) can equivalently be regarded as the evolution equations of two-dimensional rotation matrices parametrized by θ_i. Higher-dimensional matrix generalizations of the Kuramoto model exist in which the rotation group is replaced by any compact classical Lie group.[12] For example, the N Eqs. (1) can be generalized to $Nd(d-1)/2$ independent equations for elements of the rotation matrices $O_i \in SO(d)$ in any dimension $d \geqslant 2$ and has synchronization properties similar to those of the Kuramoto model. Rigorous results, for general matrix models, such as the existence and stability of phase-locked states have been obtained.[13]

Besides the matrix models, for which the trajectories lie on the compact group manifold, there are vector models with trajectories in d dimensions that are confined to the unit sphere S^{d-1}. For $d=2$, these reduce to the Kuramoto model, where the unit 2-vector is given by $\boldsymbol{x}_i = (\cos\theta_i, \sin\theta_i)$. Synchronization occurs with properties similar to those of the Kuramoto model.[12,14,15]

A common feature of these generalizations is that trajectories are restricted to compact manifolds, but the possibility that dynamical models can be extended to include noncompact manifolds was previously noted,[12] and general matrix models have since been defined and analyzed.[16] Several points of difficulty arise with these models, which naturally have unbounded trajectories. Firstly, singularities can appear as the system evolves, i.e., the solutions might exist only locally; secondly, the initial values of the system must generally be restricted for synchronization to occur, otherwise trajectories can rapidly diverge, preventing any possibility of synchronization. Sufficient conditions for the global existence of solutions, with restricted initial values, and the existence of phase-locked states have been derived.[16] These results show that the concept of synchronization extends to matrix models with noncompact symmetry groups, and also, as we show here by example, to vector models with an indefinite inner product.

In the case of matrix models, we choose the noncompact group $SO(1,1)$ and derive a hyperbolic form of the Kuramoto model which we analyze in detail in Sec. III. We find an exact solution for $N=2$, which points to possible behaviours of the general system, and also discuss measures of synchronization, with numerical observations.

We obtain the same hyperbolic Kuramoto equations from the vector model using an indefinite metric in Sec. IV, in which trajectories are confined to hyperbolas in the plane, and show in Sec. V that this model describes the synchronization of relativistic particles in Minkowski space-time in $1+1$ dimensions. This interpretation requires several modifications to the equations of the system; firstly, particle space-time separations must be time-like in order for interactions to occur, which then leads to a time-dependent network topology and secondly, since interactions cannot occur instantaneously in a relativistic system, we must allow for time delays.

II. MATRIX MODELS ON NONCOMPACT MANIFOLDS

We formulate a hyperbolic form of the Kuramoto model by selecting the noncompact Lorentz group $SO(1,1)$ as the symmetry group for Eq. (1.3) in Ref. 16; specifically, we start with the system of N matrix equations

$$\dot{X}_i X_i^{-1} = \Omega_i + \frac{\kappa_i}{2N}\sum_{j=1}^{N}\lambda_i\lambda_j\left(X_j X_i^{-1} - X_i X_j^{-1}\right), \tag{2}$$

where X_i is a group element located at the ith node and Ω_i is an element of the corresponding Lie algebra. We allow for node-dependent coupling coefficients κ_i and also include real multiplicative parameters λ_i, as shown in (2). For simplicity, we assume that $\lambda_i > 0$ for all i. Let G be the diagonal $d \times d$ matrix

$$G = \mathrm{diag}(\underbrace{1,\ldots 1}_{p\text{ times}}, \underbrace{-1,\ldots,-1}_{q\text{ times}}), \tag{3}$$

then $G^2 = I_d$ and elements M_i of $SO(p,q)$ are real matrices which satisfy $M_i^{\mathsf{T}} G M_i = G$ with $M_i^{-1} = G M_i^{\mathsf{T}} G$, where M_i^{T} denotes the transpose of M_i and elements Ω_i of the Lie algebra of $SO(p,q)$ satisfy $\Omega_i^{\mathsf{T}} G + G\Omega_i = 0$. Equation (2) now reads, upon setting $X_i = M_i$ and $X_i^{-1} = G M_i^{\mathsf{T}} G$, as

$$\dot{M}_i G M_i^{\mathsf{T}} = \Omega_i G + \frac{\kappa_i}{2N}\sum_{j=1}^{N}\lambda_i\lambda_j\left(M_j G M_i^{\mathsf{T}} - M_i G M_j^{\mathsf{T}}\right), \tag{4}$$

where Ω_i is an element of the Lie algebra of $SO(p,q)$. For the compact case $G = I_d$ these equations are equivalent to Eq. (5) in Ref. 12, namely, (setting $M_i = O_i$)

$$\dot{O}_i O_i^{\mathsf{T}} = \Omega_i + \frac{\kappa_i}{2N}\sum_{j=1}^{N}\lambda_i\lambda_j\left(O_j O_i^{\mathsf{T}} - O_i O_j^{\mathsf{T}}\right). \tag{5}$$

For $d=2$, the symmetry group is $SO(2)$ and with the parametrization $O_i = \begin{pmatrix} \cos\theta_i & \sin\theta_i \\ \sin\theta_i & \cos\theta_i \end{pmatrix}$, (5) reduces to the Kuramoto model (1).

Because the RHS of (4) is antisymmetric, it follows[12,16] that $M_i^{\mathsf{T}} G M_i$ is a constant of motion and provided that $M_i^{\mathsf{T}} G M_i = G$ holds at the initial time $t=0$, then elements M_i remain on the group manifold for all $t>0$. For general properties of the system (2), and hence also for (4), we refer to Ref. 16, in which rigorous results are obtained which ensure the global existence of solutions and the existence and uniqueness of phase-locked states.

III. THE HYPERBOLIC KURAMOTO MODEL

We now choose $G = \mathrm{diag}(1,-1)$ and parametrize $M_i \in SO(1,1)$ according to

$$M_i = \mathrm{e}^{\alpha_i J} = \begin{pmatrix} \cosh\alpha_i & \sinh\alpha_i \\ \sinh\alpha_i & \cosh\alpha_i \end{pmatrix}, \tag{6}$$

for hyperbolic angles α_i, where

$$J = \begin{pmatrix} 0 & 1 \\ 1 & 0 \end{pmatrix}. \tag{7}$$

To be precise, (6) parametrizes a subgroup of $SO(1, 1)$ containing the identity. We define $\Omega_i = \omega_i J$ for real parameters ω_i, then $\Omega_i^{\mathsf{T}} G + G\,\Omega_i = 0$ and so Ω_i belongs to the Lie algebra of $SO(1, 1)$ as required. The equations of motion (4) reduce to

$$\dot{\alpha}_i = \omega_i + \frac{\kappa_i}{N}\sum_{j=1}^{N} \lambda_i \lambda_j \sinh(\alpha_j - \alpha_i), \tag{8}$$

which is a hyperbolic form of the Kuramoto model (1).

The defining Eqs. (4) are covariant under constant hyperbolic rotations, which for $SO(1, 1)$ reduces to the invariance of (8) under $\alpha_i \to \alpha_i + \alpha^0$ for any constant α^0. The model is also covariant with respect to hyperbolic rotating frames of reference, i.e., the transformation $\alpha_i \to \alpha_i + \omega^0 t$ is equivalent to a shift of the parameters ω_i according to $\omega_i \to \omega_i - \omega^0$.

We can find a constant of integration of (8) by dividing throughout by κ_i and summing over i. From the antisymmetry of the summand under $i \leftrightarrow j$, we obtain

$$\sum_{i=1}^{N} \frac{\dot{\alpha}_i}{\kappa_i} = \sum_{i=1}^{N} \frac{\omega_i}{\kappa_i}, \tag{9}$$

which we integrate to obtain the following relation, which holds at all times:

$$\sum_{i=1}^{N} \frac{\alpha_i(t)}{\kappa_i} = \sum_{i=1}^{N} \frac{\alpha_i^0}{\kappa_i} + t\sum_{i=1}^{N} \frac{\omega_i}{\kappa_i}, \tag{10}$$

where $\alpha_i^0 = \alpha_i(0)$.

A. Exact solutions for $N = 2$

It is useful to obtain exact solutions for $N = 2$ in order to investigate the basic properties of (8), such as the appearance of synchronized solutions as well as the possibility of singularities. For simplicity (but without loss of generality), we choose $\lambda_1 = \lambda_2 = 1$, then (8) reduces to

$$\dot{\alpha}_1 = \omega_1 - \frac{\kappa_1}{2}\sinh(\alpha_1 - \alpha_2), \tag{11}$$

$$\dot{\alpha}_2 = \omega_2 + \frac{\kappa_2}{2}\sinh(\alpha_1 - \alpha_2), \tag{12}$$

with the initial values $\alpha_i^0 = \alpha_i(0)$. Let $\alpha = \alpha_1 - \alpha_2, \omega = \omega_1 - \omega_2$ and $\kappa = (\kappa_1 + \kappa_2)/2$, then we have $\dot{\alpha} = \omega - \kappa\sinh\alpha$, which has the solution (as follows from Ref. 17, 2.441 3)

$$\omega\tanh\left[\frac{\alpha(t)}{2}\right] = 2c\tanh[c(t - t_0)] - \kappa, \tag{13}$$

where $2c = \sqrt{\kappa^2 + \omega^2}$; t_0 is the constant of integration which is fixed by imposing $\alpha(0) = \alpha_1^0 - \alpha_2^0$. The form of the solution restricts the possible values of $\alpha_0 = \alpha(0)$, in particular at $t = 0$ we must have, using $\tanh(-ct_0) < 1$

$$\frac{\omega}{|\omega|}\tanh\left(\frac{\alpha_0}{2}\right) < \sqrt{1 + \frac{\kappa^2}{\omega^2}} - \frac{\kappa}{|\omega|}. \tag{14}$$

If $\kappa > 0$, the RHS of this inequality is less than unity which restricts the possible values of α_0, i.e., $\omega\,\alpha_0/|\omega|$ cannot be arbitrarily large and positive. Provided (13) is satisfied at $t = 0$, however, the solution exists for all $t > 0$, because $\tanh[c(t - t_0)]$ is an increasing function of t.

Since $c > 0$, the separation $\alpha(t)$ approaches a constant value α_∞ as $t \to \infty$ which from (13) is given by

$$\frac{\omega}{|\omega|}\tanh\left(\frac{\alpha_\infty}{2}\right) = \sqrt{1 + \frac{\kappa^2}{\omega^2}} - \frac{\kappa}{|\omega|}. \tag{15}$$

This equation has a solution only if $\kappa > 0$, since otherwise the RHS is larger than unity, whereas the LHS is bounded by unity.

From (10), we obtain

$$\frac{\alpha_1(t)}{\kappa_1} + \frac{\alpha_2(t)}{\kappa_2} = \left(\frac{\omega_1}{\kappa_1} + \frac{\omega_2}{\kappa_2}\right)t + \frac{\alpha_1^0}{\kappa_1} + \frac{\alpha_2^0}{\kappa_2}, \tag{16}$$

and by combining (13) and (16), we obtain the exact solution for α_1, α_2 for any initial values α_1^0, α_2^0. Asymptotically, we have for any $\kappa > 0$,

$$\alpha_i(t) = \alpha_i^\infty + \omega_{\mathrm{av}} t + O\left(\mathrm{e}^{-t\sqrt{\kappa^2 + \omega^2}}\right), \tag{17}$$

for $i = 1, 2$, where

$$\omega_{\mathrm{av}} = \left(\frac{\omega_1}{\kappa_1} + \frac{\omega_2}{\kappa_2}\right) \Big/ \left(\frac{1}{\kappa_1} + \frac{1}{\kappa_2}\right), \tag{18}$$

and where the coefficients α_i^∞ can be expressed explicitly in terms of α_i^0 and κ_i, ω_i.

For the special case $\omega_1 = \omega_2$, for which $\omega = 0$, the equation $\dot{\alpha} = -\kappa\sinh\alpha$ has the solution (as follows from Ref. 17, 2.423):

$$\tanh\left[\frac{\alpha(t)}{2}\right] = \mathrm{e}^{-\kappa(t - t_0)}, \tag{19}$$

where t_0 is again fixed by requiring that $\alpha(0) = \alpha_1^0 - \alpha_2^0$ and in this case, the asymptotic separation α_∞ is zero provided that $\kappa > 0$.

Generally, the asymptotic trajectories $\alpha_1(t)$ and $\alpha_2(t)$ are parallel straight lines separated by α_∞, and for identical ω_i converge to a single trajectory. The property (17) signifies that the system has synchronized, as we discuss in Sec. III B.

From these exact solutions for $N = 2$, we draw the following conclusions:

1. Global solutions exist only if the initial values of the system are suitably restricted, which is consistent with previous general observations.[16]
2. The asymptotic form (17), which signals that the system has synchronized, holds only for $\kappa > 0$, similar to the

Kuramoto model, where nodes with positive couplings are attractive but otherwise are repulsive.

3. In contrast to the Kuramoto model, synchronization occurs for any $\kappa > 0$, and there is no critical value for κ. Similarly, there are no restrictions on the parameters ω_i for synchronization to occur.
4. System (8) develops singularities if $\kappa < 0$, a possibility that is discussed in general in Ref. 16. This singularity is immediately evident for solution (19) (for $\omega_1 = \omega_2$), since for $\kappa < 0$, the solution exists only for $t < t_0$; otherwise, the RHS increases to values larger than unity. A similar observation holds for (13), which shows that the LHS is bounded in magnitude by $|\omega|$, while for $\kappa < 0$, the RHS is an increasing function of t which exceeds this bound at a certain critical time $t = t_c$, and so the solution fails to exist for $t \geqslant t_c$.
5. Synchronization of the system occurs for any $\kappa > 0$, which requires only $\kappa_1 + \kappa_2 > 0$. It is therefore possible for synchronization to occur even if one node has a small negative coupling constant. We find numerically that this occurs also for general $N > 2$, provided that one, and only one node, has a small negative coupling constant.

B. Synchronization in the hyperbolic Kuramoto model

For $N > 2$, system (8) synchronizes with properties similar to those for $N = 2$, as it follows from known general results[16] applied to $SO(1, 1)$. We define synchronization as the phase-locking of states, as defined precisely in Ref. 16 (Definition 2.3). Although the results as stated in Ref. 16 apply only to uniform couplings κ and uniform parameters λ, they would be expected to generalize to the case of distributed parameters κ_i, λ_i.

The existence of unique smooth local solutions $X_i(t)$ to (2) is proved in Proposition 2.1,[16] and global solutions are shown to exist provided that the initial ratios $X_i X_j^{-1}$ lie sufficiently close to the identity (Proposition 3.1). Phase-locking is defined by means of the ensemble diameter $D(t)$, which itself is defined (Definition 3.1) for any solutions $M_i(t)$ by

$$D(t) = \max_{1 \leqslant i < j \leqslant N} ||M_i(t) M_j^{-1}(t) - I_2||, \tag{20}$$

where $M_i \in SO(1,1)$ are the matrices defined in (6) and I_2 is the 2×2 identity matrix. The norm $||\,.\,||$ is the Frobenius matrix norm. By substituting from (6), we find explicitly:

$$||M_i M_j^{-1} - I_2||^2 = 8 \cosh(\alpha_i - \alpha_j) \sinh^2\left(\frac{\alpha_i - \alpha_j}{2}\right). \tag{21}$$

Phase-locking, or asymptotic entrainment, occurs when the asymptotic limit of $M_i(t) M_j^{-1}(t)$ exists, i.e., when $M_i(t) M_j^{-1}(t)$ approaches a constant matrix for all i, j (Definition 2.3[16]). Since $M_i M_j^{-1} = \mathrm{e}^{(\alpha_i - \alpha_j) J}$, this definition is equivalent to the requirement that the $t \to \infty$ limit of $\alpha_i(t) - \alpha_j(t)$ should exist. For the Kuramoto model, this definition of synchronization corresponds to frequency locking (see Ref. 18, Definition 3.1), or equivalently to asymptotic phase-locking,[19] i.e., we require that $\lim_{t \to \infty} \dot{\alpha}_i(t) - \dot{\alpha}_j(t) = 0$ for all nodes i, j. The global existence of solutions and phase-locking occurs generally for system (2) under the conditions of Theorem 5.1,[16] such as restricted initial values and a sufficiently large coupling constant. Stability of the phase-locked states is proved in Theorem 5.2.

For systems of identical matrices Ω_i, i.e., for identical parameters ω_i, complete entrainment or complete synchronization occurs when $M_i M_j^{-1} = \mathrm{e}^{(\alpha_i - \alpha_j) J}$ approaches the identity matrix (Definition 2.3). This requires that $\lim_{t \to \infty} \alpha_i(t) - \alpha_j(t) = 0$ for all nodes i, j, which for the Kuramoto model has been referred to as phase agreement (Ref. 18, Definition 3.2), or asymptotic complete-phase synchronization.[19] According to Theorem 4.2,[16] global solutions exist and $D(t)$ approaches zero exponentially fast, provided that $D(0) < 1$ and κ is greater than a fixed positive constant, and so under these conditions, complete entrainment always occurs. For $SO(1, 1)$ for $N > 2$, we find numerically that synchronization occurs whenever $\kappa > 0$, as shown for $N = 2$ in Sec. III A.

C. The synchronization manifold

Synchronization, or phase-locking, is equivalent for system (8) to the property that solutions take the asymptotic form

$$\alpha_i(t) = \omega_{\mathrm{av}} t + \alpha_i^\infty, \tag{22}$$

neglecting terms which are exponentially small, for some constant ω_{av}, where α_i^∞ are constants determined by the initial conditions and parameters of the system. Solutions (22) lie on the synchronization manifold as defined, for example, in Ref. 1. To show the equivalence of (22) to phase-locking, consider the identity

$$\alpha_i \sum_{j=1}^N \frac{1}{\kappa_j} = \sum_{j=1}^N \frac{\alpha_j}{\kappa_j} + \sum_{j=1}^N \frac{1}{\kappa_j} (\alpha_i - \alpha_j), \tag{23}$$

which holds for all $i = 1 \ldots N$. We replace the first term on the RHS by the exact integral (10), and then when asymptotic entrainment occurs, the differences $\alpha_i - \alpha_j$ in the second term approach either a constant value or zero for the case of complete entrainment, as discussed above. Therefore, asymptotically, we obtain form (22) with

$$\omega_{\mathrm{av}} = \sum_{i=1}^N \frac{\omega_i}{\kappa_i} \Big/ \sum_{i=1}^N \frac{1}{\kappa_i}, \tag{24}$$

which is consistent with (17) for $N = 2$. Theorems 4.1 and 5.1 in Ref. 16 provide estimates of lower order terms in the asymptotic expression (22). Conversely, it follows from (22) that $\lim_{t \to \infty} \alpha_i(t) - \alpha_j(t)$ exists and is zero if the constants α_i^∞ are independent of i, corresponding to complete synchronization for identical parameters $\omega_i, \lambda_i, \kappa_i$.

If (22) holds asymptotically, then from (8), the following N equations must be satisfied:

$$\omega_{\mathrm{av}} - \omega_i = \frac{\kappa_i}{N} \sum_{j=1}^N \lambda_i \lambda_j \sinh\left(\alpha_j^\infty - \alpha_i^\infty\right), \tag{25}$$

from which, or directly from (9), we again obtain the expression (24) for ω_{av}. Formula (24) remains valid for nontrivial

network topologies, i.e., if we insert the factor a_{ij} under the sum in (8) and hence also in (25), with $a_{ij} = a_{ji}$, then ω_{av} is unchanged. The fact that the N Eqs. (25) must be satisfied in the synchronized system provides a useful accuracy check for numerical computations.

Equation (25) explains why the hyperbolic model (8) allows synchronization to occur for any coupling constants $\kappa_i > 0$, in contrast to the standard Kuramoto model (1) for which we require $\kappa_i = \kappa > \kappa_c$ for some critical value $\kappa_c > 0$. The corresponding equations for the Kuramoto model have been well-analyzed, see for example Ref. 20, Sec. 3, where it is shown that solutions exist only for $K > K_c$, see also Ref. 21 (Theorem 1). By contrast, (25) can be solved for the differences $\alpha_j^\infty - \alpha_i^\infty$ for any fixed parameters $\omega_i, \lambda_i, \kappa_i$ with $\lambda_i, \kappa_i > 0$, as we show in the Appendix, essentially because the sinh function in (25) is unbounded. In particular, (25) can always be satisfied for arbitrarily small coupling constants κ_i.

The solutions (22) in the synchronization manifold are stable as follows from general results[16] (Theorem 5.2) which guarantee orbital stability for couplings K larger than a fixed value K_e, for specified initial configurations. Numerically, we also observe stability for arbitrarily small coupling constants κ_i. Let us show for the special case of identical parameters, $\omega_i = \omega_{\text{av}}$ for all i, that stability for any $\kappa_i = \kappa$ follows from the properties of a Lyapunov function L. A corresponding function is well known for the Kuramoto model.[22]

We assume without loss of generality, by means of the transformation $\alpha_i \to \alpha_i + \omega^0 t$, that $\omega_i = 0$ for all i. Define

$$L(\alpha_1, \alpha_2 \ldots \alpha_N) = \frac{\kappa}{2N} \sum_{i,j=1}^{N} \lambda_i \lambda_j \left[\cosh(\alpha_j - \alpha_i) - 1\right]. \tag{26}$$

Then, $L \geqslant 0$ with $L = 0$ if and only if $\alpha_i = \alpha_j$ for all i, j, which comprises all points on the synchronization manifold. These degenerate minima of L are related by hyperbolic rotations in which $\alpha_i \to \alpha_i + \alpha^0$. Equation (8) may be written as $\dot{\alpha}_i = -\nabla_i L$, and hence

$$\dot{L} = \sum_{i=1}^{N} \frac{\partial L}{\partial \alpha_i} \dot{\alpha}_i = -\sum_{i=1}^{N} \dot{\alpha}_i^2, \tag{27}$$

which implies $\dot{L} \leqslant 0$, with $\dot{L} = 0$ if and only if $\alpha_i = \alpha_j$ for all i, j. Hence, L strictly decreases on all trajectories which are not minima of L. It follows that trajectories on the synchronization manifold are asymptotically stable[23] (Theorem 6.5.2) for any $\kappa > 0$.

D. Measures of synchronization

In this section, we describe and compare a range of order and disorder parameters in order to quantify the long-term synchronization behaviour of (8).

The form of the ensemble diameter $D(t)$ in (20) (following Ref. 16) suggests that we define a simpler measure by calculating the maximum difference $|\alpha_i - \alpha_j|$ over all nodes. Specifically, if we define the hyperbolic phase difference by

$$P(t) = \max_{1 \leqslant i < j \leqslant N} |\alpha_i(t) - \alpha_j(t)|, \tag{28}$$

then P takes a constant value at the onset of synchronization, as is evident from (22). This measure is analogous to the phase difference used for the Kuramoto model.[19] The measures D and P take the value zero for a completely synchronized system.

Another measure of synchronization is a related disorder parameter $R(t)$ which evaluates the average deviation of the nodes from their mean trajectory

$$R(t) = \frac{1}{N} \sum_{i=1}^{N} |\alpha_i(t) - \alpha_{\text{av}}(t)|, \tag{29}$$

where $\alpha_{\text{av}}(t) = \sum_i \alpha_i(t)/N$ is the average position of the nodes at time t. We refer to R as a disorder parameter since, like D and P, it is small for trajectories which are closely correlated and is large for widely separated trajectories. At synchronization, this parameter also attains a constant value and $R = 0$ corresponds to a completely synchronized system.

The most commonly used synchronization measure for the Kuramoto model is the order parameter $r(t)$ defined by

$$\mathrm{e}^{\mathrm{i}\psi(t)} r(t) = \frac{1}{N} \sum_{i=1}^{N} \mathrm{e}^{\mathrm{i}\theta_i(t)}, \tag{30}$$

where ψ is the average phase of the system and r, which satisfies $0 \leqslant r \leqslant 1$, measures the phase coherence. A value $r = 1$ corresponds to a completely synchronized state in which all the phases are identical and $r = 0$ corresponds to a phase-balanced state. For the hyperbolic model (8), we define an order parameter similar to (30)

$$r(t) = \frac{1}{N} \sum_{i=1}^{N} \mathrm{e}^{\alpha_i(t) - \omega_{\text{av}} t}, \tag{31}$$

where ω_{av} is defined in (24). If synchronization occurs, then (22) holds asymptotically and r takes the constant value $\sum_i \mathrm{e}^{\alpha_i^\infty}/N$. Although r is not normalized in the same way as is (30) for the Kuramoto model, it provides an easily computed measure which determines the onset of synchronization.

As an example, in Fig. 1 we plot the four measures D, P, R, r as functions of t, choosing $N = 20$ with randomly generated parameters $\omega_i \in [-4, 4]$ and initial values $\alpha_i^0 \in [-3, 3]$, with $\kappa_i = 1$ for all i. The plots for R, D have been rescaled so as to be of a similar order of magnitude. Each of these measures attains a constant value at a similar time, signifying the onset of synchronization.

E. Numerical observations

We have performed numerical investigations of solutions to (8) over a range of values for $N \leqslant 100$, for random initial values α_i^0 and parameters ω_i, and for random constants κ_i and λ_i in $[0, 1]$. In all cases, we find that solutions exist globally and that synchronization occurs, meaning that (22) holds for large times, as measured by the order parameters r and P. The constants α_i^∞ in (22) are generally of the order of unity for parameters in the selected range. The hyperbolic

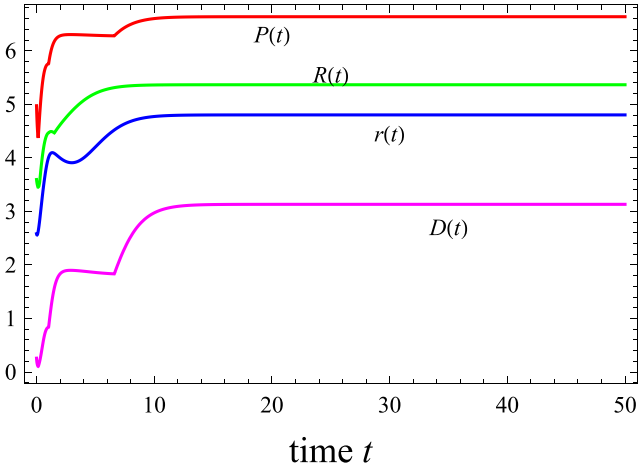

FIG. 1. The synchronization measures R, D (rescaled) and r, P plotted as a functions of t for $N=20$ nodes with random initial values $\alpha_i^0 \in [-3,3]$ and random parameters $\omega_i \in [-4,4]$, with $0<\lambda_i<1$.

angles α_i move out to infinity in a synchronized cluster (for $\omega_{\rm av} \neq 0$) as the system evolves.

As previously noted, there are no critical values for the coupling constants κ_i, rather these determine the time scale over which synchronization occurs. Increasing the spread of the initial values α_i^0 increases the time it takes for a cluster to form. Even for very widely spread initial values, the nodes still eventually synchronize.

In Fig. 2, we plot the trajectories of the N variables $\alpha_i(t)$ for $0 \leqslant t \leqslant 100$ for $N=50$, with randomly generated parameters $\alpha_i^0, \omega_i \in [-1,1]$, and $\kappa_i, \lambda_i \in [0,1]$. In this example, $\omega_{\rm av}$ is small and positive, as is evident from the positive asymptotic slope of the trajectories. Most nodes are synchronized at $t \approx 20$ units, as indicated by the constant slope of the trajectory, whereas the order parameter r shows that the onset of synchronization occurs at $t \approx 50$ units.

Another way to depict the trajectories of the system is by means of the relativistic space-time interpretation discussed in Sec. V B, where trajectories move along one branch of a hyperbola in $1+1$ dimensional space-time, parametrized by α_i. A more convenient depiction is via a

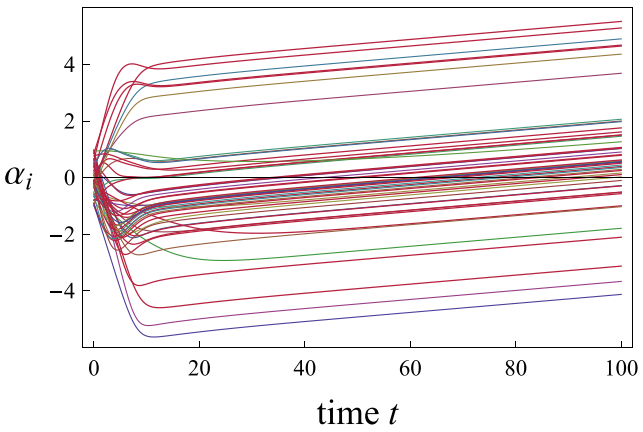

FIG. 2. The $N=50$ trajectories $\alpha_i(t)$ for randomly generated parameters $\omega_i, \lambda_i > 0, \kappa_i > 0$, showing that all trajectories synchronize with lines of identical constant slope.

stereographic projection in which the trajectories are projected onto the unit circle. Define

$$u_i = \frac{2\alpha_i}{1+\alpha_i^2}, \quad v_i = \frac{-1+\alpha_i^2}{1+\alpha_i^2}, \tag{32}$$

then $u_i^2 + v_i^2 = 1$, and so for each trajectory $\alpha_i(t)$, the corresponding point $(u_i(t), v_i(t))$ lies on the unit circle. The interval $[-1,1]$ maps to the lower half of the circle and trajectories α_i which move out to infinitely map to points close to the north pole. If $\omega_{\rm av} > 0$, the synchronized cluster moves anticlockwise around the circle and eventually approaches, but never crosses the north pole. Figure 3 uses the same parameters as Fig. 2, showing firstly the initial values α_i^0 (in red) which lie on the lower half of the circle, then the same nodes at a later time (in blue), in which some clustering of nodes is evident, and then the same nodes (in green) at a much later time showing their asymptotic positions.

In general, by choosing a frame of reference in which $\omega_{\rm av} = 0$, which is always possible by means of the time-dependent hyperbolic rotation $\alpha_i \to \alpha_i - \omega_{\rm av} t$, all nodes asymptotically approach a constant value α_i^∞, which can be projected onto the unit circle as a fixed configuration. As previously noted, if all parameters ω_i take the identical value $\omega_i = \omega$, then from (24), we have $\omega_{\rm av} = \omega$, and all asymptotic trajectories coincide, with the constants α_i^∞ being independent of i.

IV. VECTOR MODELS OF SYNCHRONIZATION

Besides the matrix models discussed in Sec. II, there are also vector models which generalize the Kuramoto model and have properties determined by an underlying Lie

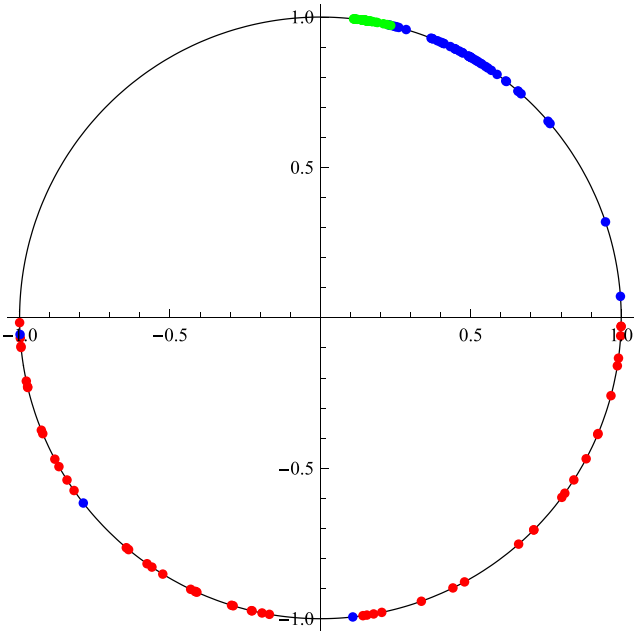

FIG. 3. Stereographic projection onto the unit circle of the trajectories at three different times (red, blue, and green). The initial values $\alpha_i^0 \in [-1,1]$ map to the lower half of the circle (red), while the configuration at a later time (blue) shows a clustering of nodes, but with some outliers, then asymptotically, all nodes approach the north pole (green).

group.[12] Located at each node i is a real vector $\boldsymbol{x}_i$ of length d which satisfies

$$\dot{\boldsymbol{x}}_i = \Omega_i \boldsymbol{x}_i - \frac{\kappa_i}{N}\sum_{j=1}^{N}(\langle \boldsymbol{x}_i, \boldsymbol{x}_i\rangle \boldsymbol{x}_j - \langle \boldsymbol{x}_i, \boldsymbol{x}_j\rangle \boldsymbol{x}_i), \tag{33}$$

where $\langle \boldsymbol{x}_i, \boldsymbol{x}_j\rangle = \boldsymbol{x}_i^{\mathsf{T}} G \boldsymbol{x}_j$ is a symmetric bilinear form in which the metric tensor G is a diagonal $d \times d$ matrix defined as in (3). This bilinear form is invariant under $SO(p, q)$. The matrices Ω_i are elements of the Lie algebra of $SO(p, q)$ and satisfy $\Omega_i^{\mathsf{T}} G + G\,\Omega_i = 0$. The overall sign of coupling κ_i in (33) is arbitrary, since it can be reversed by changing the sign of metric G.

It follows from (33) by using $\langle \boldsymbol{x}_i, \Omega_i \boldsymbol{x}_i\rangle = 0$ that

$$\langle \boldsymbol{x}_i, \dot{\boldsymbol{x}}_i\rangle = 0, \tag{34}$$

and hence $\langle \boldsymbol{x}_i, \boldsymbol{x}_i\rangle$ is a constant of motion for all i, with a value that is fixed to the initial values $\boldsymbol{x}_i^0 = \boldsymbol{x}_i(0)$.

The case $G = I_d$, which corresponds to the compact group $SO(d)$, has been previously discussed,[12] and rigorous results for any dimension d have been obtained.[14,15,24] If we choose the initial vectors $\boldsymbol{x}_i^0$ to be unit vectors, then all trajectories lie on the unit sphere S^{d-1}. Phase-locked synchronization occurs for a sufficiently large coupling constant,[15] even in the presence of a small uniform time delay.[24] The Kuramoto model (1) is regained for $d = 2$ by setting $\boldsymbol{x}_i = (\cos\theta_i, \sin\theta_i)$.

Let us now turn to the noncompact case of $d = 2$ for which $G = \mathrm{diag}[1, -1]$, where the underlying group is $SO(1, 1)$. Trajectories at each node are of two types, depending on whether the constant of motion $\langle \boldsymbol{x}_i, \boldsymbol{x}_i\rangle$ is positive or negative. For reasons explained in Sec. V, we choose the case in which $\langle \boldsymbol{x}_i, \boldsymbol{x}_i\rangle$ is negative at all nodes i, i.e., we choose initial values $\boldsymbol{x}_i^0$ such that $\langle \boldsymbol{x}_i, \boldsymbol{x}_i\rangle = -\lambda_i^2$ for parameters $\lambda_i > 0$, and hence we parametrize $\boldsymbol{x}_i$ according to

$$\boldsymbol{x}_i = \lambda_i\,(\sinh\alpha_i, \cosh\alpha_i) \tag{35}$$

for hyperbolic angles α_i. Also, we confine all trajectories to the branch of the hyperbola in which the second component of the vector $\boldsymbol{x}_i$ is positive, since otherwise particles have a space-like separation and cannot interact, as explained below. We choose, as before, $\Omega_i = \omega_i J$, where J is defined in (3).

Upon substituting (35) into (33), we obtain precisely the equations of the hyperbolic Kuramoto model (8). Synchronization occurs for system (33) as discussed previously, i.e., when α_i takes the asymptotic form (22), which holds whenever $\kappa_i > 0$.

V. SYNCHRONIZED RELATIVISTIC DYNAMICS

We describe a physical interpretation of the hyperbolic Kuramoto model in terms of relativistic mechanics, using the vector model in $1 + 1$ dimensions, where $\boldsymbol{x}_i$ now denotes the space-time coordinates of a particle of unit mass.

First, however, let us recall the physical meaning of the Kuramoto model, where for the case of zero coupling, $x_i = \cos\theta_i$ denotes the one-dimensional position of a particle of unit mass and the time derivative $p_i = -\omega_i \sin\theta_i$ is the momentum, upon using $\dot{\theta}_i = \omega_i$. Then, we have $\ddot{x}_i = -\omega_i^2 x_i$, showing that the particle motion is that of a simple harmonic oscillator of frequency ω_i. The relation $x_i^2 + (p_i/\omega_i)^2 = 1$ expresses conservation of the energy of the particle and shows that phase space trajectories are unit circles. The two-dimensional vector $\boldsymbol{x}_i = (\cos\theta_i, \sin\theta_i)$, therefore, consists of the position and (scaled) momentum components of the particle. The effect of the cubic nonlinear couplings in (33) (for the compact case in which $G = I_d$) is to synchronize a network of harmonic oscillators to a common phase-locked frequency.

By contrast, for the noncompact case, where the model is invariant under the Lorentz group $SO(1, 1)$, we regard $\boldsymbol{x}_i = (x_i^0, x_i^1)$ as the space-time coordinates of a particle of unit mass, and therefore the local time (i.e., the laboratory time) of the particle at the ith node is x_i^0 and its position is x_i^1. For clarity, we rename the previous time variable t as s, assumed to be a Lorentz-invariant quantity, which we refer to as the "s-time" of the particle, and so $\dot{\boldsymbol{x}}_i$ now means $d\boldsymbol{x}_i/ds$. We assume that there is a $1-1$ correspondence between s and the local time $x_i^0(s)$, which should be an increasing function of s. As we will see, this ensures that the Lorentz-invariant proper time τ_i of each particle is also an increasing function of s.

For a general description and discussion of special relativity, Lorentz transformations and invariant space-time intervals, we refer to Ref. 25 (Chap. 7), and to Ref. 26.

A. Invariant factors and proper time

The model (33) describes the time evolution of a network, or cluster, of relativistic particles of unit mass in $1 + 1$ dimensions which interact with each other through the cubic nonlinearity. The Lorentz-invariant quantities $\langle \boldsymbol{x}_i, \boldsymbol{x}_i\rangle$, which are also constants of the motion, may be written in the usual relativistic notation as $(\boldsymbol{x}_i)^\mu (\boldsymbol{x}_i)_\mu = (x_i^0)^2 - (x_i^1)^2$. We evaluate the speed v_i of the ith particle according to

$$v_i = \frac{dx_i^1}{dx_i^0} = \frac{dx_i^1}{ds}\Big/\frac{dx_i^0}{ds} = \frac{x_i^0}{x_i^1}, \tag{36}$$

where we have used the fact that $(x_i^0)^2 - (x_i^1)^2$ is constant in s for every i. Hence

$$1 - v_i^2 = \frac{(x_i^1)^2 - (x_i^0)^2}{(x_i^1)^2},$$

which for physical particles is positive (where the "speed of light" is unity); hence, we require the coordinates $\boldsymbol{x}_i$ all be space-like. This justifies the parametrization (35) which ensures that $\boldsymbol{x}_i$ is space-like, and we do not consider time-like vectors $\boldsymbol{x}_i$ which describe tachyons.

From (35) and (36), we obtain $v_i = \tanh\alpha_i$, where now α_i is the rapidity of the particle at the ith node. As s increases, along with the rapidity α_i, the speed approaches the relativistic limit of unity. Trajectories are confined to the branch of the hyperbola $(x_i^0)^2 - (x_i^1)^2 = -\lambda_i^2$, for which $x_i^1 > 0$. The Lorentz factor is given by $\gamma_i = 1/\sqrt{1 - v_i^2} = \cosh\alpha_i$. The

momentum p_i of each particle is given by $p_i = \gamma_i v_i = \sinh\alpha_i$ and the energy is $E_i = \gamma_i = \cosh\alpha_i$. The energy and the momentum, therefore, each increase without bound as the s-time increases, but the invariant relation $E_i^2 - p_i^2 = 1$ is always maintained.

The proper time τ_i of the particle at the ith node is given by $d\tau_i = dx_i^0/\gamma_i$ [see, for example, the definition of proper time in Ref. 25, Eq. (7.6)]; hence

$$d\tau_i = \frac{dx_i^0}{\cosh\alpha_i} = \lambda_i \frac{\cosh\alpha_i \, d\alpha_i}{\cosh\alpha_i} = \lambda_i \, d\alpha_i, \tag{37}$$

giving $\tau_i = \lambda_i \alpha_i$. Up to a constant multiplicative factor, the proper time at each node is therefore given by the rapidity α_i.

B. Particle trajectories

Let us determine the trajectory $\boldsymbol{x}(s)$ of a single particle in the absence of the cubic interaction shown in (33); in effect, we choose $N = 1$. Then, $\dot{\boldsymbol{x}} = \Omega \boldsymbol{x}$, where $\Omega = \omega J$, which implies $\ddot{\boldsymbol{x}} = \Omega^2 \boldsymbol{x} = \omega^2 \boldsymbol{x}$. In particular, the position x^1 satisfies $\ddot{x}^1 = \omega^2 x^1$ showing that the particle is subject to a linear repulsive force which flings it out to infinity along the space-time hyperbola $x^\mu x_\mu = -\lambda^2$, for some constant λ, with an increasing speed which approaches the limit 1. With the parametrization (35), we have $\dot{\alpha} = \omega$, which implies $\alpha(s) = \alpha_0 + \omega s$, and so we obtain the general solution

$$\boldsymbol{x}(s) = \lambda \, (\sinh(\alpha_0 + \omega s), \cosh(\alpha_0 + \omega s)), \tag{38}$$

where α_0 is an arbitrary constant. The local time x^0 is an increasing function of s provided that $\omega > 0$, and so there is a $1-1$ correspondence between the s-time and the local time. The proper time is given by $\tau = \lambda\alpha = \lambda\omega s$ (up to an additive constant), and so for a single isolated particle, the s-time is equivalent to the proper time τ and, as required, is Lorentz-invariant.

For $N = 2$, we have derived an exact solution in Sec. III A and conclude that the system always synchronizes in the sense that (17) holds asymptotically, provided that $\kappa > 0$. Generally, for $N > 1$, the effect of the nonlinear terms in (33) is to synchronize the trajectories, in which each coordinate $\boldsymbol{x}_i$ in (35) evolves according to Eq. (8) for α_i. Particle trajectories lie on the hyperbola $\langle \boldsymbol{x}_i, \boldsymbol{x}_i \rangle = -\lambda_i^2$ and when the system has synchronized, all particles move together according to (22) in the positive x^0 (time) direction provided that $\omega_{\rm av}$, as defined in (24), is positive.

As an example, in Fig. 4, we plot the space-time locations of $N = 20$ particles which are each restricted to the right branch of one of four possible hyperbolas (blue), corresponding to four distinct values of λ_i. As s increases, all particles move in the positive x^0 and x^1 directions with increasing speed, and eventually synchronize in the sense that the hyperbolic angles α_i asymptotically satisfy (22).

C. Relativistic restrictions

For a valid interpretation of the system as an evolving cluster of relativistic particles, there are further considerations

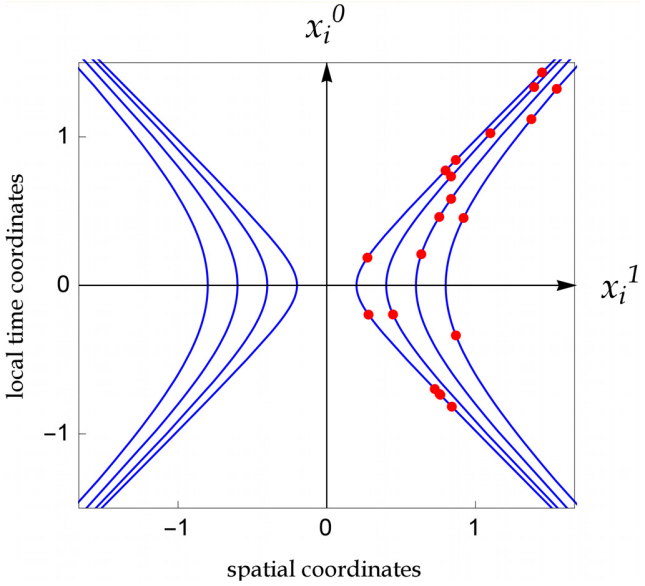

FIG. 4. A space-time plot showing the positions of $N = 20$ particles (red) distributed over the right branch of four hyperbolas (blue) satisfying $(x_i^0)^2 - (x_i^1)^2 = -\lambda_i^2$.

which we now discuss, as a result of which we impose three requirements:

1. Both the local time $x_i^0(s)$ and the proper time $\tau_i(s)$ of each particle must be strictly increasing functions of s, in order to avoid particle motion which is backwards or stationary in time.
2. The particle separation between any two interacting nodes of the network must be time-like, i.e., the two particles must be causally related, otherwise they cannot interact. We therefore introduce a coupling factor δ_{ij} into the equations, depending on s, which is unity if the nodes i and j are causally connected, but is otherwise zero.
3. The particle interactions as given in (8) are assumed to be instantaneous, whereas in a relativistic system, interactions occur with a finite speed of propagation. Hence, we introduce a time delay $\sigma_{ij} = \sigma_{ji}$ which occurs when the ith particle interacts with the jth node, assuming that there is a time-like separation between the two nodes.

Hence, we modify Eq. (8) to read as

$$\dot{\alpha}_i = \omega_i + \frac{\kappa_i}{N} \sum_{j=1}^{N} \delta_{ij}(s) \lambda_i \lambda_j \sinh\big[\alpha_j(s - \sigma_{ij}) - \alpha_i(s)\big]. \tag{39}$$

Let us consider the three listed requirements, in turn.

Each particle is subject to a repulsive force controlled by the parameter ω_i which propels the particle out to infinity along the hyperbola $\langle \boldsymbol{x}_i, \boldsymbol{x}_i \rangle = -\lambda_i^2$. There is also an attractive force between interacting nodes due to the nonlinearity in (39) which leads to the synchronization of all nodes. For random initial values α_i^0 and random parameters ω_i, the particle trajectory can move backwards with respect to the local time x_i^0, i.e., $x_i^0(s)$ can be a decreasing function of s over a range of values of s, although asymptotically we have $\alpha_i(s) \to \alpha_i^\infty + \omega_{\rm av} s$, in which case all particles move in the

direction of increasing space-time coordinates $x_i^0(s)$ and $x_i^1(s)$, provided that $\omega_{\rm av} > 0$. Figure 2 provides an example of trajectories $\alpha_i(s)$ with $\omega_{\rm av} > 0$, in which $\alpha_i(s)$ evidently decreases for some nodes i, but only for small s.

We can avoid backward motion for all local times x_i^0 by requiring that ω_i be sufficiently large so that the repulsive force due to the local dynamics ensures that $\dot{\alpha}_i(s)$ is always positive, and is therefore an increasing function of s. For example, at the initial time $s = 0$, we require the RHS of (39) to be positive, which can always be achieved by choosing sufficiently large ω_i. In effect, we transform to a hyperbolically rotating frame by replacing $\alpha_i \to \alpha_i - \omega^0 s$, which shifts the parameters ω_i to larger values. Having ensured that $\alpha_i(s)$ is an increasing function of s, it follows that the proper time $\tau_i(s) = \lambda_i \alpha_i(s)$ is also an increasing function of s, as is the local time $x_i^0(s) = \lambda_i \sinh\alpha_i(s)$.

Only those nodes in the cluster of particles that have a time-like separation can interact. We observe firstly that particles located on opposite branches of the hyperbola have a space-like separation, and therefore never interact. Let $\boldsymbol{x}_1 = \lambda_1(\sinh\alpha_1, \cosh\alpha_1)$ and $\boldsymbol{x}_2 = \lambda_2(\sinh\alpha_2, -\cosh\alpha_2)$, then the space-time separation is given by

$$\langle \boldsymbol{x}_1 - \boldsymbol{x}_2, \boldsymbol{x}_1 - \boldsymbol{x}_2 \rangle = -\lambda_1^2 - \lambda_2^2 - 2\lambda_1\lambda_2 \cosh(\alpha_1 + \alpha_2),$$

which is always negative. If we attempt to solve (33) with particles lying on different branches of the hyperbola, we find that the solution develops a singularity. We have therefore parametrized trajectories as in (35) with the result that the position x_i^1 is positive for all particles and trajectories always lie on the corresponding $x_i^1 > 0$ branch of the hyperbola, as Fig. 4 shows.

Now consider the particle separation for any fixed s and any i and j, then from (35), we obtain

$$\langle \boldsymbol{x}_i - \boldsymbol{x}_j, \boldsymbol{x}_i - \boldsymbol{x}_j \rangle = -\lambda_i^2 - \lambda_j^2 + 2\lambda_i\lambda_j \cosh(\alpha_i - \alpha_j). \quad (40)$$

This is positive for uniform λ_i because $\cosh(\alpha_i - \alpha_j) \geqslant 1$ for all i, j. Any two particles which lie on the same branch of a common hyperbola are therefore always able to maintain contact as the system evolves. Generally, the requirement that the RHS of (40) be positive for any fixed s reduces to the condition

$$e^{-|\alpha_i - \alpha_j|} \leqslant \frac{\lambda_i}{\lambda_j} \leqslant e^{|\alpha_i - \alpha_j|}. \quad (41)$$

If the parameters λ_i are not uniform, i.e., if the ratio λ_i/λ_j is not unity, then these inequalities can be violated at any value of s if, for example, α_i and α_j happen to be equal at some particular s-time. It is therefore possible for two connected particles to lose contact if they lie on different hyperbolas, because the separation can become space-like at some time $s > 0$ even if there is an initial time-like separation; the particles can, however, also subsequently reconnect.

For any two trajectories $\boldsymbol{x}_i(s), \boldsymbol{x}_j(s)$, define

$$\delta_{ij}(s) = \begin{cases} 1 & \text{if } \langle \boldsymbol{x}_i - \boldsymbol{x}_j, \boldsymbol{x}_i - \boldsymbol{x}_j \rangle \geqslant 0, \\ 0 & \text{otherwise}, \end{cases} \quad (42)$$

where the space-time separation is evaluated as in (40), then we insert this factor $\delta_{ij} = \delta_{ji}$ into the equations to be solved, as shown in (39). The effect of δ_{ij} is to introduce a time-dependent network topology into the system, since nodes can disconnect and reconnect as the system evolves, for non-uniform λ_i. It is nevertheless possible for the system to synchronize as before, provided that the connections do not become too sparse, as is known to occur for the Kuramoto model.[1,27] If the system does indeed synchronize, then the separation $\langle \boldsymbol{x}_i - \boldsymbol{x}_j, \boldsymbol{x}_i - \boldsymbol{x}_j \rangle$ as given in (40) is asymptotically independent of s, and so the network topology becomes constant. Hence, the formula (24) for $\omega_{\rm av}$ remains valid.

For the $N = 20$ particle trajectories shown for example in Fig. 4 at a certain fixed s-time, we have included the factor $\delta_{ij}(s)$ when solving the equations numerically. Initially, we found that there were frequent connections and disconnections between particles located on different branches of the four hyperbolas as the system evolved, but asymptotically the connectivity of the network remained constant, as expected. Of the $N(N-1)/2 = 190$ possible connections in the asymptotic configuration, 163 were nonzero (i.e., unity), which was sufficiently large for synchronization to take place.

Finally, in (39) we have included a time-delay $\sigma_{ij}(s)$ which allows for a finite speed of propagation for signals between any two connected nodes i and j. We suppose that σ_{ij}^2 is proportional to the time-like separation $\langle \boldsymbol{x}_i - \boldsymbol{x}_j, \boldsymbol{x}_i - \boldsymbol{x}_j \rangle$, and is therefore a function of s. We have not modelled the effect of this time delay but note that link-dependent time delays have previously been investigated[18] for the Kuramoto model, and that for vector models a small uniform time delay has no qualitative effect on synchronization.[24,28]

In summary, the system of N particles evolves from its initial configuration during a short transient time into a synchronized cluster in which each particle moves out to infinity along one branch of an invariant hyperbola, with increasing speed given asymptotically by $v_i(s) = \tanh(\alpha_i^\infty + \omega_{\rm av} s)$, which is evidently limited by unity. The proper time τ_i of each particle is given in the synchronized cluster by $\tau_i = \lambda_i(\alpha_i^\infty + \omega_{\rm av} s)$ which, up to overall multiplicative and additive constant factors, is proportional to s. The average space-time separation of the N particles can be calculated from (40) and is related to the measure P defined in (28), which is constant in the asymptotic configuration. This indicates that the N particles can each be considered as constituents of a synchronized cluster which evolves as a collective entity. For identical parameters ω_i, complete synchronization occurs and the cluster appears as a single particle, in the sense that (22) holds with $\alpha_i^\infty = \alpha_j^\infty$.

VI. CONCLUSIONS

The Kuramoto model when expressed in matrix form can be generalized to matrix models with elements belonging to a Lie group, for both compact and noncompact Lie groups. We have described a hyperbolic form of the Kuramoto model by replacing the rotation matrices of $SO(2)$ by elements of the noncompact group $SO(1, 1)$. While this leads to a model with unbounded trajectories and, in some circumstances, run-away solutions (singularities), the usual concept

of synchronization remains well defined in that trajectories cluster together as quantified by measures such as D, P, R, r, with common constants such as $\omega_{\rm av}$. If the given parameters such as ω_i are identical, then the trajectories coincide and we obtain complete synchronization. In general, there is no critical value for the coupling constants κ_i, rather synchronization occurs whenever $\kappa_i > 0$.

We have also formulated a vector model of synchronization in which the symmetry group is noncompact. While such models have been previously studied for the compact case, general properties are yet to be derived for these more general models, which also have unbounded trajectories. By choosing the symmetry group to be $SO(1, 1)$, we regain the hyperbolic Kuramoto model, and synchronization occurs as before. The vector formulation leads to an interpretation of the model as a system of interacting relativistic particles in $1+1$ dimensions, where the vector components are the space-time coordinates. For this interpretation to take effect, the hyperbolic Kuramoto model requires modifications in order to take account of relativistic requirements such as a finite speed of propagation for signals between nodes, and a time-like separation between interacting nodes. Numerical examples show that synchronization of N elements of the network can still occur, with a network topology that varies with time. The synchronized configuration can be viewed as a bound state of the N constituent nodes.

It has been observed[25] (Secs. 7.9 and 7.10) that "no satisfactory formulation for an interacting multiparticle system exists in classical relativistic mechanics, except for some few special cases," and that difficulties can arise from covariant Lagrangian formulations. We have avoided these difficulties because, firstly, we have not used a Lagrangian formulation, but have taken the equations of motion as our starting point in which the space-time coordinates evolve as functions of an invariant parameter s (denoted θ in Ref. 25). Hence, Lorentz covariance of the system as a whole is maintained. Secondly, we have avoided the introduction of external forces and the problems of "action at a distance," since all interactions occur through assumed nonlinear interactions between constituent particles. These particle interactions occur only for time-like separations and although we have not modelled the effects of a finite time of propagation of signals between the constituents of the system, these could, in principle, also be included.

The generalization of these results to other groups is of interest, for example, the choice of the noncompact Lorentz groups $SO(1, 2)$ and $SO(1, 3)$ would be expected to lead to relativistic models in $1+2$ and $1+3$ dimensions.

ACKNOWLEDGMENTS

The work of A.G.W. was supported by the Australian Research Council through the ARC Center of Excellence for Particle Physics (CoEPP) at the Terascale (Grant No. CE110001004).

APPENDIX: EXISTENCE OF SOLUTIONS

We show here that the N Eqs. (25) can be solved to find the differences $\alpha_j^\infty - \alpha_i^\infty$ for all $i, j = 1 \ldots N$, for any $\omega_i, \lambda_i, \kappa_i$ with $\lambda_i, \kappa_i > 0$. The exact solution given in Sec. III A for $N = 2$ shows that $\kappa_1 + \kappa_2 > 0$ is necessary for synchronization to occur, but we assume, in general, stronger condition $\kappa_i > 0$ for all i. We write (25) as

$$\omega_{\rm av} - \omega_i = \frac{\kappa_i \lambda_i}{2} \left(\rho\, {\rm e}^{-\alpha_i^\infty} - \bar\rho\, {\rm e}^{\alpha_i^\infty} \right), \tag{A1}$$

where

$$\rho = \frac{1}{N} \sum_{j=1}^N \lambda_j {\rm e}^{\alpha_j^\infty}, \quad \bar\rho = \frac{1}{N} \sum_{j=1}^N \lambda_j {\rm e}^{-\alpha_j^\infty}. \tag{A2}$$

If $\omega_i = \omega_{\rm av}$ for all i, i.e., for identical parameters ω_i, we obtain ${\rm e}^{\alpha_i^\infty} = \sqrt{\rho/\bar\rho}$ for all i from (A1), with $\sqrt{\rho\bar\rho} = \sum_i \lambda_i / N$. In this case, ${\rm e}^{\alpha_i^\infty}$ is independent of i and (25) is satisfied by setting $\alpha_j^\infty = \alpha_i^\infty$ for all i and j, corresponding to complete synchronization.

Otherwise, if $|\omega_i - \omega_{\rm av}| \neq 0$ for one or more values of i, we observe that (A1) is quadratic in ${\rm e}^{\alpha_i^\infty}$ with two roots, only one of which is positive, and so we obtain

$${\rm e}^{\alpha_i^\infty} = \frac{\omega_i - \omega_{\rm av} + \sqrt{\rho\bar\rho\, \kappa_i^2 \lambda_i^2 + (\omega_i - \omega_{\rm av})^2}}{\bar\rho\, \kappa_i \lambda_i}, \tag{A3}$$

from which follows

$${\rm e}^{-\alpha_i^\infty} = \frac{-\omega_i + \omega_{\rm av} + \sqrt{\rho\bar\rho\, \kappa_i^2 \lambda_i^2 + (\omega_i - \omega_{\rm av})^2}}{\rho\, \kappa_i \lambda_i}. \tag{A4}$$

By substituting (A3) into (A2), we obtain

$$\begin{aligned} \rho &= \frac{1}{\bar\rho\, N} \sum_{i=1}^N \frac{\omega_i - \omega_{\rm av} + \sqrt{\rho\bar\rho\, \kappa_i^2 \lambda_i^2 + (\omega_i - \omega_{\rm av})^2}}{\kappa_i} \\ &= \frac{1}{\bar\rho\, N} \sum_{i=1}^N \frac{\sqrt{\rho\bar\rho\, \kappa_i^2 \lambda_i^2 + (\omega_i - \omega_{\rm av})^2}}{\kappa_i}, \end{aligned} \tag{A5}$$

where we have used $\sum_i (\omega_i - \omega_{\rm av})/\kappa_i = 0$, as follows from the definition (24) of $\omega_{\rm av}$. We therefore obtain the following equation for $\rho\bar\rho$:

$$\rho\bar\rho = \frac{1}{N} \sum_{i=1}^N \frac{\sqrt{\rho\bar\rho\, \kappa_i^2 \lambda_i^2 + (\omega_i - \omega_{\rm av})^2}}{\kappa_i}. \tag{A6}$$

We obtain the same equation if we substitute (A4) into the expression (A2) for $\bar\rho$. We wish to solve (A6) for $\rho\bar\rho$, for then we obtain $\bar\rho\, {\rm e}^{\alpha_i^\infty}$ from (A3) for all $i = 1 \ldots N$, as well as $\rho\, {\rm e}^{-\alpha_j^\infty}$ from (A4) for all $j = 1 \ldots N$. On multiplying these two quantities, we obtain $\rho\bar\rho\, {\rm e}^{\alpha_i^\infty - \alpha_j^\infty}$, and hence, since $\rho\bar\rho$ is now known, ${\rm e}^{\alpha_i^\infty - \alpha_j^\infty}$ for all $i, j = 1 \ldots N$ as required.

Let $x = \rho\bar\rho$ and define the linear polynomial p_i and the function f for $x \geqslant 0$ by

$$p_i(x) = x\, \kappa_i^2 \lambda_i^2 + (\omega_i - \omega_{\rm av})^2, \quad f(x) = \frac{1}{N} \sum_{i=1}^N \frac{\sqrt{p_i(x)}}{\kappa_i}, \tag{A7}$$

then (A6) reads $x = f(x)$. f is continuous and differentiable and is also positive for all $x \geqslant 0$, in particular,

$$f(0) = \frac{1}{N}\sum_{i=1}^{N}\frac{\sqrt{p_i(0)}}{\kappa_i} = \frac{1}{N}\sum_{i=1}^{N}\frac{|\omega_i - \omega_{\rm av}|}{\kappa_i}, \qquad \text{(A8)}$$

and so $f(0) > 0$, since $\kappa_i > 0$ for all i.

First, we show that $f(x) = x$ has at most two solutions. Let $g(x) = x - f(x)$, then $g''(x) = -f''(x)$. Since $f'' < 0$, we have $g'' > 0$ and so g is strictly convex on $[0, \infty)$. Therefore, g has at most two distinct positive roots.

Also, for sufficiently large x, we have $f(x) < x$. This follows from the Cauchy-Schwarz inequality that

$$\left(\frac{1}{N}\sum_i \frac{\sqrt{p_i(x)}}{\kappa_i}\right)^2 \leqslant \frac{1}{N}\sum_i \frac{p_i(x)}{\kappa_i^2} = ax + b, \qquad \text{(A9)}$$

for positive coefficients a and b which can each be deduced from the formula (A7) for $p_i(x)$. Hence, $f(x) \leqslant \sqrt{ax + b}$ for all $x > 0$ which implies $f(x) < x$ for sufficiently large x. Together with $f(0) > 0$ and the continuity of f, this implies by the intermediate value theorem that there exists at least one solution $x > 0$ to the equation $f(x) = x$. The strict convexity of g shows that this is the only solution, i.e., there exists exactly one solution $\rho\bar{\rho}$ to (A6) for any $\kappa_i > 0$. It is straightforward to find this solution numerically by standard root-finding methods.

[1]A. Arenas, A. Díaz-Guilera, J. Kurths, Y. Moreno, and C. Zhou, Phys. Rep. **469**, 93–153 (2008).
[2]S. Boccaletti, V. Latora, Y. Moreno, M. Chavez, and D.-U. Hwang, Phys. Rep. **424**, 175–308 (2006).
[3]F. Dörfler and F. Bullo, Automatica **50**, 1539–1564 (2014).
[4]J. A. Acebrón, L. L. Bonilla, C. J. Pérez Vicente, F. Ritort, and R. Spigler, Rev. Mod. Phys. **77**, 147–185 (2005).
[5]A. Pikovsky and M. Rosenblum, Chaos **25**, 097616 (2015).
[6]Y. Kuramoto, "Self-entrainment of a population of coupled non-linear oscillators," in *International Symposium on Mathematical Problems in Theoretical Physics*, Lecture Notes in Physics, edited by H. Araki (Springer, Berlin, Heidelberg, 1975), Vol. 39, pp. 420–422.
[7]M. A. Lohe, Automatica **54**, 114–123 (2015).
[8]M. A. Lohe, Phys. Scr. **89**, 115202 (2014).
[9]H. Daido, Prog. Theor. Phys. **77**, 622–634 (1987).
[10]D. Iatsenko, P. V. E. McClintock, and A. Stefanovska, Nat. Commun. **5**, 4118 (2014).
[11]V. Vlasov, E. E. N. Macau, and A. Pikovsky, Chaos **24**, 023120 (2014).
[12]M. A. Lohe, J. Phys. A: Math. Theor. **42**, 395101 (2009).
[13]S.-Y. Ha and S. W. Ryoo, J. Stat. Phys. **163**, 411–439 (2016).
[14]D. Chi, S.-H. Choi, and S.-Y. Ha, J. Math. Phys. **55**, 052703 (2014).
[15]S.-H. Choi and S.-Y. Ha, SIAM J. Appl. Dyn. Syst. **13**, 1417–1441 (2014).
[16]S.-Y. Ha, D. Ko, and S. W. Ryoo, J. Stat. Phys. **168**, 171–207 (2017).
[17]I. S. Gradshteyn and I. M. Ryzhik, *Table of Integrals, Series and Products* (Academic, 1965).
[18]G. S. Schmidt, A. Papachristodoulou, U. Münz, and F. Allgöwer, Automatica **48**, 3008–3017 (2012).
[19]Y.-P. Choi, S.-Y. Ha, S. Jung, and Y. Kim, Physica D **241**, 735–753 (2012).
[20]R. E. Mirollo and S. H. Strogatz, Physica D **205**, 249–266 (2005).
[21]D. Aeyels and J. Rogge, Prog. Theor. Phys. **112**, 921–941 (2004).
[22]J. L. van Hemmen and W. F. Wreszinski, J. Stat. Phys. **72**, 145–166 (1993).
[23]D. G. Schaeffer and J. W. Cain, *Ordinary Differential Equations: Basics and Beyond* (Springer, New York 2016).
[24]S.-H. Choi and S.-Y. Ha, Q. Appl. Math. **LXXIV**, 297–319 (2016).
[25]H. Goldstein, C. Poole, and J. Salko, *Classical Mechanics*, 3rd ed. (Pearson/Addison-Wesley, 2002).
[26]E. F. Taylor and J. A. Wheeler, *Spacetime Physics*, 2nd ed. (Freeman, NY, 1992).
[27]F. A. Rodrigues, T. K. D. M. Peron, P. Ji, and J. Kurths, Phys. Rep. **610**, 1–98 (2016).
[28]S.-H. Choi and S.-Y. Ha, J. Phys. A: Math. Theor. **48**, 425101 (2015).

Appendix II

This appendix contains the explicit forms of the coefficients a, b, c in (5.13). The constants a, b, c are:

$$a = \frac{-\eta\omega \sinh\alpha_0 - \eta^2 \cosh\alpha_0 \sin\theta_0 + \beta\eta \cosh\alpha_0 \cos\theta_0}{\Delta^2}$$

$$b = \frac{\sinh\alpha_0(\beta\Delta + \eta\omega) + \cosh\alpha_0 \cos\theta_0(\omega\Delta + \eta\beta) + \cosh\alpha_0 \sin\theta_0(\beta^2 - \omega^2)}{2\Delta^2}$$

$$c = \frac{\sinh\alpha_0(-\beta\Delta + \eta\omega) + \cosh\alpha_0 \cos\theta_0(-\omega\Delta + \eta\beta) + \cosh\alpha_0 \sin\theta_0(\beta^2 - \omega^2)}{2\Delta^2}$$

where $\Delta = \sqrt{\beta^2 + \eta^2 - \omega^2}$

Bibliography

[1] A. Arenas, A. Díaz-Guilera, J. Kurths, Y. Moreno, C. Zhou, *Physics Reports* **469**, 93-153 (2008).

[2] S. Boccaletti V. Latora, Y. Moreno, M. Chavez, D.-U. Hwang *Physics Reports* **424**, 175-308(2006).

[3] F. Dörfler, F. Bullo, *Automatica* **50**, 1539-1564 (2014).

[4] J.A. Acebrón, L.L. Bonilla, C.J. Pérez Vicente, F. Ritort, R. Spigler, *Rev. Mod. Phys.* **77**, 147-185 (2005).

[5] A. Pikovsky, M. Rosenblum, *Chaos* **25**, 097616 (2015).

[6] F.A. Rodrigues, T.K.DM. Peron, P. Ji, J. Kurths, *Phys. Rep.* **610**, 1-98 (2016).

[7] J. Buck, E. Buck, *Nature* **211**, 562-564 (1966).

[8] J. Pantaleone, *Phys. Rev. D* **58**, 073002 (1998).

[9] C.M. Gray, *J. Comput. Neurosci.* **1**, 1138 (1994)

[10] F. Dörfler, M. Chertkov, F. Bullo, *PNAS* **110**, 2005-2010 (2012).

[11] Y. Kuramoto, International symposium on mathematical problems in theoretical physics, Lect. Notes Theoret. Phys, **39**, 420-422 (1975).

[12] M.A. Lohe, *Automatica* **54**, 114-123 (2015).

[13] H. Hong, S.H. Strogatz, *Phys. Rev. E* **84**, 046202 (2011).

[14] Y.-P. Choi, S.-Y. Ha, S.-B. Yun, *Physica D* **240**, 32-44 (2011).

[15] S.-Y. Ha, Y. Kim, Z. Li, *SIAM J. Applied Dynamical Systems* **13**, 466-492 (2014).

[16] J.A. Acebrón, L.L. Bonilla, R. Spigler, *Phys. Rev. E* **62**, 3437-3454 (2000).

[17] F. Ritort, *Phys. Rev. Lett* **80**, 6-9 (1998).

[18] S.N. Dorogovtsev, A.V. Goltsev, J.F.F. Mendes, *Rev. Mod. Phys.* **80**, 1275-1335 (2008).

[19] J.L. van Hemmen, W.F. Wreszinski, *J. Stat. Phys.* **72**, 145-166 (1993).

[20] T. Gross, B. Blasius, *J. R. Soc. Interface* **5**, 259-271 (2007).

[21] F. Dörfler, F. Bullo, *SIAM, J. Applied Dynamical Systems* **10**, 1070-1099 (2011).

[22] D.M. Abrams, R. Mirollo, S.H. Strogatz, D.A. Wiley, *Phys. Rev. Lett.* **101**, 084103 (2008).

[23] M.A. Lohe, *J. Phys. A: Math. Theor.* **42**, 395101 (2009).

[24] M.A. Lohe, *J. Phys. A: Math. Theor.* **43**, 465301 (2010).

[25] S.-H. Choi, S.-Y. Ha, *SIAM J. Applied Dynamical Systems* **13**, 1417-1441 (2014).

[26] S.-Y. Ha, D. Ko, S.W. Ryoo, *J. Stat. Phys.* **168**, 171-207 (2017).

[27] I.S. Gradshteyn, I.M. Ryzhik, *Table of Integrals, Series and Products*. Seventh Edition, Elsevier, 2015.

[28] A.C. Kalloniatis, M.L. Zuparic, *Physica A* **447**, 21-35 (2016).

[29] N. Jeevanjee, *An Introduction to Tensors and Group Theory for Physicists*. Second edition, Springer International, Switzerland (2015) .

[30] Y.-P. Choi, S.-Y. Ha, S. Jung, Y. Kim *Physica D* **241** 735-753 (2012).

[31] S.-Y. Ha, T. Ha, J.-H. Kim, *Physica D*, **239** 1692-1700 (2010).

[32] K.T. Alligood, T. Sauer, J. Yorke, *Chaos: An introduction to dynamical systems*. First edition, Springer, United States of America (1996).

[33] H. Hong, S.H. Strogatz, *Phys. Rev. Lett.* **106**, 054102 (2011).

[34] D. Yuan, M. Zhang, J. Yang, *Phys. Rev. E* **80**, 012910 (2014).

[35] D. Yuan, J. Yang, *Commun. Theor. Phys.* **59**, 684-688, (2013).

[36] K. Wiesenfeld, P.Colet, S. H. Strogatz, *Phys. Rev. E* **57** 1563-1569 (1998).

[37] H. Sakaguchi, Y. Kuramoto, *Prog. Theor. Phys.* **76** (1986).

[38] S. Shinomoto, Y. Kuramoto, *Prog. Theor. Phys.* **75**, 1105 (1986).

[39] M.A Lohe, *J. Phys. A: Math. Theor.* **50** 505101 (2017).

[40] S.-H. Choi, S.-Y. Ha *J. Phys. A: Math. Theor.* **48** 425101 (2015).

[41] H. Goldstein, J. Safko, C. Poole, *Classical Mechanics*. Third edition, Pearson, United States of America (2014).

[42] F.J. Harris, *Proceedings of the IEEE* **66**, 51-83 (1978).

[43] M.E.J. Newman, *SIAM Review* **45**, 167-256 (2003).